UNIVERSITY OF CALIFORNIA

Los Angeles

From Rupture to Recovery: Integrating Probabilistic Building Performance Assessment, Decision-Making and Socioeconomic Vulnerability to Model Post-Earthquake Housing Recovery

A dissertation submitted in partial satisfaction of the requirements for the degree Doctor of Philosophy in Civil Engineering

by

Hua Kang

2018

ABSTRACT OF THE DISSERTATION

From Rupture to Recovery: Integrating Probabilistic Building Performance Assessment, Decision-Making and Socioeconomic Vulnerability to Model Post-Earthquake Housing Recovery

by

Hua Kang

Doctor of Philosophy in Civil Engineering

University of California, Los Angeles, 2018

Professor Henry V. Burton, Chair

Housing plays a primary role in post-earthquake recovery because all sectors of the economy rely on residents having healthy living conditions so that they will remain in the affected region. Therefore, understanding the time-dependent effects of earthquake events on housing is critical for improving post-earthquake trends through policy and planning interventions. This study develops an integrated framework for modeling post-earthquake housing recovery that combines probabilistic building performance with the decisions, actions and socioeconomic vulnerability of the affected populations. Building performance is characterized using limit states such as post-earthquake occupiability and repairability, which are explicitly linked to community functionality and recovery. Fragility functions are used to link the probability of exceeding these limit states to ground shaking intensities. Household decisions are modeled using empirical probabilistic utility models. Probabilistic discrete state models are implemented to represent post-earthquake recovery trajectories at the building, neighborhood and community scales. These models, which are inherently stochastic, can be purely empirical, such that the temporal parameters are sampled from an appropriate probability distribution. Alternatively, a simulation-based model can be employed to explicitly account for the effect of resource-availability on the time to complete relevant recovery activities. Socioeconomic vulnerability and other exogenous (external to household) and endogenous (external to household) factors are statistically linked to the temporal recovery parameters. The proposed model can be used to assist policy-makers, municipal governments and planners in understanding the possible interdependencies, interventions, and tradeoffs associated with post-earthquake housing recovery.

The dissertation of Hua Kang is approved.

Scott Joseph Brandenberg

Yingnian Wu

Ali Nejat

Henry V. Burton, Committee Chair

University of California, Los Angeles, 2018

2018

Table of Contents

List of Tables

List of Figures

Acknowledgements

The research presented in this paper is supported by the National Science Foundation CMMI Research Grant No. 1538747. Any opinions, findings, and conclusions or recommendations expressed in this paper are those of the authors and do not necessarily reflect the views of the sponsor.

The authors would like to thank Professor Scott Miles of University of Washington for generously sharing ideas and suggestions. Their contribution is greatly appreciated.

HUA KANG

EDUCATION

University of California, Los Angeles, Los Angeles, USA

Master of Science in Statistics (*Sept. 2015- Jun. 2018*)

Columbia University, New York, USA

Master of Science in Civil Engineering (*Sept. 2013-Dec. 2014*)

Tianjin University, Tianjin, China

Bachelor of Science in Civil Engineering (*Sept. 2009- Jun. 2013*)

Bachelor of Science in Management (*Sept. 2009- Jun. 2013*)

JOURNAL PAPER

Kang, H. and Burton, H. V. (2018). "*Replicating the recovery following the 2014 South Napa earthquake using stochastic process models*," Earthquake Spectra, https://doi.org/10.1193/012917EQS020M.

Burton, H. V., Miles, S.B. and **Kang, H.** (2018). "*Integrating performance based engineering and urban simulation to model post-earthquake housing recovery*," Earthquake Spectra (accepted for publication).

Miles, S.B., Burton, H. V., and **Kang, H.** (2018). "*Towards a community of practice for disaster recovery modeling*," Natural Hazards Review (accepted for publication).

Kang, H., Yi, Z., and Burton, H. V. (2018). "*Effect of Los Angeles soft-story ordinance on the post-earthquake housing recovery of impacted residential communities*," Natural Hazards (submitted).

CHAPTER 1: Introduction

1.1 Motivation and Background

During the period following a major disaster, affected communities are expected to cope with a myriad of challenges that span the various sectors that support their daily economic activity. The lives of residents are severely disrupted when there is major damage to the built infrastructure that underpins normal community functionality. These disruptions can vary both spatially and temporally affecting some groups and places more than others at different times during the recovery-period. With the goal of overcoming these challenges, many have advocated the implementation of pre-event planning (Wilson, 1991; Geis, 1996; Wu and Lindell, 2004), whereby procedures and guidelines outlining deliberate post-event actions and operating-protocol are developed towards achieving desirable short-, medium- and long-term outcomes.

The relative infrequency and spatiotemporal scale of large-scale post-earthquake housing recovery events makes longitudinal collection of quantitative data difficult (Chang, 2010). In light of this, modeling is one critical research advancement necessary for understanding and quantifying the complex processes driving post-earthquake housing recovery and the myriad of influences on decision and outcome trajectories over time (Miles and Chang, 2011). There have been efforts in the last few decades towards modeling disaster recovery in urban regions (Nejat and Damnjanovic, 2012; Miles and Chang, 2011; Comerio and Blecher, 2010; Schneider and Schauer, 2006; Miles and Chang, 2006; Rose and Liao, 2005). However, especially for earthquakes, the effect of immediate post-event building conditions on recovery-related decisions, activities and trajectories has not been adequately addressed. Existing models take a qualitative approach or represent building states as economic loss. These models do not represent the limit states of buildings in a way that can be explicitly linked to decisions and outcomes related to repair, reconstruction, and abandonment. Meaningful quantification of post-earthquake housing recovery requires an assessment of building performance limit states that inform owner and occupier decisions and possible ameliorative actions over time.

1.2 Objectives

The objective of this study is to develop an integrated post-earthquake housing recovery model that combines robust assessments of building performance with characterization of post-earthquake decisions and actions, socioeconomic vulnerability and temporal processes. The broader objective of the project is realized through the completion of the following tasks:

1. Explore and summarize the previous work that have been done in disaster recovery modeling including their limitations and future research needs.
2. Develop and implement a probabilistic building performance assessment methodology that can be incorporated to model possible recovery-based limit states such as loss of functionality (e.g. due to utility disruption), building unsafe to occupy, irreparable damage and collapse. Fragility curves will be used to link ground shaking intensity to the probability of exceedance of those limit states.
3. Formulate two types of discrete-state stochastic process models to capture recovery trajectories: (a) discrete-time, state-based models which characterize transition probabilities based on the time elapsed in a given state and (b) time-based models which sample from the probability density function of time to complete various processes. These two models can be purely-empirical or simulation-based.
4. Apply advanced statistical tools including machine learning algorithms to statistically link various explanatory variables (exogenous and endogenous factors related to damage, neighborhood, and socioeconomic vulnerability) to the pace of recovery.
5. Conduct a case study using building damage and reconstruction data from the 2014 South Napa Earthquake to validate and calibrate a stochastic process post-earthquake recovery model.
6. Propose decision making models at household level using two alternative approaches: (a) empirical probabilistic and (b) theoretical deterministic utility-based models. The latter is developed using the results of a survey of households in the City of Los Angeles.
7. Perform a case study using five target neighborhoods in Los Angeles to evaluate the effect of (a) measures to mitigate building seismic vulnerability (e.g. soft-story retrofit ordinance) and (b) household decision-making on post-earthquake housing recovery trajectories.

1.3 Organization and Outline

The main body of the current study consists of five chapters. Most chapters are adopted from a research paper which is cited at the beginning of the chapter.

Chapter 2 begins with a literature review of the studies on disaster recovery categorized by modeling methods: (1) resource-constraint models, (2) statistical curve-fitting models, (3) agent-based models, (4) stochastic simulation models, (5) discrete event simulation models and (6) network models. The chapter concludes with a summary of the similarities and differences in the modeling techniques, including the benefits and drawbacks of each approach and their suitability to the context and application of the recovery model.

Chapter 3 begins with a description of building performance limit states that inform post-earthquake recovery and functionality of residential communities. To follow, probabilistic (fragility) models are used to represent limit states. The chapter ends by presenting a method to map the loss-based fragility function parameters used in risk assessment platform such as HAZUS and OpenQuake, to the "recovery-based" ones considered in this study.

Chapter 4 begins with an overview of two types of stochastic process models (time- and state-based) that can be used to model post-earthquake recovery. These models are developed to the be either "empirically- or simulation-based". For the empirically based models, the temporal parameters (e.g. time-to-permit) are sampled from an assumed probability distribution using parameters that are calibrated using data from prior recovery events. The simulation-based model explicitly incorporates the effect of resource constraints (e.g. availability of building inspectors) on the time to complete relevant recovery processes. A case study is performed using building damage and permit acquisition and completion date data from the 2014 South Napa earthquake to validate and calibrate the recovery models.

Chapter 5 beings with a description of an inventory of 8,000 buildings located in five Los Angeles neighborhoods. Analytical building level damage fragility curves are developed using the results nonlinear analyses of structural models representing each archetype. A scenario-based damage assessment is performed using shaking intensities generated from the Southern California ShakeOut scenario and a discrete-time state-based stochastic process model is used represent post-earthquake recovery. The quantified effect of the Los Ordinance soft-story retrofit on post-earthquake housing recovery is investigated.

Chapter 6 begins with a literature review of decision-making models. The formulation of theoretical deterministic and empirical probabilistic decision-models for predicting post-disaster household decision-outcomes is then presented. A survey of 96 Los Angeles households was conducted and used to develop the empirical probabilistic decision-model. A summary of the survey design is presented. A description how the data was collected a is also presented. A multilevel statistical analysis is implemented to develop the decision-model. The chapter concludes by applying the developed-decision-model to the Los Angeles case study presented in Chapter 5.

Chapter 7 synthesizes the developments and findings from the earlier chapters and discusses the limitations and opportunities for future advancements.

CHAPTER 2: Modeling Post-Disaster Restoration of Socio-Technical Systems: A State of the Art Review

This chapter is partly based on the following publication:

Miles, S.B., Burton, H. V., and Kang, H. (2018). "Towards a community of practice for disaster recovery modeling," *Natural Hazards Review* (accepted for publication).

2.1 Overview

This chapter presents a literature review that has been conducted to assess the state-of-the-art on modeling post-disaster restoration (recovery) of socio-technical systems. Research efforts on disaster recovery modeling date back to as early as 1985 and the topic has become increasingly popular, particularly within the last 10 to 15 years. It is an appropriate time to present this review because of the increased frequency of large scale natural disasters and some recent applications of simulation models in pre-disaster recovery-planning. The review is organized around the different ways that the dynamic processes of recovery are mathematically represented. Six main types of models are described and compared to assess the time-dependent effects of hazard events on the built environment. Resource-constraint model describes recovery process using mathematical equations and rules based on available resources. Statistical curve-fitting model is the most straight forward method where data from previous disaster is employed to fit recovery curve or to study trends on building characteristics. Agent-based model models recovery process as a dynamic system of interacting agents so that individual entities that may speed or constraint the pace of disaster recovery process and their interdependencies inherent between key agents can be investigated. Stochastic simulation model performs a sampling-based computational simulation that keeps track of recovery process with random increments over any time interval. Therefore, this method is complemented with stochastic process and Monte-Carlo simulation. Discrete event simulation (DES) model assumes each event occurs at a particular instant in time and changes the state of the system. Contrasting to continuous simulation, no change is allowed between consecutive events. Network Models use a series of links that connect a supply node and multiple demand nodes as the neuron-like units to optimize system. The studies utilizing each of the six modeling approaches are described, focusing on (a) the mechanisms and processes that are represented, (b) the key variables and nomenclature, (c) relevant equations, (d) the approach (or lack

thereof) used to represent boundary conditions, (e) relevant datasets and visualization and (e) case studies used for validation and testing.

2.2 Resource-Constraint Models

Resource-constraint models represent post-disaster restoration processes using mathematical equations and rules that either explicitly or implicitly incorporate the spatial and temporal effects of available resources (labor finances etc.). The models can be deterministic or probabilistic and are generally based on empirical observations from past disasters including information garnered from affected populations and the various agencies that are responsible for mitigating the effects of extreme hazard events on communities. Isumi et al. (1985) developed a model to predict the post-earthquake behavior of lifeline systems (gas, water and power). The model provides predictions of seismically induced damage to the relevant infrastructure systems or "hard" damage, the initial loss of functionality or "soft" damage and the recovery of both the physical infrastructure and systems' functionality. Hard damage to individual elements of a lifeline system is described by the relationship between the ground shaking intensity and rate of damage. The damage rates are probabilistically described using a Poisson distribution where the rate term describes the number of "damaged" points within a census region. Examples of damaged points include loosened pipelines (gas system), fallen poles (electrical system) and leaking pipes (water distribution system). The severity of damage within an element is not considered. Soft damage is quantified using indices that capture the loss of functionality of the lifeline system. These indices describe the percentage of customers within the study area who can use a utility (gas, electricity and water). An analytical model or "closed-form" equation describes the repair of damaged points within a lifeline system.

$$D_i(t+\Delta t) = D(t) - \Delta t \cdot r_i(t) \tag{2.1}$$

where $D_i(t)$ i is number of damaged points occurring in the i^{th} i$^{\text{th}}$ division. The repair work rate, $r_i(t)$ r$_{\text{i}}$(t), is determined by the number, efficiency and scheduling of repair workers in the i^{th} division. The repair rate also accounts for the density of damage within the division. The number of customers $V_i(t)$ who can use a utility service is also modeled using an analytical equation.

$$V_i(t+\Delta t) = V_i(t) + \Delta t O_i(t) \tag{2.2}$$

where $O_i(t)$ is the number of gas meters opened per a unit of time. The repair activities described in equations 2.1 and 2.2 are based on a series relationship i.e. restoration of service occurs after repairs are completed.

The Isumi et al. model was used to predict the restoration of water, gas and power systems following the 1978 Off-Miyagi earthquake. The damage rates for each system was determined from observations from the same earthquake. Monte Carlo simulation was used to generate multiple realizations of damage. GIS mapping was used to visualize the distribution of damage. The restoration strategies for the actual earthquake was used to model the distribution of workers. Fig. 2-1 shows the relationship between the observed and predicted recovery trajectory for the gas system. Similar plots were developed for the water and electric systems. The plot shows that the prediction model reasonably captures the restoration of gas within the region. Multiple restoration curves are shown for each lifeline representing the effect of different repair strategies including (a) no prioritization of repairs, (b) prioritizing heavily damaged areas and (c) prioritizing areas with minor damage.

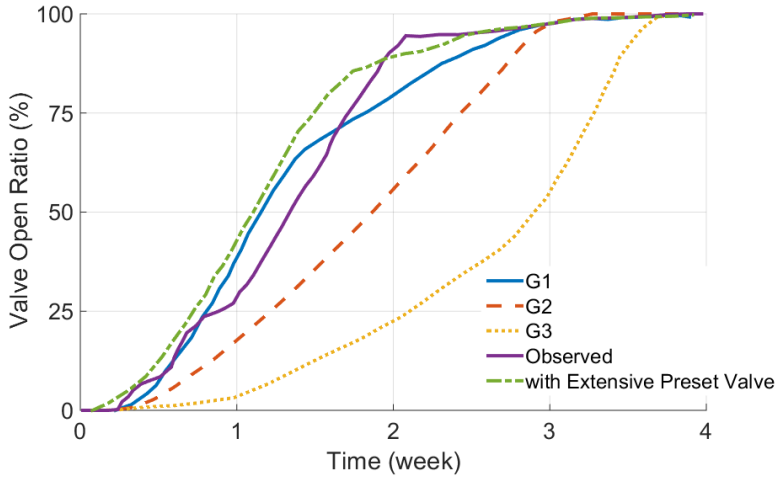

Fig. 2-1. Comparing simulated and observed restoration of gas system (adapted from Isumi et al. 1985)

Ballantyne and Taylor (1990) estimated the restoration times for the various components that comprise Seattle's water distribution system based on the time it would take for a crew of workers to repair different types (damage to pipes, pumping equipment etc.) and degrees (e.g. pipe leaks, pipe breaks) of damage. It was assumed that larger events would place greater constraints on available resources due to increased disruptions to other types of lifeline systems (electric power, telecommunication, transportation) that are needed to carry out repair activities within the affected water distribution system. A similar approach was implemented

in the HAZUS loss modeling platform (Whitman et al., 1997). The number of available workers was taken as a fixed percentage of the study region and estimates of the number of pipe leaks and breaks that could be repaired by a single worker are provided.

Improving on an earlier model that estimated water service restoration times solely based on census-level pipe break densities (Chang et al. 1996), Chang et al. (1999) adopted the resource constraint approach in a study of the Memphis Light, Gas and Water Division. Anecdotal evidence from past earthquakes was used to inform key assumptions in the new model. For example, observations from the Kobe earthquake showed that it was reasonable to assume that the least damaged areas would be restored more quickly than areas with greater damage. However, restoration times were not strongly correlation with census-level damage densities. Moreover, the Kobe earthquake data did not support the assumption by Ballantyne that the number of available workers was proportional to resident population. In the improved Chang et al. model, the spatial distribution damage to the water supply network is obtained from Monte Carlo simulation based on some scenario earthquake. For a given damage pattern, a system flow analysis was performed and the ratio of supplied to demanded flow was assessed. The restoration of supply was modeled based on an assumed rate and spatial sequencing of repairs.

Cimellaro et al. (2010) proposed an analytical approach for quantifying disaster resilience, which is based on an earlier conceptual framework developed by the Multidisciplinary Center for Earthquake Engineering Research (MCEER) (Bruneau et al., 2003). A resilience curve was used to capture the initial hazard-event-induced loss of functionality of the considered system and the temporal restoration of functionality. The initial loss of functionality was assumed to be a function of economic losses. Three simple analytical functions (linear, exponential and trigonometric) were suggested for modeling the recovery of functionality. The authors noted that the choice of the recovery function can be based on the level of preparedness and availability of resources to support the recovery.

2.3 Statistical Curve-Fitting Models

Another approach to modeling post-disaster restoration of socio-technical systems is to use "purely" empirically-based statistical models, which provides predictions of recovery-outcomes for future disasters, solely based on observations from past disasters. Several researchers have employed various regression techniques to simulate disaster recovery

trajectories and/or investigate the variables that most influence the different sectors following a major hazard event.

The ATC-25 (FEMA, 1991) document uses regression modeling to estimate the fraction of pre-event capacity of lifeline systems as a function of time since the earthquake, which is conditioned on the Maximum Mercalli Intensity (MMI). The overall framework starts with establishing empirically-based analytical relationships between *MMI* and the damage factor (DMG) for a given damage state and the restoration time (TR).

$$DMG = \exp(a)MMI^{b} \tag{2.3}$$

$$T_R = \exp(c)DMG^{d} \tag{2.4}$$

where *a*, *b*, *c* and *d* are regression coefficients. Equations 3 and 4 are used to develop restoration curves for each *MMI* by fitting a line through the restoration time associated with discrete restoration levels (e.g. 30%, 60% and 100% of pre-earthquake capacity), which results in the following regression function:

$$R = f + (g)(T_R) \tag{2.5}$$

Where *R* is the percentage of functionality restored (relative to the pre-earthquake functionality level) and *f* and *g* are regression coefficients. Example restoration curves for ports/cargo handling equipment corresponding to different *MMIs* are shown in Fig. 2-2. As one would expect, the slope of the restoration curve decreases as the *MMI* value increases.

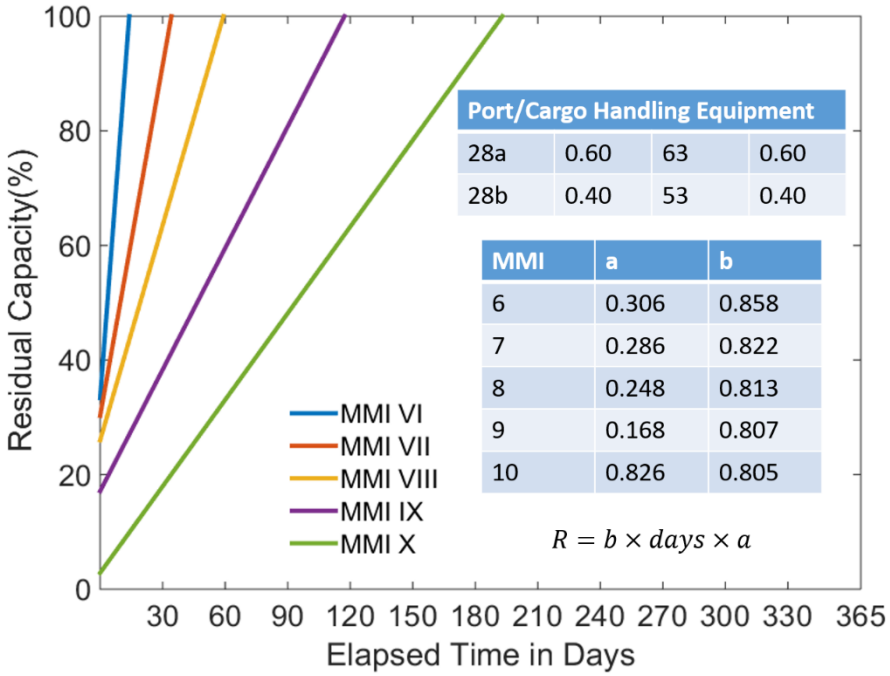

Port/Cargo Handling Equipment			
28a	0.60	63	0.60
28b	0.40	53	0.40

MMI	a	b
6	0.306	0.858
7	0.286	0.822
8	0.248	0.813
9	0.168	0.807
10	0.826	0.805

Fig. 2-2. Restoration curves for ports/cargo equipment (adapted from ATC-25 Figure 3-6)

Liu et al. (2007) used acceleration failure time (AFT) models to estimate post-disaster power restoration times. *AFT* is a type of survival analysis model that is used to statistically analyze time-to-event data. The *AFT* model is described using the following equation:

$$\ln(T_i) = x_i^T \beta + \varepsilon_i \tag{2.6}$$

where T_i is a random variable representing the duration (survival time) of the i^{th} outage, x_i is a vector of predictors describing the i^{th} outage, β is the vector of regression coefficients and ε_i is an error term that is assumed to be independent and identically distributed. Data from six hurricanes and eight ice-storms were used to construct *AFT* models for the two types of hazard events. Six continuous predictor variables were considered including the maximum wind speed, duration of strong winds, 7-day rainfall, thickness of ice, total number of outages in the storm, outage start time (relative to the first outage), number of customers affected by the outage and population density. Models were also developed using categorical predictors including identifiers for specific hurricane and ice storm events, the type of device affected and the type of land cover in the outage location. Parametric *AFT* models were developed using the maximum likelihood method assuming Weibull, log-logistic and log-normal distributions for the outage duration and a normally distributed error term. The Weibull model was found to have the best fit based on the Akaike Information Criterion (Akaike, 1998).

Data from one of each type of event was excluded from the model for testing. Comparisons between the model predictions and observations from the test data are shown in Fig.2-3 for a real hurricane. Two predicted cases are shown. In the first case, the values of the explanatory variables are taken from the actual hurricane. In the second case, the explanatory variable values are sampled from parametric distributions developed using historical hurricane data. A similar plot (not shown in this chapter) was developed for real ice storm. Fig.2-3 shows that both prediction models capture the shape of the restoration curves but under-predicts the restoration time.

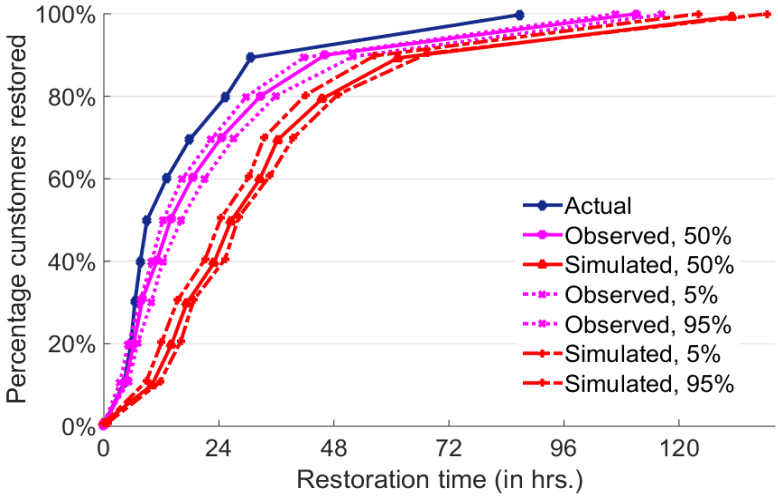

Fig.2-3. Comparing restoration curves from prediction model and observed data for a real hurricane (adapted form Liu et al. 2007)

Han et al. (2009) highlighted the fact that the Liu et al. model for predicting hurricane outage durations requires assumptions of how to represent the categorical variables, which are based on specific hurricane events. The authors noted that it is difficult to know what specific characteristics of a hurricane are captured by these categorical variables. Moreover, the Liu et al. model uses information that only becomes available after the hurricane makes landfall. To address these limitations, Han et al. developed a statistical model of hurricane-induced power outage duration using only information that is measurable prior to the hurricane making landfall. Examples of such variables include the time since the last hurricane landfall and the mean annual precipitation. Generalized linear models were used for the regression analysis. The dataset used to construct the statistical model was transformed through principal component analysis to avoid issues related to strong correlation among predictor variables. The relative importance of each of the explanatory variables was evaluated based on the relative change in the mean outage duration with respect to a unit change in the predictor.

Nateghi et. al (2011) assessed the effectiveness of five types of statistical models, including machine learning algorithms, in predicting the duration of power outages due to hurricanes. Included in the assessment are *AFT* regression, Cox Proportional Hazards (Cox PH) regression, Bayesian Additive Regression Trees (BART), Classification and Regression Trees (CART) trees and Multiple Adaptive Regression Splines (MARS). The *AFT* model has been described in the summary of the Liu et al. study. Like *AFT*, *Cox PH* regression also incorporates a survival analysis, where the log of the instantaneous rate of power restoration h_i, is taken as the linear combination of a set of predictor variables. However, in contrast to *AFT, Cox PH* is a semi-parametric model which makes no assumptions about the probabilistic distribution of the rate of power restoration, which makes the model output more difficult to interpret. *CART, BART* and *MARS* are machine learning algorithms. *CART* is a tree-based method, which recursively divides the data-space into subspaces until some pre-defined termination criteria is achieved. The dependent variable is taken as the mean or median value at the terminal node. The tree is subsequently pruned back starting from the terminal nodes, to avoid an overfitted prediction model. *BART* is also a tree-based algorithm that is used for classification and regression. *BART* is a fully Bayesian probability model that is constructed by aggregating the weighted estimates from many small trees, which are independently constructed using bootstrap resampled versions of the training data. *BART* provides a methodology for evaluating the relative influence of the different predictor variables. *MARS* is a nonlinear regression model that can capture interactions between different predictor variables. It consists of a series of linear splines and is often used in statistical models that comprise of many predictors. The models were first evaluated using a data-set from Hurricane Ivan, which was used for both training and testing. The prediction model from the Ivan data-set was then applied to two additional hurricanes: Katrina and Dennis. By comparing the mean absolute deviation and the root mean squared error of each method, the results showed that *BART* outperforms all other statistical methods.

Zhang et al. (2009) developed linear regression models that capture the temporal evolution of property values for single family homes in Miami-Dade County following Hurricane Andrew, which occurred in 1992. The models were used to investigate several hypotheses related to the effect of occupant tenure and neighborhood income and ethnic minority composition on the pace of recovery. Factors affecting property abandonment, home sales and land use change were also examined. The model was constructed using data from over 60,000 single-family homes located in South Dade. The data comprised of (1) housing tax

appraisal information from 1992 (just before the hurricane) to 1996, (2) parcel-level county land use and housing transaction data from 1991 to 1999 and (3) 1990 census data at the block group level. Explanatory variables related to the building (age number of bedrooms and bathrooms and level of hurricane damage), household (owner-occupied versus renter-occupied) and neighborhood (income and percentage ethnic minorities) were used to construct the panel models as multilevel, mixed-effects, linear regression. These predictors were found to be statistically significant based on a confidential level of 0.01. The effect of housing tenure and percentage of Hispanics at the neighborhood level on the recovery of property values is shown in Fig. 2-4. It shows that the value of owner-occupied houses recovered at a faster rate than renter-occupied houses. An inverse relationship between the percentage of ethnic minorities within a neighborhood and the rate of recovery of property values.

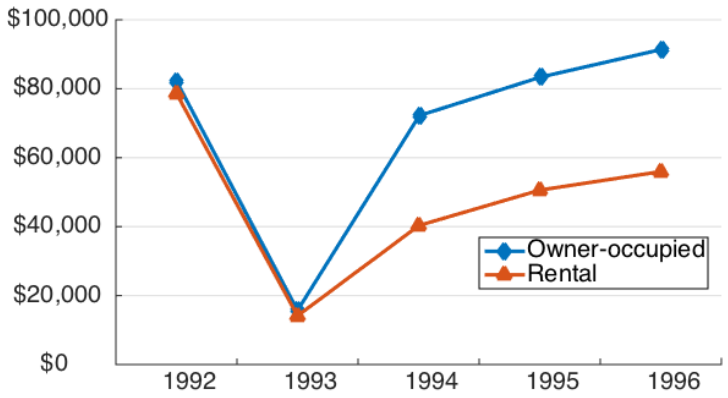

(a)

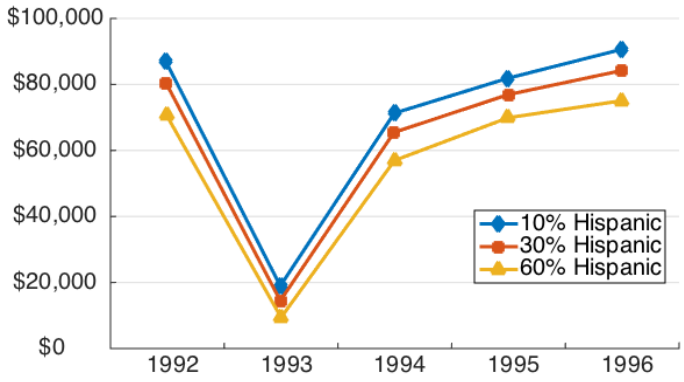

(b)

Fig. 2-4. Effect of (a) tenure (owner-occupied versus rental) and (b) percentage of Hispanics at the neighborhood level on the recovery of home values

Nejat et. al (2016) used linear regression to predict post-disaster household-level decisions (rebuild or repair damaged houses; wait and stay in temporary housing; relocate) and their impact on community-level recovery. Data related to a wide range of internal and external attributes (demographic, socioeconomic, exposure parameters, external signals and spatial activities) was collected in Staten Island, New York after Hurricane Sandy (2012). The data was acquired through 126 surveys of occupied homes and temporary shelters. Categorical housing recovery decisions (repair or wait/relocate) were used as the dependent variable. The Least Absolute Shrinkage and Selector Operator (LASSO) method (Tibshirani, 1996) was used to perform the regression. The *LASSO* method is often used in multi-variate regression when there is multicollinearity in the data representing the explanatory variables. Multicollinearity, which refers to the presence of strong correlations among predictor variables, can lead to inaccurate estimates of the regression coefficients, inflated standard errors and deflated partial t-test values in the regression coefficients. Of the 23 predictor variables considered in the regression model, the availability of insurance, tenure or place attachment, and availability of funding from external resources such as federal, state, local, and charities, were found to be statistically significant. The authors used anecdotal evidence from previous disasters (Comerio, 1998 and Wu et. al 2004) to validate the results obtained from their prediction model.

2.4 Agent-Based Models

Agent-based modeling (ABM) is a computational method that is used to analyze the collective behavior complex social systems comprised of autonomous agents that interact with an environment (N. Gilbert, 2008). Agents are used to represent social entities such as people, organizations, communities or nation states, whose behavior are governed by rules that account for preferences, competitive bidding and resource and budget constraints (Grinberger & Felsenstein, 2016). Several researchers have explored the use of *ABM* to represent the dynamic community-driven recovery processes that follow a disaster. In the context of disaster recovery modeling, agents are used to represent various social actors within a community (individuals, households, businesses), whose actions and interactions have the effect of increasing or reducing the pace at which various recovery processes are completed.

Nejat (2011) used *ABM* to model the post-disaster dynamic interactions among homeowners and between homeowners and insurance companies. These two types of

interactions influence homeowners' decisions regarding whether to repair, sell or abandon damaged property, which in turn affects the overall recovery trajectory of their community. The temporal behavior of agents (homeowners and insurance companies) are represented using both theoretical and empirical models. In the theoretical model, interactions among homeowners were represented as rational agents seeking to maximize their utility, which is a function of the gains/losses associated with specific post-event actions. The empirical household-interaction model is based on the results of experiments that are designed to mimic the conditions following a real disaster. The theoretical model for the homeowner-insurer bargaining process is based on game theory while the empirical model is also based on an experiment. The homeowner-homeowner and homeowner-insurance interaction models are placed in a Multi-domain Multi-agent system (Fig. 2-5) to represent the behavior of individual neighborhoods or communities. In the spatial domain, the relative location of entities drives interactions. For example, homeowner decisions are also affected by their location relative to commercial properties, educational institutions and essential lifelines. In the organizational domain, interactions are based on the social dynamics among homeowners and between homeowners and insurance companies.

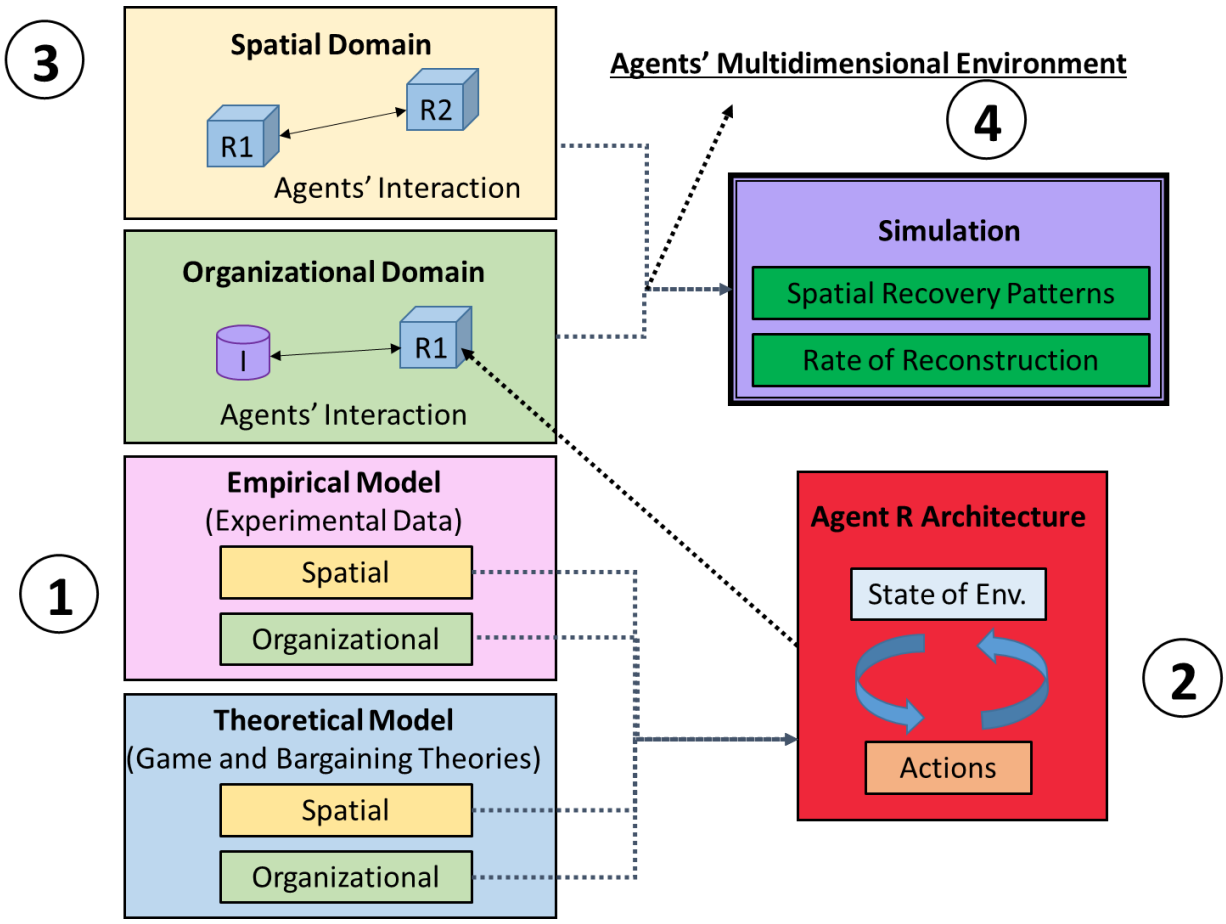

Fig. 2-5. Interactions in Multi-domain environment (adapted from Nejat, 20011)

To date, the most comprehensive model of disaster recovery is *ResilUS* developed by Miles and Chang (2003, 2006, 2011, 2014). The recovery model contains elements of both agent-based modeling and stochastic simulation (described in the next section). In *ResilUS*, households and businesses are represented as socioeconomic agents located within neighborhoods, which make up the larger community. The model starts with a description of the impact of the hazard event (earthquake) on the built environment (damage to buildings and lifeline systems) and socioeconomic agents (economics and personal health). The ability of agents to perform the activities necessary to bring about recovery is driven by both exogenic and endogenic variables. For example, the ability of households or businesses to reconstruct their residence or facility is influenced by their financial resources and the construction capacity of the community. Fig. 2-6 shows an overview of the various entities that are part of ResilUS with some examples of the attributes, behaviors and functional dependencies that were considered. ResilUS was implemented in the MATLAB/Simulink modeling platform, where the recovery dynamics are captured using Markov chains, which randomizes the state-transitions of various entities over time. The processes represented in the Markov chains

include building and lifeline restoration, health recovery, business demand recovery, business production recovery and whether an agent leaves the community. With the goal of calibrating parts of the model and performing sensitivity analyses, ResilUS was used to simulate the recovery dynamics following the 1994 Northridge earthquake. Results from the case study include an assessment of the spatial distribution of building damage (residential and commercial), repair and reconstruction, household injury, impacts on business demand and employment and business and household recovery. Fig. 2-7 shows examples of recovery trajectories for businesses and households following the Kobe earthquake and Fig. 2-8 shows the spatial is one of the simulation results which includes simulated recovery of households, businesses, buildings, and lifeline network. The general predictions that lifeline recovers fastest, household and businesses lag on recovery process, building recovered to only the level of 0.5 after 5 years are reasonable in reality. Visualization is also considered in Miles' work which is the least explored area by current researchers. A custom geo-visual interface was designed. The advantage of visualization is to represent the hyper-dimensionality and complexity of community resilience in an efficient, manageable and comprehensive way.

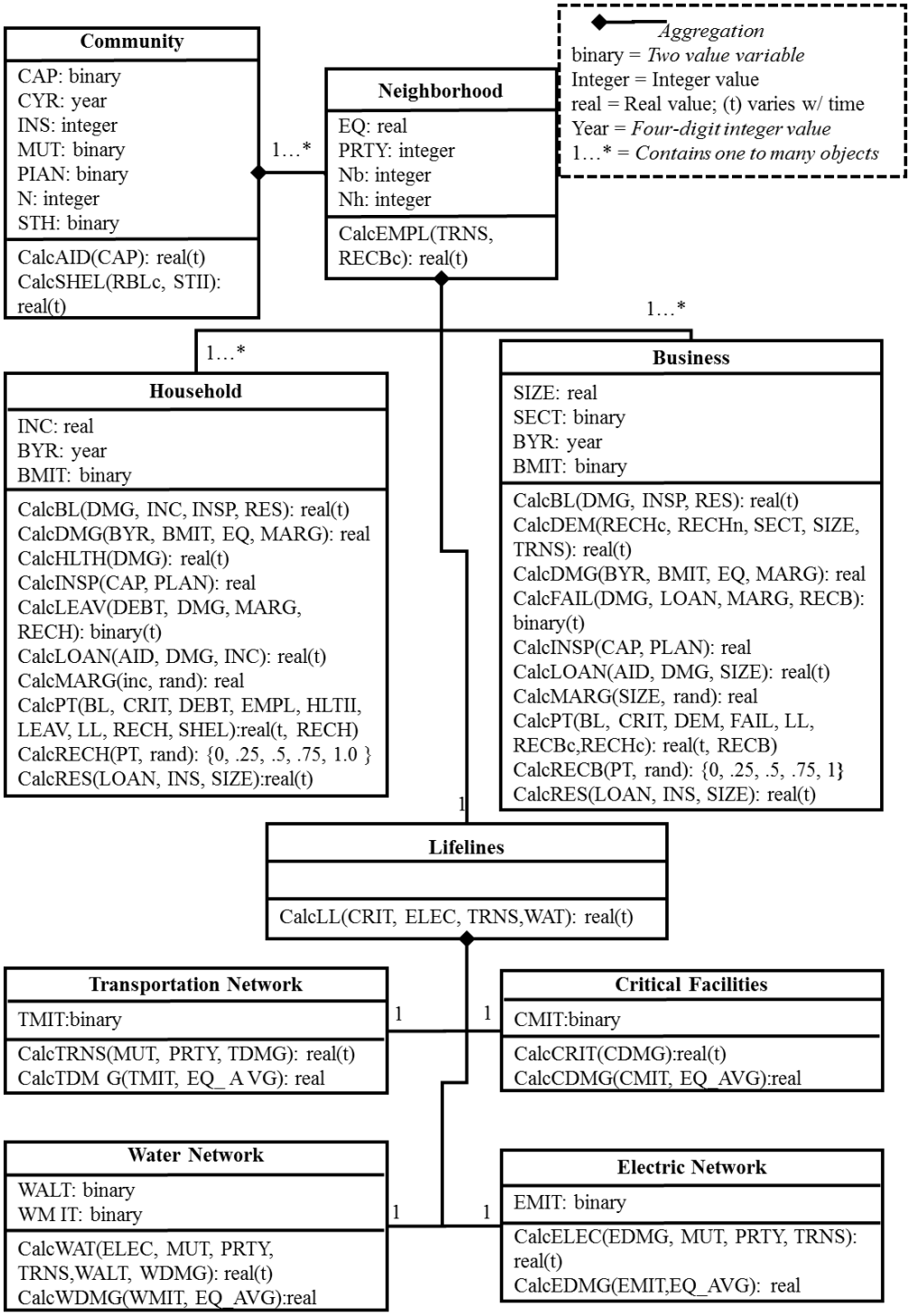

Fig. 2-6. Main objects in conceptual model. The three parts of each box respectively indicate the object's name, attributes and behaviors or functions (adapted from Miles and Chang, 2006)

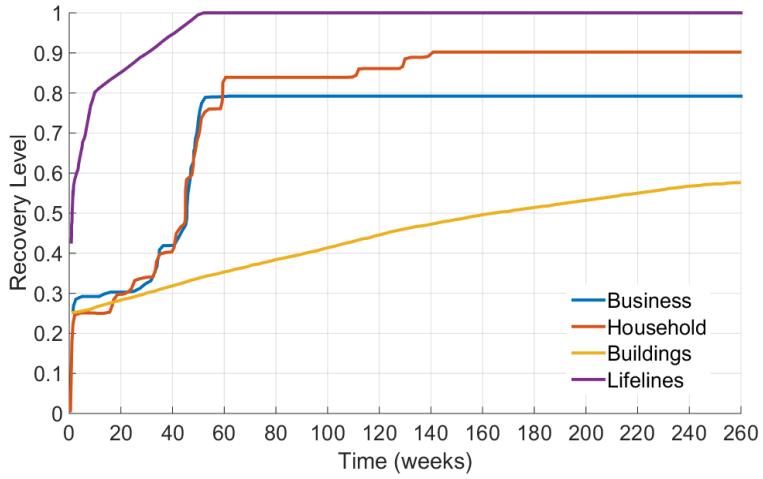

Fig. 2-7. Simulated recovery of businesses, households, buildings and lifelines following the Kobe earthquake (adapted from Miles and Chang, 2006)

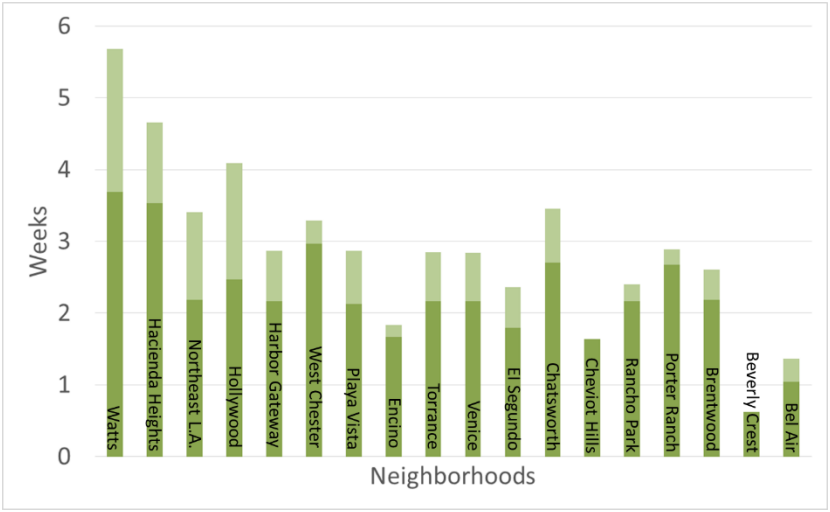

Fig. 2-8. Spatial variation of recovery following the 1994 Northridge earthquake (adapted from Miles, 2014)

Grinberger and Felsenstein (2014, 2015a and b, 2016) used *ABM* to simulate the economic welfare consequences of disaster recovery. The change in the value of residential and non-residential properties is evaluated at the income-group scale to inform the differences in the ability of different social classes to cope with disasters. A conceptual representation of the simulation architecture used to construct the *ABM* is illustrated in Fig. 2-9. A detailed spatial database of the urban environment is integrated with an urban dynamics simulation model to inform land-use dynamics and population flows. Macro-level post-disaster outcomes are governed by agent-citizens who function as residents, consumers and producers, their environment (residential and commercial buildings) and the rules that govern their spatial behavior. The urban dynamics simulation model is separated into supply and demand sides.

On the demand side, the agents comprise of individuals and households, who interact with their environment by making three types of decisions: (1) the number and location of out-of-home activities and path taken between them, (2) workplace decisions and (3) relocation and migration decisions, which includes population flows within and between urban areas. On the supply side, environmental entities (buildings and census tracts) are subject to changes (land-use, housing price) based on the shock of the hazard event or the collective behavior of agents. For example, a commercial building can be converted to housing because of change in population demands. The model is applied to a case study of an earthquake in Jerusalem, where the urban setting consists of two major commercial spaces with adjacent residential districts. Building damage is described using a resilience score, which is determined based on the earthquake magnitude, distance from the epicenter and the number of stories. Buildings receiving a resilience score below a minimum threshold, are assumed to be demolished. Fig. 2-10 shows an example results from the case study, showing recovery trajectories for the residential building stock and its average value. Other relevant results include the spatial distribution of turnover (change in ownership) rates average household income.

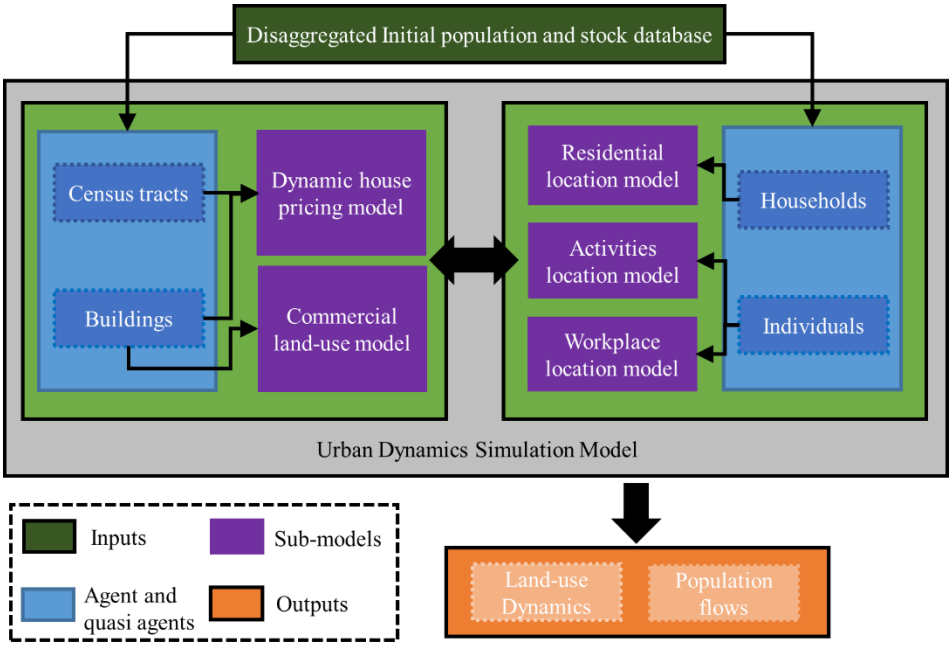

Fig. 2-9. Conceptual representation of architecture of simulation model (adapted from Grinberger and Felsenstein, 2016).

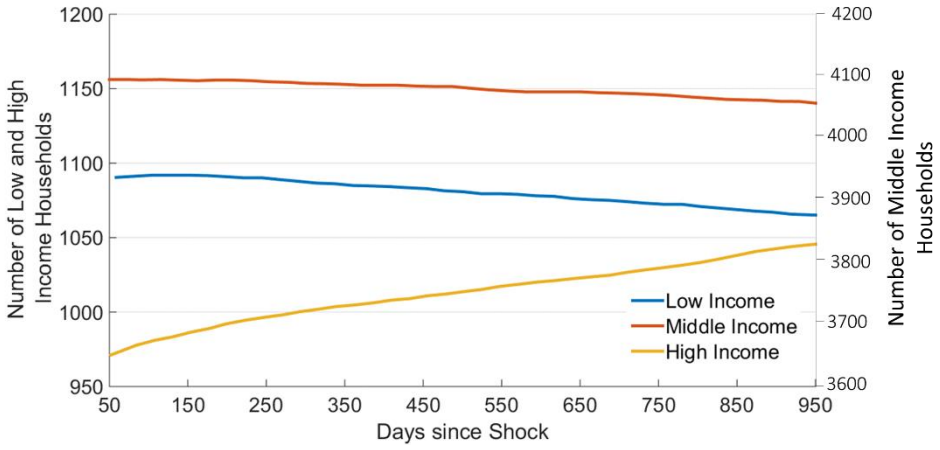

(a)

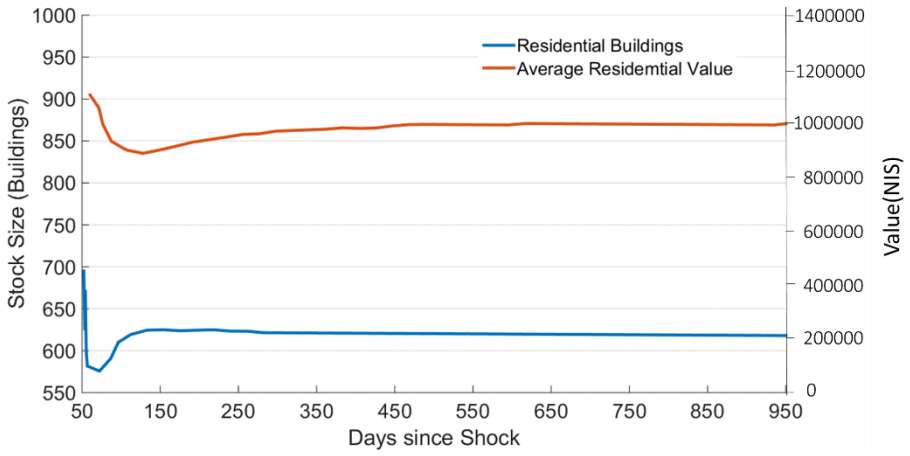

(b)

Fig. 2-10. Recovery trajectory of (a) the residential building stock (number of buildings) and (b) their value (adapted from Grinberger and Felsenstein, 2016).

2.5 Stochastic Simulation Models

Stochastic simulation modeling is a sampling-based computational method that is used to generate realizations of random variables that vary spatially, temporally or both. The recovery of different social (households, businesses, communities) and constructed physical systems (buildings and lifelines) can be described using discrete states that change with space and time. As such, stochastic simulation models can be used to represent different disaster recovery processes Two types of stochastic simulation models can be used to quantify recovery trajectories of built infrastructure and social systems: discrete-time, state-based models and time-based models (Mishalani and Madanat, 2002). Discrete-time state-based models, such as Markov chains, characterize the probability that the system transitions to a higher (or lower)

recovery state at a given discrete time. Time-based models on the other hand, characterize a probability density function of the time it takes to transition to a higher (or lower) state (also referred to as state duration). In both the time- and state-based models, statistical models can be used to link the parameters that define the probabilistic distributions governing state transition to a set of explanatory variables that are known to affect the transition time (e.g. extent of damage to a building, neighborhood demographics or income).

Some researchers have incorporated stochastic simulation models as a sub-routine within some of the other recovery modeling approaches described in this state-of-the-art review. For example, as noted earlier Miles and Chang (2003, 2006, 2011, 2014) used Markov chains to govern the behavior (state transitions) of households and businesses within an *ABM* recovery simulation platform (ResilUS). In other cases, stochastic simulation is used as the primary modeling technique. Kozin and Zhou (1990) used discrete-state, discrete time Markov processes to model the post-earthquake restoration of the functioning capacity of spatially distributed lifeline systems. The capacity state of the lifeline system as a function of time, $S(t)$, is assumed to take on discrete states $S_1, S_2, \mathrm{K}\ S_M$ at time t following the earthquake. The transition probability, describes the probability of transitioning from a lower to higher recovery state, conditioned on the available resources. Restoration is modeled as a non-decreasing process, where, within a given time interval, the system either stays within the current state or transitions to a higher one. The transition probabilities for all states can be described using a state transition matrix.

Research performed by Bocchini et al. (2012) and Deco et al. (2013) was directed towards developing a probabilistic framework for assessing the seismic resilience of bridges. The "resilience and rapidity" of a bridge subjected to a single seismic event was described using a functionality curve, which is schematically represented in Fig. 2-11. The curve captures the initial loss of functionality at the time of the event and the restoration of functionality during the period following the event. Fragility analysis is used to probabilistically quantify the seismically induced damage which causes the functionality to drop to some residual value. The post-event recovery is subsequently described in two phases. An idle time interval describes the first phase, during which the functionality remains constant with time. The activities preceding the repair of the damaged bridge takes place during this stage. The restoration of functionality to some fraction of the pre-event level occurs during the second phase. The recovery trajectory is described using a six-parameter sinusoidal-based continuous function.

The uncertainty in the overall restoration is considered by modeling these parameters with probability distribution functions, which the authors describe as a parametric representation of a stochastic process. Building on their previous work, Karamalou and Bocchini (2016) developed a framework for capturing the characteristics of the restoration function for various types of bridges with different levels of damage, which considers the availability of resources for carrying out repairs. The simulation-based approach is described in four stages: (1) system definition is used to classify the key components of the bridge, (2) damage-states and the repair activities needed to ameliorate these states are defined for each component, (3) random variables describing the duration associated with each repair task are defined and (4) the restoration schedule for the bridge is defined and implemented.

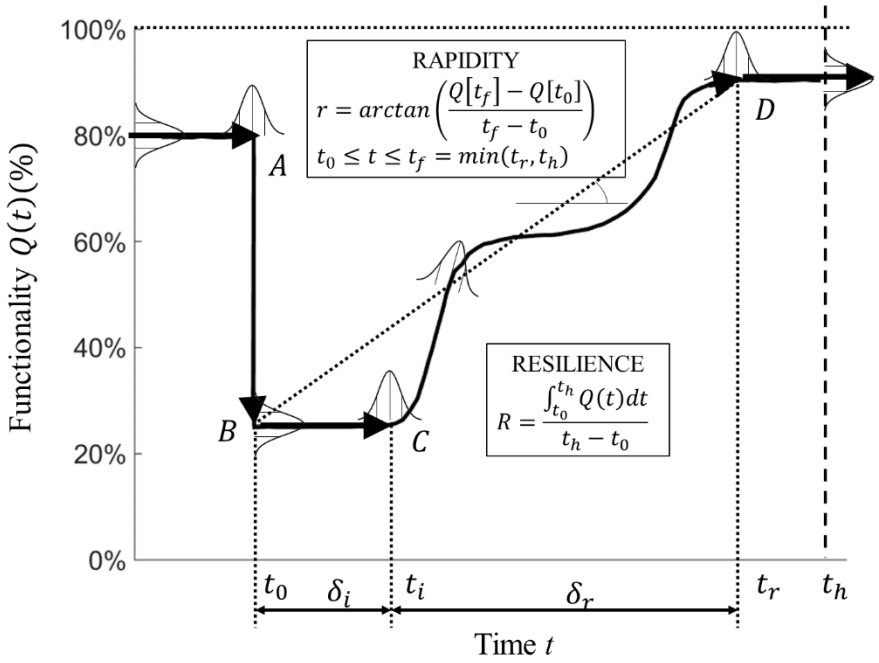

Fig. 2-11. Schematic representation of the seismic "resilience and rapidity" of a bridge (adapted from Deco et al. 2013)

Iervolino et al (2015) also used discrete-state, discrete time Markov processes to model post-earthquake recovery, while accounting for the case where the restoration of functionality is impeded by aftershocks. The overall recovery is simulated by combining two Markov chains: one to represent the process of recovery and another to capture the degrading effect of aftershocks (Fig. 2-12). The analytical formulation of the combined process is described in equation 2.9.

$$Q(t) = q_0 + q_c(t) - \sum_{i=1}^{N(t_0,t)} \Delta q_i \tag{2.9}$$

where $Q(t)$ is the performance level gained at time t during recovery, q_0 is the starting performance level immediately after the mainshock, $q_c(t)$ is the accumulation of recovery effort at time *t*, Δq_i is the degradation in performance caused by a single aftershock, and $N(t_0,t)$ is the total number of aftershocks. The performance function is discretized into *n* states where state *1* represents the highest level of performance and state *n* represents the lowest. The transition matrix for the Markovian recovery process is shown in equation 2.10.

$$\left[P_R(k,k+1)\right] = \begin{bmatrix} 1 & 0 & \Lambda & 0 \\ \Lambda & \Lambda & \Lambda & \Lambda \\ P_{R,(n-1),1}(k,k+1) & P_{R,(n-1),2}(k,k+1) & \Lambda & 0 \\ P_{R,n,1}(k,k+1) & P_{R,n,2}(k,k+1) & \Lambda & P_{R,n,n}(k,k+1) \end{bmatrix} \tag{2.10}$$

Where $P_{R,j,i}(k,k+1)$ represents the probability of transitioning from performance level *j* to *i* between the time interval *k* and *k + 1*. *i* represents a performance level that is equal to or higher than *j*. The zero elements above the principle diagonal indicates that recovery processes can only lead to a higher performance level. The transition matrix used to capture the degradation of functionality due to aftershocks in shown in equation 2.11.

$$[P_E(k)] = \begin{bmatrix} P_{E,11}(k) & P_{E,12}(k) & \Lambda & P_{E,1n}(k) \\ 0 & P_{E,22}(k) & \Lambda & P_{E,2n}(k) \\ \Lambda & \Lambda & \Lambda & \Lambda \\ 0 & 0 & \Lambda & 1 \end{bmatrix} \tag{2.11}$$

where $P_{E,ij}(k)$ represents the probability of transitioning from performance level *j* to *i* between the time interval *k* and *k + 1*. *j* represents a performance level that is equal to or lower than *i*. The zero elements below principle diagonal indicates that aftershocks can only lead to a lower performance level. The combined transition matrix is formulated by applying total probability theorem in equation 2.12 where $\lambda(k)$ is the rate of occurrence of aftershock between time interval k and k+1.

$$[P(k,k+1)] = \lambda(k)[P_E(k)]\left[P_R(k,k+1)\right] + (1-\lambda(k))\left[P_R(k,k+1)\right] \tag{2.12}$$

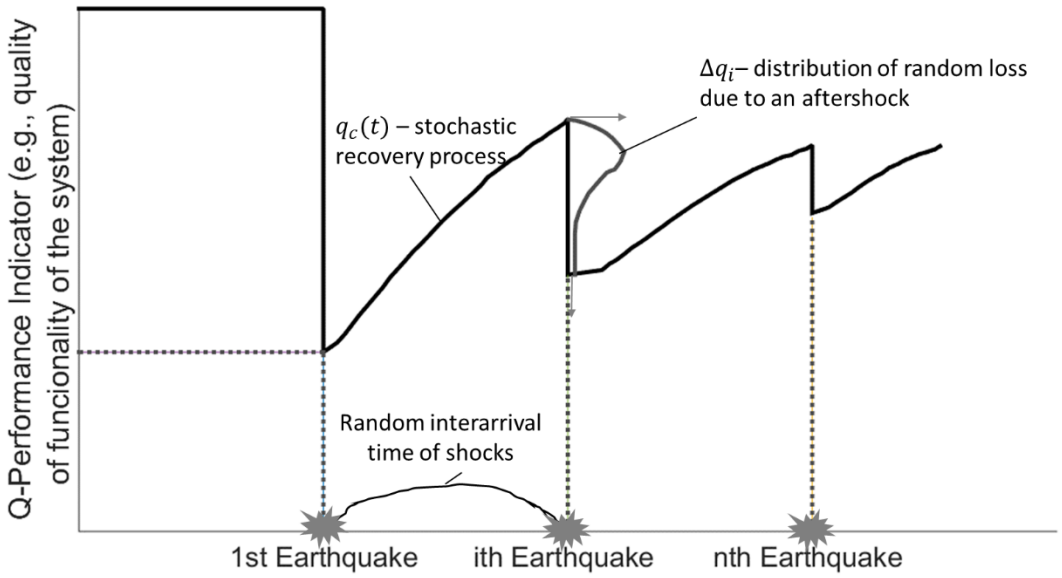

Fig. 2-12. Schematic representation of post-earthquake recovery trajectory affected by aftershocks (adapted from Iervolino et al. 2015)

Burton et al. (2015) used the concept of recovery paths to model the restoration of functionality of earthquake-damaged buildings. The recovery paths are described by discrete functioning states and the time spent within each state. The functioning states represent the changing condition of the building with respect to its ability to facilitate its intended operation. Fig. 2-13 shows a conceptual representation of a recovery path used to model the restoration of functionality of a residential building. Three functioning states are shown: (1) the building is unsafe to occupy (*NOcc*), (2) the building is safe to occupy but unable to facilitate normal functionality (*OccLoss*), and (3) the building is fully functional (*OccFull*). These three states are specific to residential buildings and would need to be redefined for other building types. The Burton et al. framework starts with an assessment of the probabilistic distribution of building-level limit states, which are linked to functionality and recovery (functional loss, unsafe to occupy, irreparable and collapse). Each building-level limit state is associated with a unique recovery path which captures the relevant activities and time spent within each functioning state. For example, a building that is unsafe to occupy immediately after a hazard event must be inspected, building permits acquired and the relevant repairs carried out before it can transition from the *NOcc* to *OccLoss* functioning state. A stochastic time-based approach is used to generate multiple realizations of building-level recovery by sampling from the probabilistic distribution of the recovery paths (which is based on that of the damage states) and temporal parameters (e.g. inspection time, time to obtain permits, repair time). The

trajectory of the expected recovery function (also shown in Fig. 2-13), which is taken as the mean of all realizations, is shown to be influenced by the probability distribution of building-level limit states and the parameters (1st and 2nd moments) that define the probability distribution function of the temporal parameters.

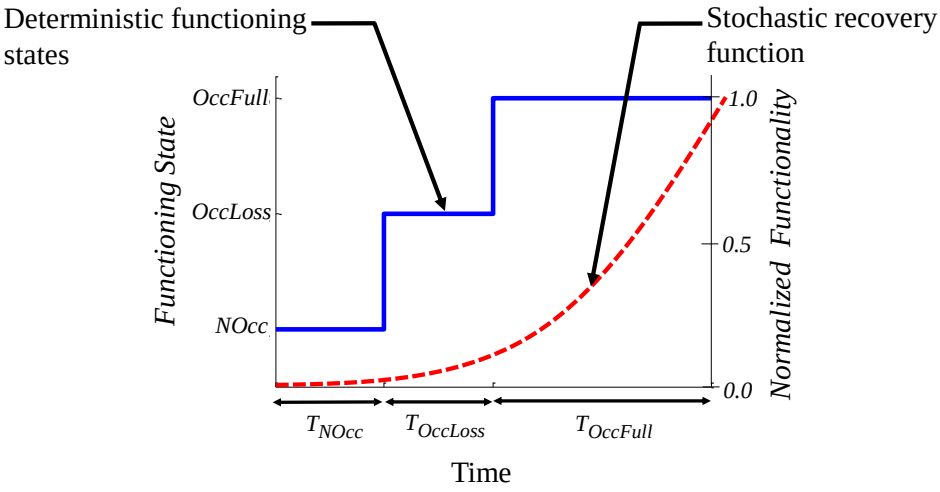

Fig. 2-13. Schematic representation of building recovery path and stochastic recovery function (adapted from Burton et al. 2015)

2.6 Discrete Event Simulation Models

Discrete event simulation (DES) models (Jerry, 1984) represent the behavior of a complex system as a discrete sequence of events which occur at discrete points in time. The core elements *DES* models include entities, attributes, events, resources and time. Entities are used to represent specific objects within the system, which have attributes, experience events and consume resources over time. Attributes are a set of features that are specific to each entity, the accumulation of which defines the state of that entity at any given point in time. Events are occurrences that can affect the state of an entity and resources are objects that provide services to entities. In the context of a disaster recovery model, entities are used to represent the various physical and social systems within a community. The recovery of functionality during the period following a hazard-event is represented as state-changes within these entities, which are brought about by different restorative actions and events, many of which require human and financial resources. The state-changes can be modeled as deterministic and stochastic.

Cagnan et al (2004, 2006, 2007) used *DES* to model the recovery of electric power following an earthquake in Los Angeles. The model includes an assessment of the seismic hazard, damage and loss of functionality of the physical infrastructure, and restoration of

service. The seismic hazard is described in terms of the spatial distribution of peak ground acceleration resulting from some pre-defined earthquake scenario. Using the appropriate fragility functions, the damage model is used to characterize the physical damage and loss of functionality in high-voltage transmission substations. For the restoration model, *DES* is used to keep track of the state-changes of key components within the electric system during the period following a scenario earthquake. Transmission substations and power plants are modeled as entities. Plant operators, damage assessment teams, and repair teams serve as the resources. The maim events in the *DES* model include the initial inspection, damage assessment, repair and re-energizing of key components. The level of physical damage and functionality of various entities define the state of the system. The *DES* model was applied to Los Angeles Department of Water and Power (LADWP) high-voltage transmission network to study the process of restoring power after major earthquakes. The model was based on a collection of qualitative and quantitative damage and recovery data from the Northridge earthquake, *LADWP's* emergency response plan, interviews with *LADWP* personnel and tours of the facility. Results from the study include (1) restoration curves showing the percentage of customers with restored power, (2) the spatial variation of power rapidity, which describes the full probability distribution of all possible combinations of percentage of customers and durations (Fig. 2-14) and (3) an evaluation of the adequacy of available *LADWP* stored material and restoration crews. Xu et al. (2007) extended the Cagnan et al. model to determine the inspection, damage assessment and repair schedule that is needed to optimize the post-earthquake restoration of the electric power system. The average power outage time for each customer was used as the objective function and genetic algorithms were used to obtain the optimal schedule.

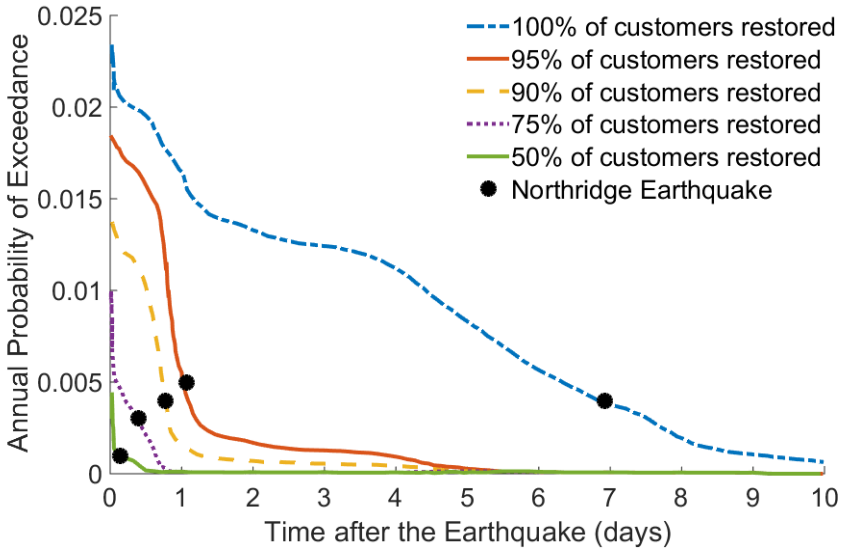

Fig. 2-14. Rapidity risk curves for the LADWP electric power system (adapted from Cagnan et al. 2006)

Another direct extension of the Cagnan et al. framework is the work by Tabucchi et al. (2006, 2007, 2008) and Brink et al. (2009), in which *DES* is applied to model the restoration of *LADWP's* water supply system. The Tabucchi et al. model uses the Graphical Iterative Response Analysis of Flow Following Earthquakes (GIRAFFE) (Shi, 2006╬,(Wang, 2006)) software platform to estimate the effects of earthquake ground shaking on the serviceability of the water distribution network. Like the Cagnan et al. model, the results include service restoration curves, spatial distribution of restoration and an assessment of material and crew usage. Tabucchi et al. (2010) used the Tabucchi et al. model to investigate strategies for reducing the duration of post-earthquake restorations including (1) maximizing groundwater pumping, (2) connecting raw emergency water storage to reservoirs and (3) rationing water use.

Luna et al (2011) also applied *DES* to model the post-earthquake recovery of water distribution systems. The *DES* model is divided into four modules including damage simulation, capacity loss, resource estimation and resource allocation (Fig. 2-15). In the damage simulation module, the spatial distribution of damage state probabilities for pipes within the network is received as input and realizations of damage are generated as output. The realizations of pipeline damage states are used as input for the resource estimation module, which determines the amount of resources required (material, labor, equipment etc.). The resource allocation module is used to prioritize the application of resources needed to restore the functionality of the water distribution system. The restoration activities are performed based

on the prioritization rules established in the resource allocation module. The methodology was applied to the trunk network of the Tokyo water distribution system. The damage probabilities for the trunk lines were obtained from a prior study. Recovery curves describing the percent of customers with restored service as a function time following the earthquake were developed.

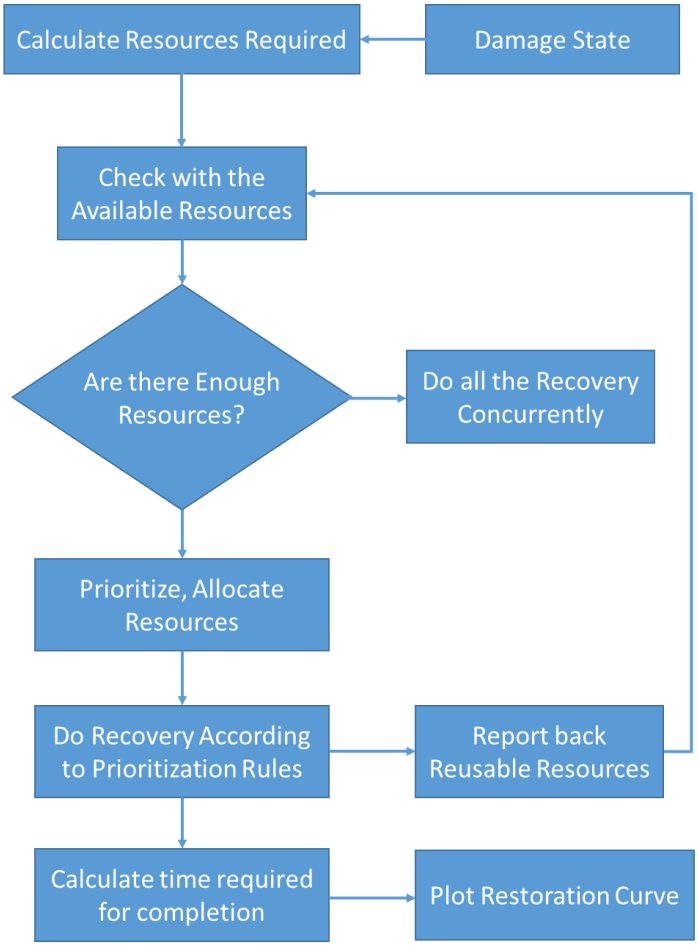

Fig. 2-15. Flow chart of simulation steps (adapted from Luna et al. 2011)

Kang and Lansey (2013) also developed a *DES* post-earthquake recovery model for water distribution systems. The overall approach was very similar to the Luna et al. model. The main steps include (1) identifying the damage state of key components, (2) calculating the required resources, (3) prioritizing resources, (4) performing recovery activities based on prioritization rules, (5) calculating system serviceability and (6) generating the restoration curve. System serviceability is defined using a serviceability index which describes the ratio of available water demand to required water demand. The model was applied to an unidentified study network consisting of nodes, reservoirs, pumping-stations and pipes, which supplies water to a primarily residential district. The generated results include system restoration curves and mapped spatiotemporal distributions of system serviceability.

Huling and Miles (2015) described how *DES* can be used to develop a comprehensive model of disaster recovery. A flowchart for the *DES* model is shown in Fig. 2-16. It starts with a definition of the modeling environment which includes (a) the entities and their attributes, (b) the events that are used to bring about state-changes in the entities and (b) the resources that are needed to perform specific recovery activities. Stakeholders such as homeowners, business owners or governmental organizations, all of who compete for resources needed for recovery, are represented as entities within the *DES* model. Recovery resources can be physical (e.g. building materials), human (e.g. construction workers) and financial (e.g. FEMA grant funds). Sequential, durational events are used to advance various recovery processes. An example of the sequence of events needed to restore the functionality of a damaged household include securing finances needed for repairs, acquiring a building permit, hiring contractors and completing the repairs. A prototype *DES* model was developed for a single recovery phenomena of homeowner reconstruction. The model was constructed using the Python programming language and the SimPy (Simulation for Python) library. The simulation results include assessments of the time needed to complete building inspections, acquire a loan and complete repairs.

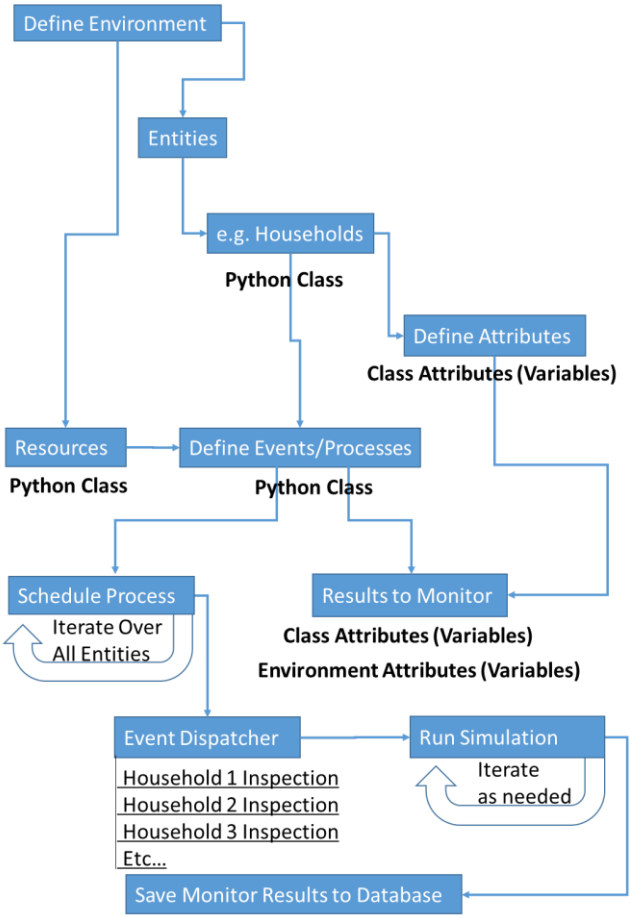

Fig. 2-16. Flowchart of DES creation in a Python environment (adapted from Huling and Miles 2015)

2.7 Network Models

Network models are used to characterize the interactions of objects within complex systems. Such systems are mathematically described using a graph structure in which vertices (or nodes) are used to represent the objects and their interactions are captured using edges (or arcs). Network models have been used to simulate the response of physical, biological, social and information systems whose overall behavior is dominated by interacting entities. Nojima and Kameda (1992) develop a network model of post-earthquake restoration of lifeline systems. A directed graph, which contains supply and demand nodes, was used to represent the configuration of the lifeline system. The performance or functionality of the network is described using metrics such as the supply-to-demand node connectivity or the supply serviceability level. Taking $h_j (j = 1,2,\Lambda\ ,n)$ as the number of users linked to a particular demand node v_j and T_j as the time after an earthquake, the restoration level, $R(T_j)$ (Fig. 2-17) is described using the following equation.

$$R(T_j) = \sum_{\sigma(k) \le \sigma(j)} (h_k / \sum_{i=1}^{n} h_i) \tag{2.13}$$

where $\sigma(j)$ is the position number assigned to each node in the recovery sequencing. The reconnection of all demand nodes to their supply nodes signifies the completion of the recovery activity of the network.

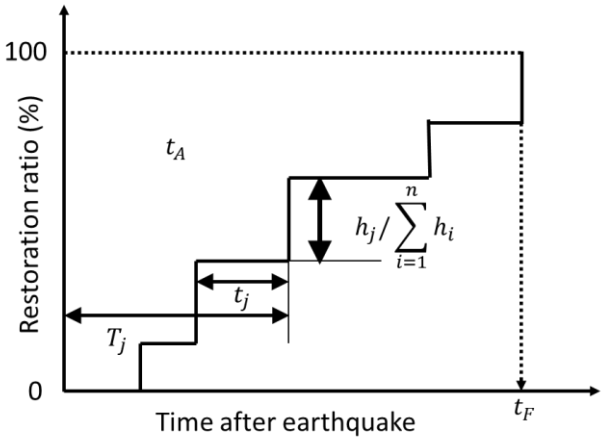

Fig. 2-17. Formulation of restoration curve (Adapted from Nojima and Kameda, 1992)

Shinozuka et al (1992) used a network model to formulate a repair strategy for gas networks. Shortest path analysis was used to determine the sequence of restoration of various components within the network. Didier et al. (2015) used a network model to simulate post-earthquake recovery of a community and its electrical power supply system. The social systems (houses, businesses etc.) within the community are viewed as the demand nodes and the electric systems as the supply nodes. The loss of resilience (LOR) during the period following an earthquake, which is conceptually represented in Fig. 2-18, is analytically described as

$$LOR = \int_{t_0}^{t_f} \langle D(t) - S(t) \rangle dt \tag{2.14}$$

Where $D(t)$ is the demand and $S(t)$ is the available supply. t_0 is the starting time of occurrence of disaster and t_f is the end of time when both demand and supply system recovered to the level before disaster happens. The recovery trajectory for the individual components that make up the social and physical systems within the community is described by a time-dependent recovery probability distribution conditioned on the damage state of that component. The methodology is applied to a virtual community comprising an electric power supply and distribution system and other social and physical entities. The subsystems that make

up the electrical grid, including the supply and distribution states are explicitly defined. However, the other physical (buildings) and social entities (homes, businesses) are aggregated at each demand node. The Weibull and Lognormal probability distributions are used to describe component-level recovery. Two types of recovery assessments are performed: scenario-based assessment and probabilistic seismic hazard analysis (PSHA) based assessments. Plots of *LOR* versus moment magnitude were generated for the scenario-based assessment while the results of the *PSHA*-based assessment were described in terms of the mean annual frequency of exceeding a particular *LOR.*

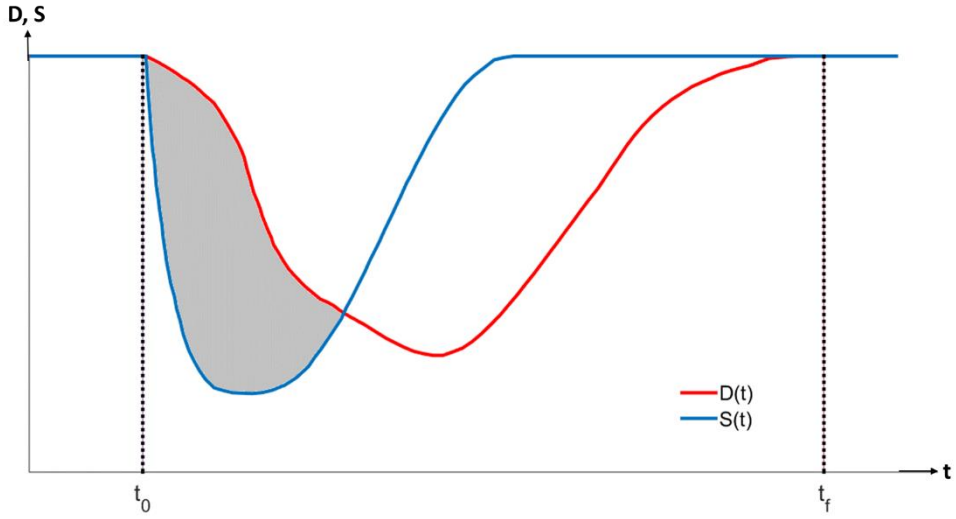

Fig. 2-18. Loss of Resilience of EPSS (adapted from Didier et al. 2015)

2.8 Summary and Conclusion

This chapter presented a review of the literature on disaster recovery modeling of socio-technical systems. The review is organized around the mathematical formulations and simulation frameworks that are used to represent those dynamic processes that are perceived to most affect the recovery-outcome, based on the (social or built infrastructure) system and metric of interest. However, the reviewed studies also vary in terms of the social and/or built infrastructure (technical) system and recovery-metric of primary interest, the availability and use of data from past disasters, the visualization of results and the extent to which the models were validated and tested.

2.8.1 Summary of Modeling Approaches

Within the engineering community (and as reflected in this review), the modeling approaches that have been developed are primarily focused on predicting the recovery of built

infrastructure systems that are impacted by a hazard event. This includes both the physical restoration of key the key components that comprise the system as well as its functionality. It is therefore not surprising that the earliest efforts to model disaster recovery were primarily focused on explicitly capturing these repair and replacement activities needed to restore system functionality and the effect of available resources on the time it takes to perform these activities. This is a defining characteristic of the resource-constraint model developed by Isumi et al. (1985), which, based on this review, is the first documented attempt to model disaster recovery of built infrastructure (water, power and gas) systems. Simple analytical equations were used to describe the restoration of each utility service based on the number of damaged components, the time to repair each component and the availability of workers to conduct the repairs. Later, studies by Ballantyne, Whitman et al. (HAZUS), Chang et al. would adopt and build on this approach. occurs during a major hazard event. The main improvements to the Isumi et al. model came from the use empirical data from subsequent earthquakes to inform key assumptions. As part the MCEER resilience framework, Cimellaro et al. proposed a resource-constraint-type modeling approach in which simple analytical functions were selected based on the level of preparedness and availability of resources to support recovery.

An early alternative to the resource-constraint model was the use of statistical curve fitting to develop regression models in which the dependent variable is a measure of (or activity that influences) the recovery-outcome of the considered system. Examples of such dependent variables include the time to (full or partial) recovery and categorical decision-outcomes that affect the recovery. The explanatory variables used to construct the regression models are based on observable and measurable factors that are assumed to affect the recovery outcomes. The earliest statistical curve fitting models (ATC-25) incorporated only a single explanatory variable such as the level of component and/or system damage. More recent curve fitting models are reflective of the availability of larger datasets and more advanced statistical models (including machine learning algorithms). The more recent models (e.g. Liu et al., Han et al. and Nateghi et al.) incorporate a large (relatively speaking) number of predictor variables. It should be noted that resource-constraint can be incorporated in curve fitting models through the inclusion of the appropriate explanatory variables. Only a couple of studies (by the same author) on predicting recovery-decision outcomes using regression models (Nejat et al.). Regression models have also been used to examine the factors that influence recovery (Zhang et al.).

More recently, the recovery modeling community has adopted more advanced techniques such as agent-based modeling and discrete event simulation. These two techniques are well-suited to disaster recovery modeling because of their ability to incorporate detailed representation of large numbers of processes (and sub-processes) and the interaction between agents/entities. The most comprehensive, currently-available model of disaster recovery, ResilUS (Miles and Chang), was developed using agent-based modeling. ResilUS can represent the recovery of households, neighborhoods and businesses including the effect of lifeline damage and restoration and the availability of resources. However, it should be noted that, because of the "all-encompassing" nature of the model, the recovery processes for each of these agents is somewhat simplistically represented. The agent-based recovery model developed by Grinberger and Felsenstein is also fairly comprehensive. It captures the restoration of the residential and commercial building stock, households and businesses. It also incorporates a dynamic pricing model that captures the temporal evolution in residential and commercial property value. Agent-based models have also been used to model the decisions and interactions of homeowners and insurance companies following a disaster (Nejat).

Most of the discrete event simulation recovery models have been used to capture, with a great level of detail, the restoration of utility service provided by lifeline systems (eater, power gas). The models capture the damage, inspection, and scheduling and performing the repairs to the individual components that comprise the lifeline system (Cagnan et al., Xu et al. Tabucchi et al., Brink et al., Luna et al. and Kang and Lansey). The effect of available resources for conducting repairs can also be explicitly considered in discrete event simulation recovery models. In some cases, the discrete event simulation models have been used to schedule the various recovery activities to optimize the restoration of system functionality (Xu et al., Tabucchi et al. Huling and Miles developed a discrete event simulation recovery model that, like previous models developed by one of the authors, captured the recovery of businesses, households and neighborhoods including the effect of available resources.

Stochastic simulation has been shown to be effective for capturing the uncertainty associated the temporal evolution of the discrete states that a system takes on (Mishlani and Madanat). As such, this technique is well-suited for modeling disaster recovery of socio-technical systems. Various types of stochastic models such as time- and state-based models have been used as the main recovery simulation technique (Kozin and Zhou, Bochini et al., Deco et al. and Burton et al.) or incorporated as part of a larger framework such as agent-based modeling or discrete event simulation (Miles and Chang). A somewhat unique application of

stochastic simulation that as found in the literature was the development of a conceptual model to represent the effect of both restoration (e.g. repair) and degrading (aftershocks) events (Iervolino et al. 2015).

The strong emphasis that is placed on capturing the interdepdence and interactions of spatially distributed entities (either between components in a single type of systems or across different systems) makes network models suitable for representing disaster recovery. The earliest application of network models in the context of disaster recovery was to simulate the restoration of functionality of spatially distributed lifeline systems (Nojima and Kameda, Shinozuka et al.). In addition to predicting restoration outcomes, these models were used to establish the optimal sequence of repairs to the damaged components within the network. More recent applications of network models attempt to capture the interactions of social systems (businesses and households) and lifelines (Didier et al.). the predicted recovery-outcomes are based on the difference in supply (utility service provided by lifelines) and demand (homes and businesses). The restoration lifeline (electrical) functionality is explicitly represented using time-dependent probability distributions (e.g. Weibull Functions) defined at the component level. However, the other social and physical systems are aggregated into a single entity and represented in a somewhat simplistic manner.

It is clear from the review of the literature that the recent works on disaster recovery modeling have adopted more advanced simulation techniques such as agent-based and network models and discrete event simulations. As noted earlier, the strength of these techniques lie in their ability to explicitly model the complex interactions of multiple entities. While agent-based and network models and discrete event simulations are computationally expensive (relatively speaking), the increased availability and manageable costs of advanced computing platforms make them feasible. Stochastic simulation can be embedded in these three techniques to ensure the rigorous treatment of uncertainties for key variables. Statistical curve fitting models are unable able to explicitly model the dynamic processes of recovery and system and sector interactions. It is also more difficult to transfer these models from one location to the next. However, they are still useful in cases where key recovery processes are not well understood. In fact, one can envision a hybrid simulation approach in which the well-understood processes are modeled using *DES, ABM* or networks and the less-understood processes represented using regression models.

2.8.2 Summary of Socio-Technical Systems Considered

The earliest models of post-disaster restoration were developed for lifeline systems including water, power and gas networks. These models were primarily used to predict the recovery of the utility service provided by these networks. Even today, the overwhelming majority of studies on modeling post-disaster restoration are focused on lifeline systems. Besides lifelines, there have been studies that have solely focused on modeling the recovery of housing. Models have been developing for simulating the recovery of only the residential building stock, while others, in additional to the physical infrastructure, have incorporated socio-economic metrics of recovery such as property value and health of household. Businesses and commercial buildings has been included as part of more comprehensive models focused on multiple sectors but have not been the primary focus of any of the recovery modeling studies. A couple of very recent studies have had as their sole focus, modeling the restoration of bridges.

2.8.3 Limitations of Current State of the Art

Recovery modeling is ultimately an empirical science. While it is possible to develop theoretical frameworks to describe and measure disaster recovery, the uniqueness and place-based nature of each disaster is such that simulation models will always be data driven. The data-needs of disaster recovery models vary based on the system or sector being represented and simulation technique. For modeling the restoration of functionality of built infrastructure systems, information on repair sequencing, task durations, availability and use of resources and organizational structures is critical. For socioeconomic metrics of recovery, longitudinal studies on the health and wellbeing of affected populations (e.g. household and businesses) is needed. Information on the drivers of key recovery-related decisions is needed for all systems and sectors. This includes the decisions of stakeholders (e.g. households and businesses) as well as local, state and federal officials tasked with managing the recovery process. Currently, the lack of data is one of the main challenges facing the recovery modeling community. While there are almost always efforts to gather empirical information following major disasters around the world, there are currently no systems to support the proper capture, curation, search, sharing and storage of this data. The general scarcity data is also reflected in the fact that very few studies on validation (particularly cross-validation) and testing of recovery models can be found in the literature.

A major challenge in creating an effective recovery model is capturing the interaction between (or interdependence of) the different social and built infrastructure systems or even

economic sectors that support community functionality. For example, if the focus is on simulating housing recovery, the modeler must decide how to incorporate the effect of lifeline systems as well as other economic sector that can influence housing recovery. The dynamic process within these other systems and sectors can be implicitly or explicitly represented. Explicit representation refers to when a process is directly represented in the mathematical formulation of the simulation environment. Implicit representation uses empirical rules and judgements to capture effect of a process on the recovery outcome of interest. Having a comprehensive recovery model makes it somewhat easier to consider interactions, however, these models often deal with individual sectors in a simplistic manner. Ultimately, the primary objective of the recovery model should inform how and if specific systems and sectors are incorporated. However, more work is needed to develop systematic procedures for modeling the interdependence and interactions of the various entities within a recovery mode. This is particularly relevant to single-system or single-sector recovery models that require careful characterization of the boundary conditions which reflect the influence of those systems, sectors and processes not explicitly represented in the simulation environment.

Because of the broad spatiotemporal distribution of the entities and processes that are represented, recovery-modeling outcomes are often described using large datasets. Providing easily digestible visual access of this data is key to effectively communicating the results of recovery simulations. Most of the studies review in this chapter utilize a recovery curve which shows time on the horizontal axis and some measure of functionality on the vertical axis. Some authors use GIS maps to illustrate the spatial variation of impacts at specific time-points (most immediately following the hazard-event). Miles (2014) illustrated how customizable, arrayed geo-visual interfaces can be used to support decisions for enhancing disaster recovery. However, more efforts are needed to develop visualization tools that can be used to communicate compelling stories of both simulation- and empirical-based disaster recovery.

CHAPTER 3: Recovery-Based Limit State Assessment of Residential Buildings

This chapter is partly based on the following publication:

Burton, H. V., Miles, S. B., and Kang, H. (2018). "Integrating performance based engineering and urban simulation to model post-earthquake housing recovery," *Earthquake Spectra* (accepted for publication).

3.1 Building Performance Limit States that Inform Post-Earthquake Recovery and Functionality of Residential Communities

This study is built on the premise that quantifying the long-term impact of a major earthquake event on a residential community requires an assessment of building performance in a manner that can be explicitly linked to recovery decisions and actions. Metrics related to functionality, inhabitability and repairability have been identified as key to understanding and modeling the relationship between building performance and the earthquake-induced socioeconomic disruption of communities (Poland et al. 2009; Burton et al. 2015). As such, the spatiotemporal distribution of building limit states that capture these metrics can be directly linked to policy-level decisions and other mitigation or recovery interventions.

A probabilistic assessment of four discrete "recovery-based" building performance limit states is a key step in the proposed recovery modeling methodology. Each limit state is related to a unique combination of decisions and actions needed to restore residential building functionality (Fig. 3-1). The first limit state, *functional loss* (*LS1)*, refers to the condition where the building is structurally safe, occupiable and accessible but has *experienced service disruptions* (e.g. electricity, water, elevator). The building is considered fully functional when these services are restored. The *uninhabitable (LS2)* limit state is used to represent a building that is either *inaccessible or unsafe to occupy* following an earthquake due to structural and/or non-structural damage. Repair of safety- and accessibility-related damaged components is needed to make the building inhabitability and functionality is restored with the reestablishment of lost services. A building that is damaged to the extent that repair becomes technically or economically infeasible, necessitating demolition and replacement is represented using the *irreparable* limit state *(LS3).* The *collapse (partial or complete)* limit state *(LS4)* also

triggers complete building replacement and is also relevant to incorporating the effect of injuries and fatalities on household recovery.

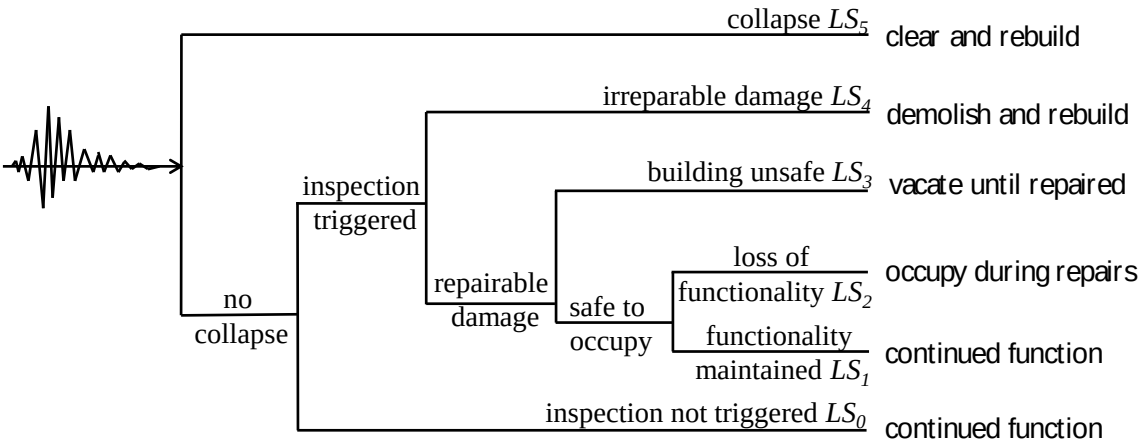

Fig. 3-1. Event tree showing link between building performance limit states and recovery actions

3.2 Performance-Based Assessment of Recovery-Based Limit States

The current framework uses fragility functions to link earthquake shaking intensity to the probability of exceeding each of the building performance limit states described in the previous section. These fragility functions for individual buildings can be developed using performance-based assessments, which combine hazard characterization, structural response simulation and component-level damage assessments (Burton et al. 2015). Fragility functions for the collapse and irreparable limit states can be obtained through statistical analysis of engineering demand parameters (EDPs) generated from nonlinear structural response simulation. Collapse is defined as the point of dynamic instability where a small increase in the intensity of the ground motion would result in an unbounded increase in the drift demands on the structure (Haselton et al. 2011). In previous studies, residual drifts have been used as the primary measure of the point at which structural damage renders a building irreparable (Ramirez and Miranda 2012). However, observations from prior earthquakes have shown that demolition can also be triggered by direct economic losses that exceed the limit set by insurance providers triggering full-value pay-out (Marquis et al. 2017). Fault tree analyses have been used as the basis for evaluating functional loss (Porter and Ramer 2012) incorporating both structural response simulation and component-level damage assessment. Ideally, this type of assessment will also need to model the disruption to utilities caused by off-site damage (Burton et al. 2015). Computational approaches to assessing the post-earthquake safety and occupiability of damaged buildings also combine structural and damage analyses (Mitrani-Reiser et al. 2016).

A typology of index buildings can be established and evaluated using the previously described methodologies to develop generalized fragility functions for the building inventory within a target region for the purpose of recovery modeling.

3.3 Mapping from Loss-Based Damage States to Recovery-Based Limit State Fragility Functions

Risk modeling platforms such as HAZUS (FEMA 2012) and OpenQuake (Silva et al. 2014) use damage fragility functions that relate earthquake ground shaking intensity to building damage. These "loss-based" damage states are used to compute direct economic losses that result from having to repair or replace damaged buildings. The damage states, which include slight, moderate, extensive and complete damage, are classified based on construction type and described in terms of the type and extent of physical damage to the building. Recognizing the potentially insurmountable computational expense involved in doing performance-based assessment of index buildings, a second but supplemental approach to establishing the fragility functions for the recovery-based limit states is proposed. In this alternative approach, fragility function parameters from the loss-based damage states are mapped to those of the recovery-based limit states described in the previous section. There is an obvious correlation between these two types of building performance descriptors. Both are discrete, sequential and mutually exclusive with the higher states being associated with more extensive damage. This link will be used as the basis for mapping the fragility function parameters between them. The methodology will be illustrated using woodframe single- and multi-family residential buildings. A detailed description of the loss-based limit states for this building type (also classified as light woodframe construction) is presented in Section 5.3.1 of HAZUS.

The first step in the mapping process is estimating the conditional probability of being in a recovery-based limit state $(RBLS)$ given the occurrence of a loss-based damage state $(LBDS)$. $P(RBLS = rbls_i \mid LBDS = lbds_j)$ is the probability that recovery-based limit state i occurs given that loss-based damage state j has been observed. To illustrate the procedure, engineering judgement-based estimates of these conditional probabilities for woodframe single and multi-family buildings are shown in Table 1. They were obtained by examining the descriptions of loss-based damage states provided earlier and inferring the likelihood that this type of damage would trigger each of the four (*LS1* through *LS4*) recovery-based limit states. More representative estimates can be obtained from heuristic data using techniques such as the

Cooke's method (Cooke 1991), which can be used to harvest expert opinions on the probabilistic relationship between these two types of limit states. The conditional probabilities can also be computed directly from field observations following an earthquake by categorizing observations of building damage in terms of both the loss- and recovery-based states. In Table 1, each row provides the probability of being in each of the recovery-based limit states given the occurrence of the loss-based limit state in the first column of that row. For example, it can be observed that for a building that is in the loss-based limit state corresponding to moderate damage, the probability of being in recovery-based limit states LS*1* and *LS2*, is 0.75 and 0.20 respectively with a zero probability of being in *LS3* and *LS4.* Given that the recovery-based limit states are mutually exclusive and collectively exhaustive, each row must sum to one.

Table 3-1. Example of conditional probabilities used to map fragility parameters for loss-based damage to recovery-based limit states

Loss-Based Damage States	$P(RBLS = rbls_i \mid LBDS = lbds_j)$				
	LS0 Fully Functional	*LS1* Loss of Functionality	*LS2* Unsafe to Occupy	*LS3* Damaged Beyond Repair	*LS4* Collapse
None	1.00	0.00	0.00	0.00	0.00
Slight	0.20	0.80	0.00	0.00	0.00
Moderate	0.05	0.75	0.20	0.00	0.00
Extensive	0.00	0.20	0.40	0.30	0.10
Complete	0.00	0.00	0.00	0.20	0.80

In HAZUS, the fragility function that describes the conditional probability of exceeding loss-based damage state j is log-normally distributed and defined by the median $\left(\bar{S}_{d,lbds_j}\right)$ and log-standard deviation $\left(\beta_{d,lbds_j}\right)$ of the spectral displacement demand. Using these parameters, the probability of being in a particular loss-based damage state conditioned on come spectral displacement demand $P(LBDS = lbds_j \mid S_d)$ is calculated as the difference in the probability of exceeding consecutive states. This, combined with the conditional probability estimates in Table 3.1 can be used to compute the probability of occurrence of a particular recovery-based limit state conditioned on the spectral displacement demand $P(RBLS = rbls_i \mid S_d)$by applying the total probability theorem:

$$P(RBLS = rbls_i \mid S_d) = \sum_{j=1}^{n_{lbds}} P(RBLS = rbls_i \mid LBDS = lbds_j) \cdot P(LBDS = lbds_j \mid S_d) \qquad (3.1)$$

where n_{lbds} is the total number of loss-based damage states. The probability of exceeding a particular recovery-based limit state $P(RBLS = rbls_i \mid S_d)$ is taken as the sum of the probabilities of occurrence of all limit states equal to and greater than i.

$$P(RBLS > rbls_i \mid S_d) = \sum_{i}^{n_{rbls}} P(RBLS = rbls_j \mid S_d) \tag{3.2}$$

where n_{rbls} is the total number of recovery-based limit states. The median spectral displacement, $\bar{S}_{d,rbls_i}$ and dispersion $\beta_{d,rbls_i}$ for the recovery-based limit state fragilities can be obtained by applying the maximum likelihood method to the conditional probabilities of exceedances computed in Equation 3.2. Fig. 3-2 provides a comparison of the recovery- and loss-based fragility functions for light wood frame buildings with high-code seismic design.

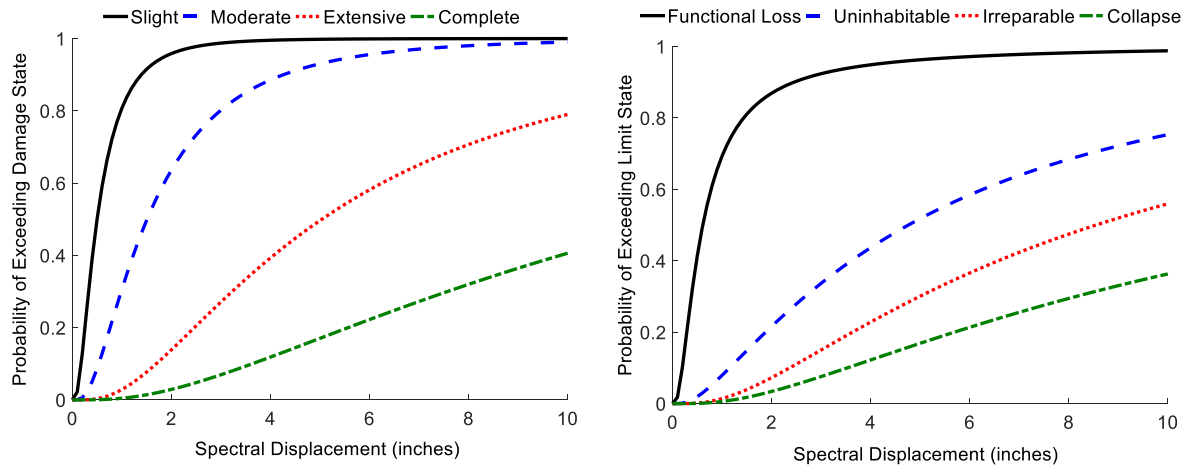

(a) (b)

Fig. 3-2. Fragility curves for (a) loss-based and (b) recovery based limit states for light wood frame buildings with high-code seismic design (building type description based on HAZUS)

CHAPTER 4: Stochastic Process Models of Post-Earthquake Recovery

This chapter is partly based on the following publication:

Kang, H., Burton, H. V., and Miao, H. (2018). "Re-Enacting the Recovery Following the 2014 South Napa Earthquake Using Stochastic Process Models," *Earthquake Spectral* (accepted for publication).

4.1 Overview

This chapter presents the development of stochastic-process models of post-earthquake recovery. Purely-empirical as well as simulation-based models are developed. For the "empirically-based" model, the temporal parameters are sampled from an assumed probability distribution with parameters that are calibrated using data from past recovery events. The simulation-based models explicitly consider the effect of resource-constraints (e.g. availability of contractors) on the time to complete specific recovery processes. Building damage, permitting and repair data from the 2014 South Napa Earthquake are then used to evaluate the proposed models. Damage data was obtained for 1470 buildings and permitting and repair-time data was obtained for a subset (456) of those buildings. A "blind" simulation is shown to adequately capture the shape of the recovery trajectory despite overpredicting the overall pace of the recovery. Using the mean time-to-permit and repair time from the acquired dataset significantly improves the accuracy of the recovery simulation. A generalized simulation model is formulated by establishing statistical relationships between key time parameters and endogenous and exogenous factors that have been shown to influence the pace of recovery.

4.2 Empirically-Based Stochastic Process Models of Post-Earthquake Recovery

Stochastic process models are used to represent different types of discrete and continuous phenomena that randomly evolve in space and/or time. The recovery of social (households, businesses, communities) and built (buildings and lifelines) infrastructure systems following an earthquake can be described using discrete states that, with a great degree of uncertainty, change with space and time making stochastic process simulation models useful for representing different disaster recovery processes. In this study, two types of discrete-state stochastic simulation models are used to quantify recovery trajectories for damaged buildings:

discrete-time, state-based models and time-based models (Mishlani and Madanat, 2002). Discrete-time state-based models, such as Markov chains, characterize the probability that the building transitions to a higher recovery state within a discrete time interval conditioned on a set of explanatory variables such as the extent of damage to the building, neighborhood demographics or, in the case of residential buildings, household income. Time-based models on the other hand, characterize a probability density function of the time it takes to transition to a higher recovery state (also referred to as state duration) given the same explanatory variables. The formulation of both models starts with defining the discrete states that capture the recovery trajectory. The recovery states can be selected based on the entity that is being represented and the information that is available to characterize these states within the simulation environment. In previous studies, recovery states for buildings have been characterized based on damage (Miles and Chang, 2003), loss, functionality (Burton et al. 2015) and recovery activities (Burton and Kang, 2017).

Fig. 4-1 shows a conceptual recovery path that describes the repair/reconstruction of a damaged building using the states described earlier, which are based on the issuance of construction and completion permits. The continuous stochastic recovery function is also shown in Fig. 4-1. The basic assumption is that there is a probabilistic relationship between the various exogenous and endogenous factors described earlier and the time spent in each state. Additionally, the sequence of state transitions for a given recovery path is pre-determined and based on the order in which the activities that comprise the recovery path will occur. The variables used to construct the discrete state probabilistic models include the cumulative continuous recovery level, $Q(t)$, the vector of observed explanatory variables, $\overline{X}$, and the discrete state of the building, $Y(t)$, at time t, measured from the time of the earthquake. The time spent within state i is denoted by T_i. The time spent in the *PreCon*, *Con* and *Com* states is denoted by T_{PreCon}, T_{Con} and T_{Com} respectively. Since the recovery is modeled as a stochastic process, T_i is a random variable. After establishing the discrete states associated with a recovery path, the discrete-time state-based model is constructed as a series of independent Poisson processes, each with their own mean rate of occurrence. Given the current time, t_i, the probability of transitioning out of state i to the subsequent state $i+1$ at some future time $t_i + \Delta$ is the probability of $i+1$ occurring at time $t_i + \Delta$ conditioned on state i being

observed at time t_i. This conditional probability, $P(t_i < T < t_i + \Delta \mid T > t_i)$, is described using the following equation.

$$P(t_i < T < t_i + \Delta \mid T > t_i) = \frac{P(t_i < T < t_i + \Delta)}{P(T > t_i)} = \frac{F(t_i + \Delta) - F(t_i)}{1 - F(t_i)} \tag{4.1}$$

where $F(t_i) = 1 - e^{-\lambda_i t_i}$ is the CDF of the exponential distribution. The mean rate of transitioning from the current state is $\lambda_i = \frac{1}{\mu_i}$, where the mean time to complete the activities involved in that state, μ_i, can be obtained from empirical data from past earthquakes. Substituting the exponential CDF into Equation 4.1 produces the following functional form for the transition probability which is used in the state-based model:

$$P(t_i < T < t_i + \Delta \mid T > t_i) = 1 - \frac{e^{-\lambda_i (t_i + \Delta)}}{e^{-\lambda_i t_i}} \tag{4.2}$$

For the time-based model, the uncertainty in the duration of each recovery state is (e.g. time to acquire construction permit, repair time) is considered by randomly sampling the duration T_i. Monte Carlo simulation is used for both the time- and state-based models to generate multiple realizations of the recovery path. For the state-based model, a single realization of a recovery path is generated by randomly sampling the state at incremental points in time using the transition probabilities from equation 4.2. For the time-based model, a single realization of a recovery path is constructed by randomly sampling the duration of each recovery state using their associated exponential distribution parameters. The extension of the discrete-state (time- and state-based) probabilistic models to include the explanatory variables can be achieved by developing a statistical model in which $\overline{X}$ is the vector of independent variables and μ_i (or λ_i) is the dependent variable.

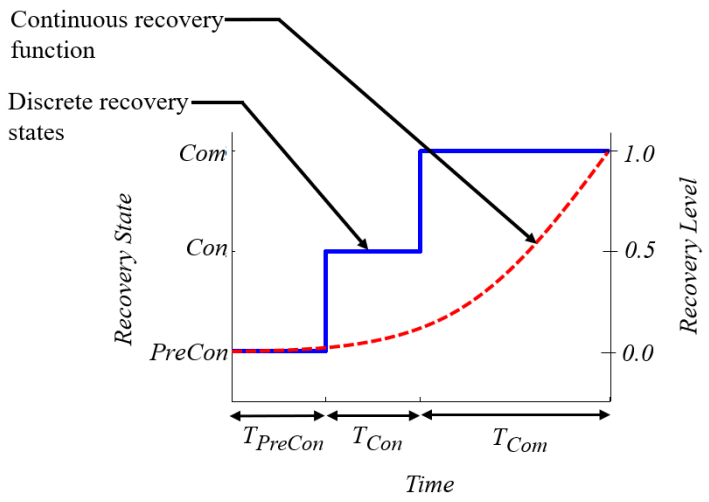

Fig. 4-1. Conceptual representation of stochastic process modeling of building-level recovery using discrete states derived from on the issuance of construction and completion permits

4.3 Simulation-Based Stochastic Process Models of Post-Earthquake Recovery

The simulation-based model captures the spatiotemporal distribution of building recovery states, occupancy, household decisions and recovery-related resources at the jurisdictional scale and is more explicit in its representation of the housing recovery process and interactions with other actors (e.g. building department, lifelines, insurance companies). Examples of such relevant housing recovery processes include building inspection and damage assessment, permitting, acquisition of finances and repair and reconstruction. The probabilistic durations of these processes, which are also related to the time spent in the recovery states described earlier, can be obtained either using the empirically-based stochastic process model, their inclusion in the simulation environment or a combination of both i.e. some processes simulated, while others are based on theoretical probability distributions. Note that the empirically-based representation is more reliant on observations and curated data from past events. The simulation-based approach is less dependent on data but requires detailed knowledge of the recovery process.

Given the spatial distribution of residential building damage within a jurisdiction, the process of inspecting each residence can be operationalized in a simulation environment. Key inputs for the simulation model include the number of inspection teams, their work schedule (e.g. number of hours per day) and the sequencing and duration (including travel time) of inspections. The outcomes of this simulation include the time it takes for each building to be inspected, which, again, is directly related to the recovery state durations, and the utilization of resources over time. Note that the inspection process can be affected by other factors (e.g.

disruption of transportation network, emergency activities). These factors can be addressed through their explicit inclusion in the simulation model or by applying impedance factors to the inspection duration parameters.

Other recovery processes such as permitting, financing and repair and reconstruction, can also be operationalized within the simulation environment. The permitting process can be modeled using a queuing algorithm that captures the order in which the building department processes permits, the time it takes to process each permit and the available resources (the capacity of the building department). A similar algorithm can be used for the repair and reconstruction process where, after obtaining the necessary financing, each building that needs repairs, enters a queue. The main inputs include the number of contractors available to perform repairs, the capacity (number of teams) and work-schedule of each contractor and the number of work-hours needed to repair or replace the building. The process of acquiring financing for repairs is influenced by multiple actors (household, bank loans, insurance, local and federal aid) and will be more difficult (compared to the other processes) to operationalize. The simulation model will need to consider the amount of savings available within the household to finance repairs. In cases where insurance, bank loans or local or federal aid are sources of financing, explicit knowledge of the application and approval mechanisms is needed to simulate these sub-processes.

4.4 Replicating the Recovery Following the 2014 South Napa Earthquake Using Empirically-Based Stochastic Process Models

4.4.1 Introduction

The M_w 6.0 South Napa earthquake struck on August 24, 2014 and caused damage to buildings and lifeline systems in the cities on Napa, American Canyon and Vallejo. With an epicentral location at N 38.22 W 122.13, approximately 8 km south-southwest of Napa, the event produced peak ground accelerations as high as 0.61g (GEER, 2014). There were two fatalities and three hundred injuries (PEER, 2016). More than 2,000 structures, mostly residential buildings, suffered damage that could be characterized as moderate to severe (PEER, 2016). The economic loss from the earthquake in the affected region is estimated to range from $500 million to $1 billion (PEER, 2016).

The damage to woodframe residential buildings was primarily the result of two well-understood seismic vulnerabilities: unbraced chimneys and unbraced, unbolted cripple wall

foundations. Chimney damage ranged from minor cracking and spalling of bricks to complete collapse. Numerous cases of partial and complete collapse of cripple wall foundations were observed. Although less prevalent than chimney and cripple wall damage, there were also recorded cases of damaged gas lines and collapsed carports (FEMA, 2015). Structural and non-structural damage to commercial buildings triggering yellow or red tags was the primary cause of business disruption in downtown Napa. Structural damage occurred in older buildings with unreinforced masonry and non-ductile concrete frames. Various types of non-structural and content damage were observed including broken storefront glazing, façade damage and broken sprinkler pipes (FEMA, 2014). The earthquake directly impacted approximately 50 wineries with damage that included broken wine bottles, collapsed wine-barrel stacks and buckled tank walls (PEER, 2016; FEMA, 2014).

The earthquake caused varied levels of damage and disruption to transportation (road and bridges) and utility (water distribution, sewer and electric power) systems. The city of Napa benefitted from the redundancy in the water supply system. As such, despite damage to pipelines and storage tanks, there was minimal disruption to potable water service. Wastewater treatment operations was disrupted for about 3 days due to the flow of spilled wine into major sewers. Damage to various components within the electricity distribution system (e.g. pole transformers, overhead wires and conductors) resulted in power outage. However, power was restored to the overwhelming majority of customers within 24 hours of the earthquake. Damage to bridges and roads were mostly minor and did not have a significant lasting impact on vehicular traffic (FEMA, 2014).

The disruptive effects of the earthquake on households and businesses throughout Napa and Solano counties were primarily a result of onsite structural and non-structural damage to buildings. As noted earlier, while there were utility service interruptions, these were restored within a few days after the earthquake occurred. Following any major hazard event, the ability of affected households and businesses to make progress towards recovery depends on several factors including the availability of financing, the general economic conditions and the presence of effective disaster management systems in the affected region (Wu and Lindell, 2014).

Previous researchers have advocated and demonstrated that pre-impact planning can have a major net positive impact on both short and long term disaster recovery outcomes (Wilson, 1991; AGCI, 1996; Wu and Lindell, 2004). While most current disaster risk models

focus on quantifying immediate probable impacts (NIST, 2010), the growing emphasis on urban resilience has spurred the development of simulation models for quantifying post-event recovery of the built infrastructure (e.g. buildings and lifelines) and the social systems (housing, businesses etc.) that they support. Several simulation techniques have been employed in modeling post-earthquake recovery (reconstruction and restoration) including resource constraint models (Isumi et al., 1985; Ballantyne and Taylor, 1990; Whitman et al., 1997; Chang et al., 1999; Cimellaro et al., 2010), statistical curve fitting (Wu and Lindell, 2004; Liu et al., 2007; Han et al.,2009; Zhang and Peacock, 2009; Nateghi et al., 2011; Nejat and Ghosh, 2016), agent-based modeling (Nejat and Damnjanovic, 2011; Miles and Chang, 2003, 2006, 2011, 2014; Grinberger and Felsenstein, 2014, 2015, 2016, 2017), discrete event simulation (Cagnan et al., 2004, 2006, 2007; Xu et al., 2007; Tabucchi et al., 2007, 2008, 2010; Luna et al., 2011; Kang and Lansey, 2013; Huling and Miles, 2015), stochastic process simulation (Kozin and Zhou, 1990; Deco et al., 2013; Karamlou and Bocchini, 2016; Iervolino and Giorgio, 2015; Burton et al., 2015; Burton and Kang, 2017) and network modeling (Nojima and Kameda, 1992; Shinozuka et al., 1992; Didier et al., 2015). Most studies have focused on modeling the restoration and/or reconstruction of specific built infrastructure systems such as lifelines (Isumi et al., 1985; Ballantyne and Taylor, 1990; Liu et al., 2007; Han et al., 2009; Nateghi et al., 2011) and buildings (Wu and Lindell, 2004; Zhang and Peacock, 2009; Burton et al., 2015; Burton and Kang, 2017). Other studies incorporate both the social and built infrastructure systems within specific economic sectors such as households and businesses (Nejat and Damnjanovic, 2011; Miles and Chang, 2003, 2006, 2011, 2014; Grinberger and Felsenstein, 2014, 2015, 2016, 2017; Nejat and Ghosh, 2016). However, due to a general lack of available data, very little work has been done to validate and test these simulation models. The proposed recovery model can assist policy-makers, municipal governments, and planners in understanding and acting upon necessary solution alternatives for enhancing community resilience. The general approach is extendable to other disasters, such as hurricane and floods.

In this case study, stochastic process simulation models are used to re-enact the recovery of the damaged building stock following the 2014 South Napa earthquake. According to Haas et al. (1977), disaster recovery comprises three phases: (1) the emergency phase immediately after an event, (2) the restoration period when damaged property and utilities are made operable to some degree, and (3) the reconstruction phase when community resources, such as housing stocks, are rebuilt. The recovery model presented in this chapter is primarily focused on simulating the reconstruction phase. The study serves two purposes. First, the

modeling technique is evaluated by comparing recovery predictions with empirical data on building repair and reconstruction following a real earthquake. Secondly, the empirical data is used to update the simulation model for application to future earthquakes, recognizing the inherent place- and event-specific nature of the model.

4.4.2 Description of Study Region and Key Data

A building damage dataset for the city of Napa was obtained from the Earthquake Engineering Research Institute (EERI) clearinghouse website (http://eqclearinghouse.org/map/2014-08-24-south-napa/). 1470 damaged buildings are included in the dataset, which contains several types of building-specific information that are relevant to this study including location (address, latitude and longitude), occupancy type, post-earthquake inspection date, ATC-20 (1995) placard (yellow and red) and a brief description of the damage caused by the earthquake. Of the 1470 buildings, 14% have commercial occupancy and 86% are residences. 90% of the 1470 buildings were assigned yellow tags and the remaining 10% were red-tagged. For the residential buildings that were assigned yellow or red tags, about half had chimney damage and about 10% had damage to the foundations (mostly cripple wall damage). Other types of damage to residential buildings included damaged fireplace, stucco cracking and front porch collapses. Damage to commercial buildings was more varied when compared to residential buildings (e.g. brick facia separated from building structure, floor buckling, collapse of masonry wall). Fig. 4-2 shows a map of the city of Napa with the location of the damaged buildings and the epicenter of the earthquake. The map is divided into five zones, which are labelled north, south, east, west and center. The markers identifying the individual buildings are color-coded to indicate the ATC-20 post-earthquake inspection tag (yellow and red). The map shows that the damage was widespread, extending from the Browns Valley District in the west to as far east as Shurtleff neighborhood. Additionally, while much of the damage was concentrated in the southern and center zones (e.g. Downtown, Central, Fuller Park), the damage extended as far north as the Springwood Estates neighborhood. The percentage of red-tagged buildings in the center, eastern, northern, southern, and western zones is 14%, 11%, 3%, 9%, and 5% respectively.

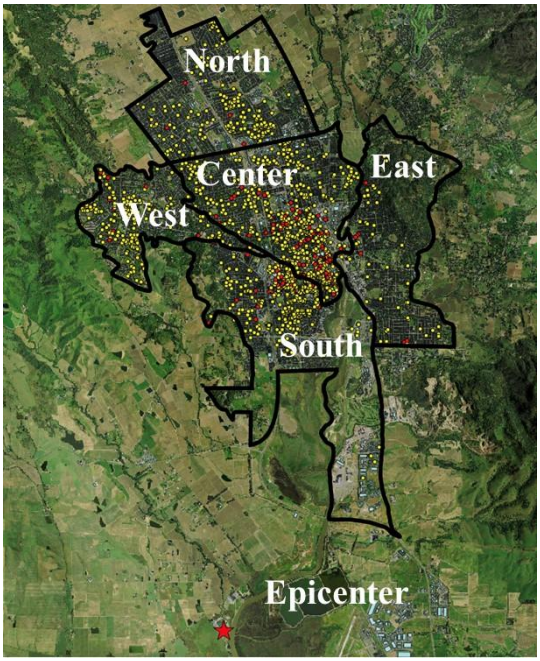

Fig. 4-2. Map of Napa showing the spatial distribution of building damage based on the assigned ATC-20 inspection tags

Previous empirical research on disaster recovery has shown that physical factors related to a building (e.g. age, construction type, level of damage), socioeconomic factors related to the property owners (e.g. access to financing for repairs) and the scale of damage in a particular jurisdiction, can have an impact on the repair/reconstruction time for damaged buildings (Zhang and Peacock, 2009; Comerio, 2010). Later in the paper, statistical models are formulated that link the various recovery time parameters to explanatory variables that are related to these exogenous and endogenous factors. Additional building and census-level data acquired as part of this study, are used to construct these statistical models. The number of stories and estimates of the floor area of the buildings contained in the dataset were obtained from Google Maps and Google Street View. This information was used to account for the size of the building when estimating repair/reconstruction times using statistical models. Information on year of construction, property value and floor area for individual buildings was obtained from Zillow (http://www.zillow.com/) and Homesnap (http://www.homesnap.com/): two online real estate database companies.

The sociodemographic characteristics included in the regression models described later are chosen based on a review of previous studies on the factors that affect the pace of disaster recovery. For example, a study by Zhang and Peacock (2009) found that disaster housing recovery trajectories are strongly correlated with household income, tenure (renter or owner

occupied) and the percentage of ethnic minorities in a community. Another study by Elliott (2014) found that tenure, the education level and number of children in a household are highly correlated with disaster recovery. Based on the findings of these and other researchers, the following sociodemographic factors, which were obtained from census data (https://www.census.gov/), are assigned to individual buildings and used in the models described in Section 4.2:

1 Percent of households where they speak English (PH_ENGLISH)
2 Percent of the population 25 years and over that have at least a regular high school diploma (PHS_DIPLOMA)
3 Percent of the total population that is Hispanic or Latino (PHISLAT)
4 Percent of the total population that is Black or African American (PAFRICAN)
5 Percent of the total population that is Asian (PASIAN)
6 Percent of households with no presence of people under 18 years (PH_NO18UNDER)
7 Per capita income in the past 12 months (INCOME)
8 Percent of occupied housing units that are owner occupied (PHU_OWNED)

4.4.3 Classification of Building Damage Using HAZUS States

The stochastic process recovery simulation methodology described in Burton et al. (2015), which is adapted as part of this study, requires an assessment of the spatial distribution of building damage for the scenario earthquake of interest. The outcome of this assessment is each building being assigned a discrete damage state. As described in Burton et al., these damage states should ideally be characterized in a manner that is explicitly linked to post-earthquake functionality and recovery (e.g. functional loss, unoccupiable, irreparable). However, the dataset that is being used for this study does not include information on the functionality or occupiability of the damaged buildings. As such, the damage states described in HAZUS (FEMA 2015), which are primarily used for quantifying earthquake-induced economic losses, are adopted for the recovery model described in Section 4.2. Based on the description of damage included in the dataset, each building is assigned one of the four HAZUS damage states (slight, moderate, extensive and complete). This subjective exercise involves matching as best as possible, the damage descriptions from the field inspection with the description of one of the four HAZUS damage states, which is categorized by building construction type. A few examples of the damage classification are presented in Table 4-1, which includes the field

inspection damage description, ATC-20 Tag, and the assigned HAZUS damage state and description. Based on the classification that was performed for the full dataset (1470 buildings), 21.9%, 63.4%, 9.5% and 5.2% of buildings are in the slight, moderate, extensive and complete damage states respectively. Fig. 4-3 shows the spatial distribution of damage based on the HAZUS damage states. The building markers are color-coded green, yellow, orange and red to represent the slight, moderate, extensive and complete damage states respectively.

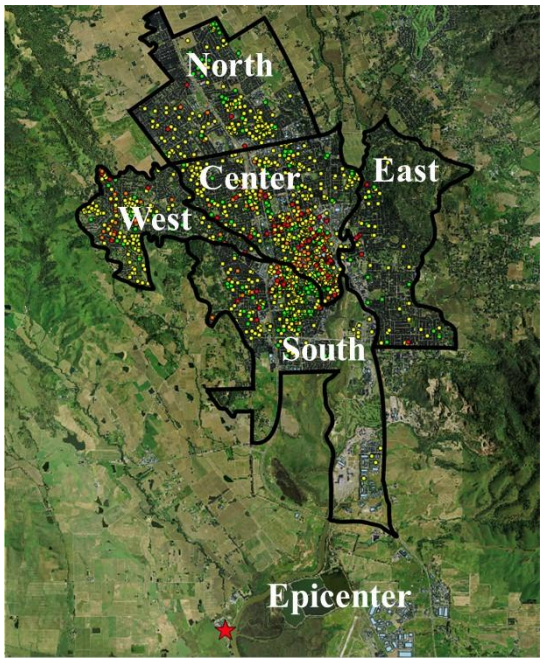

Fig. 4-3. Spatial distribution of building damage using HAZUS classifications

Table 4-1. Examples of HAZUS damage state classifications for buildings included in the dataset

Building No.	Field Inspection Damage Description	ATC-20 Tag	HAZAUS Damage State Description	HAZUS Damage State
1	Top of brick chimney fell down	Yellow	Toppling of tall masonry chimneys	moderate
2	Racking, cracking and separation of cripple walls; floors uneven/waving; unstable house	Red	Large foundation cracks, some structures may slip and fall off the foundations, and may collapse	complete
3	Minor cracks in chimney; no structural issues; suggest inspect chimney for integrity	Yellow	Small cracks in masonry chimney	slight
4	Numerous wall cracks throughout living room kitchen and dining room; chimney collapsed	Yellow	Large diagonal cracks across wall panels or plywood joints; toppling of most brick chimneys	extensive
5	Collapse imminent	Red	Structural colllapsed occurred or is imminent due to failure of cripple wall or the lateral load resisting system	complete

4.4.4 Developing Observed Building Trajectories

The permit-issue and completion date for repair-work related to the Napa earthquake was acquired for 456 of the buildings (31.0%) included in the damage dataset described earlier. This information was obtained from the online permitting and project review website (http://etrakit.cityofnapa.org/etrakit2/) for the city of Napa. Using these two pieces of information, the time-to-permit is taken as the number of days from the date that the earthquake occurred to the permit-issue date and the repair time is estimated as the number of days from permit-issue to the completion date. 93.6% of the buildings included in the "permit-issue-completion" dataset were assigned yellow tags and 6.4% were red-tagged. 21.9%, 64.0%, 8.6% and 5.5% of buildings in the permit-issue-completion dataset are deemed to have slight, moderate, extensive and complete damage respectively based on the HAZUS damage states. Fig. 4-4 shows histograms of the time-to-permit and repair times. Red-tagged buildings took on average 154 days to be issued a permit and 163 days to be repaired while the mean time-to-permit and repair time for yellow tagged buildings was 98 days and 94 days respectively. The standard deviation of time-to-permit is 97.8 (approximately 63% of mean) and 110.2 (approximately 68% of mean) for red-tagged and yellow-tagged buildings respectively while the standard deviation of the repair time is 105.2 (107% of mean) and 155.1 (158% of mean) respectively.

The two-sample Kolmogorov-Smirnov (KS) test (Massey Jr 1951) is performed on the time-to-permit and repair time data shown in Fig. 4-4 to determine the appropriate probability distribution to be used in the stochastic process model. Based on the observed skewness in the histograms, the Exponential and Lognormal distributions are considered. The null hypothesis for the KS test is that the empirical data follow Exponential and/or Lognormal distributions. The output of the tests is expressed in the form of a *p-value*, which corresponds to the probability that there is a match between the empirical and theoretical distributions. A *p-value* of 5% is used as the acceptable margin. If the *p-value* obtained from the hypothesis test falls below 5%, then the difference between the theoretical and empirical distributions is deemed significant. The results from the KS test showed that, for both the time-to-permit and repair time data, the *p-values* were greater than 5% for the Lognormal and Exponential distributions. Based on this finding, the Lognormal distribution was used to model the recovery state durations in the stochastic process models, which are described later in the chapter.

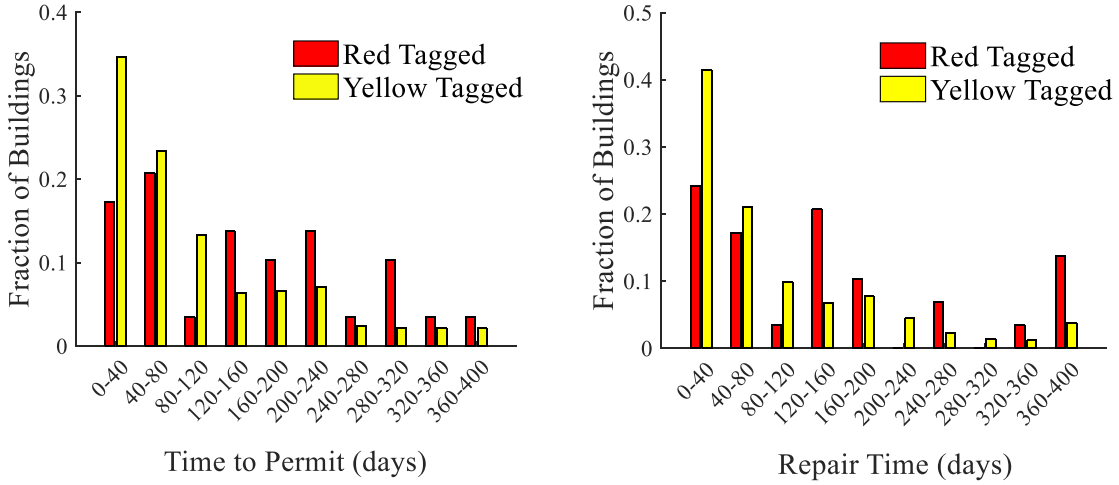

(a) (b)

Fig. 4-4. Histogram of (a) time-to-permit and (b) estimated repair times for buildings in permit-issue-completion dataset

A key objective in this study is to evaluate the efficacy of the stochastic process model in estimating the recovery trajectory of the buildings damaged during the earthquake. This is done by comparing the simulated and observed recovery trajectories, the latter of which is generated using the permit-issue-completion dataset. To establish the observed recovery trajectory, three building-level recovery states are defined. At any given time *t* (days) following the earthquake, a building is described as being in the *pre-construction (Pre-Con)* state if the building permit has not yet been issued. Between the permit-issue and completion date, a building is in the *construction (Con)* state. After the completion permit is issued, the building is in the *completion (Com)* state. We recognize that the issuance of a completion permit may not correspond to the restoration of full functionality or occupancy in the building. However, given the lack of data related to the functionality and occupancy of individual buildings, in this study, the issuance of the completion permit (*Com*) is used as the penultimate recovery state. To facilitate generating the recovery curve, the *Pre-Con* and *Com* states are assigned numerical values of 0 and 1, respectively. The *Con* state was assigned a value of 0 for the red-tagged buildings and 0.5 for the yellow-tagged buildings.

Fig. 4-5 shows the observed recovery trajectory for the 456 buildings in the permit-issue-completion dataset. For this subset of buildings, the general trend is that the reconstruction is rises sharply immediately following until around 300 days from the time of the earthquake, after which the slope of the recovery curve gradually declines towards the tail end. In Fig. 4-6a, the observed recovery trajectory is disaggregated based on the HAZUS

damage states. As one would expect, the recovery generally becomes increasingly slower as the severity of the damage state increases. In fact, the greater the separation between damage states, the earlier bifurcation of the recovery curves. For example, the recovery curves corresponding to the moderate, extensive and complete damage states bifurcate from the slight damage curve at 43 days, 15 days and 7 days following the earthquake respectively. Fig. 4-6a also shows that for the buildings in the complete damage state, the recovery curve is stagnant up to about 50 days following the earthquake. This reflects the fact that the heavily damaged buildings require much longer "lead" times (time for inspection, assessments, acquiring financing etc.) prior to the start of construction. This, combined with the longer repair/reconstruction times, also leads to a longer recovery period. For example, the overall recovery period for the buildings in the complete damage state is 756 days compared to 527 days, 594 days and 666 days for those in the slight, moderate and extensive damage states. It should be noted that, most of the buildings with slight damage had a recovery time that was much less than 527 days. However, for one of the slightly damaged buildings, there was cracking in the chimney and the building was deemed "occupiable". The lengthy recovery time is primarily due to the time it took the building owners to acquire a permit and begin the necessary repairs. Fig. 4-6b shows the recovery curves disaggregated based on the zones identified in Fig. 4-2. It shows that the center zone, which has the highest number of red-tagged buildings in the permit-issue-completion dataset, is the slowest to recover (756 days). The eastern zone has the shortest recovery time, which is consistent with the fact that, within the permit-issue-completion dataset, there are no red-tagged buildings in that zone.

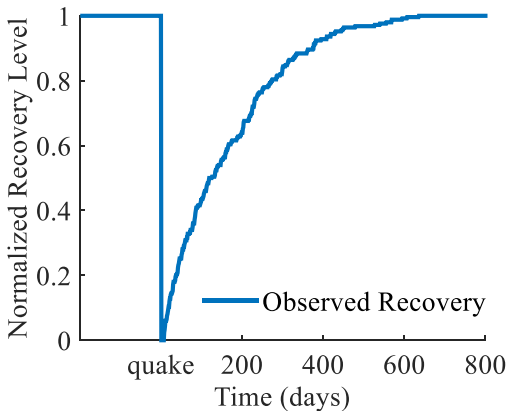

Fig. 4-5. Observed recovery trajectory for all 456 buildings in the permit-issue-completion dataset

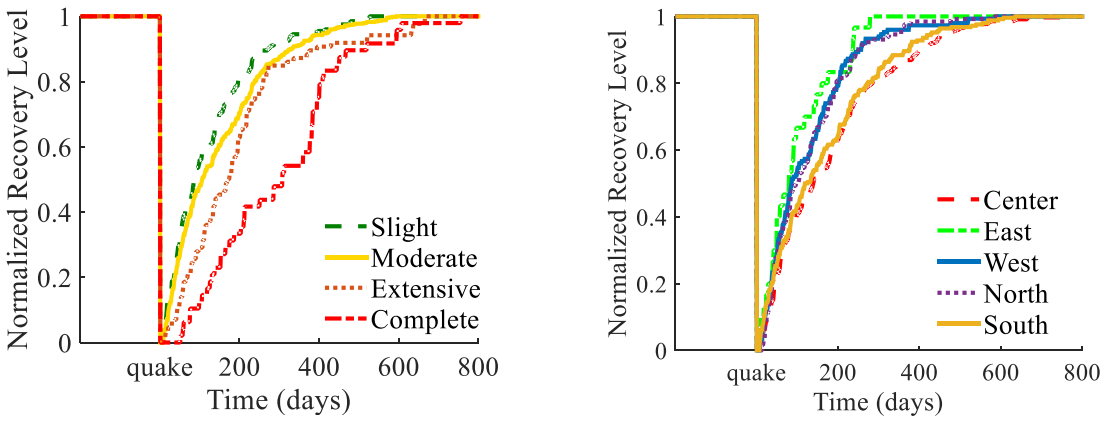

(a) (b)

Fig. 4-6. Observed recovery trajectory disaggregated based on (a) HAZUS damage state and (b) sub-jurisdictions within Napa

4.4.5 Application of the Time-Based Stochastic Process Model

In this section, the time-based stochastic process model is used to recreate the reconstruction of the damaged buildings following the 2014 South Napa Earthquake with two objectives in mind; (a) evaluating the simulation model and (b) formulating a model that can be used to predict recovery trajectories for future earthquakes. The state-based model was also used to generate recovery predictions, however, for brevity, the results are excluded from the paper.

The model is evaluated by performing a blind prediction of the reconstruction trajectory of the buildings in the permit-issue-completion dataset. Note that the term "blind" prediction is used to indicate that the permit-issue and repair times obtained for buildings damaged by the 2014 event were not incorporated. The goal here is to evaluate the model used to simulate recovery trajectory (not the damage simulation model). As such, the observed spatial distribution of damage is used for the blind prediction.

The formulation of the time-based stochastic process model starts with defining the discrete states that are used to describe the recovery path. Tables 15.10 of HAZUS (FEMA 2003) provides estimates of the overall recovery times for different building types conditioned on the damage state, which represent estimates of the median time (obtained from empirical data) for repair, reconstruction, delays for decision-making, acquiring permits, financing etc. The recovery times for the building types considered in this study (primarily single-family light residential woodframe buildings) are 5 days, 120 days, 360 days and 720 days for slight, moderate, extensive and complete damage respectively. Since the HAZUS recovery times are

aggregated, only two states are considered in the blind prediction model: (a) the building is damaged and (b) the building is fully recovered, which are assigned recovery levels of 0 and 1 respectively.

For the time-based model, the recovery time is modeled using a lognormal probability distribution function with mean values and standard deviation corresponding to the recovery times provided in HAZUS. A single realization of the recovery trajectory for the time-based model is obtained by sampling the recovery time for each building from the exponential probability distribution and constructing a recovery curve for the building portfolio. The uncertainty in the recovery trajectory is incorporated by generating 200 realizations of the recovery curve, which is shown in Fig. 4-7a along with the observed recovery trajectory. The number of realizations is chosen such that the maximum coefficient of variation in the mean recovery curve is less than or equal to 5%.

For the blind prediction, all realizations of the recovery curve are shown along with the mean curve. Since the observed damage states are used to generate the blind prediction recovery curve, the dispersion is effectively zero at the time of the event and increases with time. Towards the tail end of the recovery curve, the dispersion in the recovery level is reduced as the number of buildings that are not recovered tends towards zero. At any time during the recovery period, a probability distribution in the recovery level can be obtained, which is defined by a mean and dispersion in the recovery level. Fig. 4-8a shows the probability distribution function (PDF) of the recovery level 400 days after the earthquake and Fig. 4-8b shows the cumulative distribution function (CDF) corresponding to the same time point. The mean recovery level at this time-point is 0.88 and the coefficient of variation is 0.01. The shape of the PDF suggests that the normal distribution would be appropriate for modeling the uncertainty in the recovery level at any time following the earthquake. The CDF defines the probability that the recovery is less than a specified level conditioned on the time since the earthquake. For example, 400 days after the earthquake, there is a 90% probability that the normalized recovery level is less than 0.90. Fig. 4-7a shows that the blind prediction model adequately captures the overall shape of the recovery curve including the steep slope in the early stages and the gradual reduction in the overall rate of recovery with time. However, we also observe that the blind prediction model significantly overpredicts the recovery level from the early stages up to about the time when 80% of the buildings have recovered. For example, at 15 days and 100 days following the earthquake, the recovery level is overpredicted by factors of 2.8 and 1.2 respectively.

The fact that the overall shape of the recovery trajectory is reasonably captured suggests that the accuracy in the prediction model can be improved by using more refined estimates of the input time parameters. To test this hypothesis, a second prediction model is constructed using the mean time-to-permit and repair times from Fig. 4-4 normalized by the square footage of the building and conditioned on the inspection tag (yellow and red). The normalized mean time-to-permit is 0.066 days/ft^2 and 0.097 days/ft^2 and the repair time is 0.063 days/ft^2 and 0.104 days/ft^2 for yellow- and red-tagged buildings respectively. In Fig. 4-7b, the (mean) recovery trajectory labeled "Updated Recovery Simulation" is obtained when using these mean values and three recovery states (*Pre-Con, Con* and *Com*). It shows that the prediction model is vastly improved when the observed mean-value time parameter inputs are used. Considering the same time points used to evaluate the blind simulation model (15 days and 100 days following the earthquake), the "updated" model estimates the recovery level within 40% and 15% respectively of the observed values.

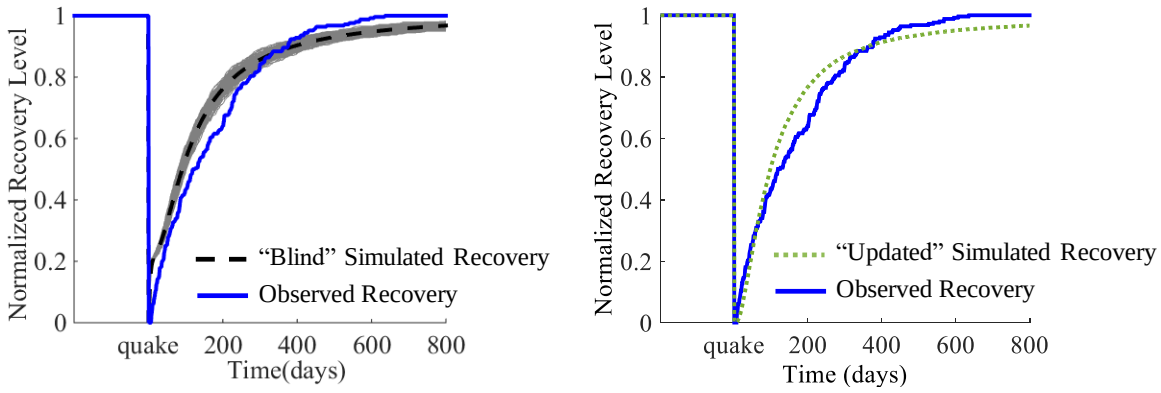

(a) (b)

Fig. 4-7. Comparing the (a) blind and (b) updated simulation results to the observed recovery trajectory for the 456 buildings in the permit-issue-completion dataset

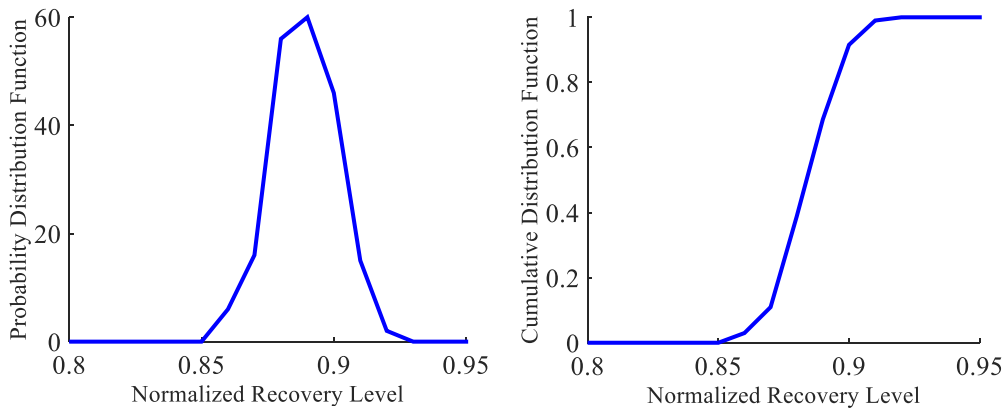

(a) (b)

Fig. 4-8. Full distribution of the normalized recovery level at 400th day including the (a) probability density and (b) cumulative distribution functions

4.4.6 Time-Based Stochastic Process Model for Predicting Future Post-Earthquake Recovery Trajectories

The goal of this section is to develop a generalized model that can be applied to incorporate a larger set of buildings in the simulated recovery trajectories for the 2014 South Napa earthquake and generate recovery predictions for future earthquakes. The first step in this process is to establish a statistical relationship between the time parameters (time-to-permit and repair time) and explanatory variables that represent different factors that are known to influence the pace of recovery.

Comerio (2006) found that areas with higher rates of severely damage buildings had a slower recovery. In the current study, the scale of damage is quantified by averaging the damage state level of all buildings within each zone. First, the buildings classified as having slight, moderate, extensive and complete damage are assigned values of 1, 2, 3 and 4 respectively. Based on these "damage values", the average damage value in each zone is taken as sum of the damage values for all buildings in that zone normalized by the total number of buildings.

The thirteen predictors used to develop the statistical model and their mean values in each zone is summarized in Table 4-2. Using these predictors and the time-to-permit and repair time as dependent variables, the Random Forest machine learning algorithm is applied to construct the regression model that will be implemented as part of the generalized recovery model. Random Forest utilizes a classification and regression tree (CART), which recursively divides the data-space into subspaces until some pre-defined termination criteria is achieved.

Fig. 4-9 shows an example of a simple *CART*, where the time-to-permit is the dependent variable. A randomly generated subset (342 buildings) of the permit-issue-completion dataset (used as the training data), which represents the highest node (root node) in the *CART* shown in Fig. 4-9, has a mean time-to-permit of 99 days. In the first division, two child nodes are generated based on the building age (< 46 years and ≥ 46 years). The predictor and split point are selected based on an attribute test which minimizes the impurity in the divided subsets. Impurity refers to how often a randomly chosen element from the training would result in an incorrect prediction result (Raileanu and Stoffel, 2004). This procedure is recursively repeated until the stopping criteria (e.g. the maximum depth of the tree, the maximum number of splits for a predictor) are met. Each point at which a split occurs is referred to as a decision node and the termination nodes are referred to as leaf nodes. For the simple tree shown in Fig. 4-9, there are three decision nodes and four leaf nodes. The time-to-repair at each leaf node is taken as the mean value for the data-subset of that node. Bootstrap sampling is used to randomly generate multiple training datasets and a *CART* is constructed for each one. For a given combination of predictor values, the corresponding value of the dependent variable from a single *CART* is taken as the mean value at the leaf node where all predictor values meet the splitting criteria for all decision nodes leading to that leaf node. The final value of the dependent variable is taken as the mean value for all randomly generated *CARTs*.

The relative importance of the thirteen predictors is also evaluated as part of the Random Forest algorithm. The importance of each predictor is assessed based on the change in the prediction error before/after permuting the predictor variable and how much the impurity is affected when that variable is used as the basis for node splitting. The results of this evaluation showed that the top five predictors (in decreasing order of importance) of the time-to-permit and repair time are the building value, floor area, age, damage state and PHS_DIPLOMA.

Table 4-2. Average damage and socioeconomic indicator values for each zone

	Central	West	East	North	South
Building Area	2,641	2,096	1,808	3,082	1,979
Building Age	72	40	62	53	74
Building Value($)	522,602	715,244	552,139	536,779	653,512
Damage State	2.19	2.00	1.53	1.78	1.82
PH_ENGLISH	88%	100%	92%	92%	93%
PH_NO18UNDER	68%	74%	66%	62%	65%
PASIAN	1%	4%	2%	3%	1%
PHISLAT	42%	9%	32%	34%	42%
PAFRICAN	1%	0%	3%	0%	0%
INCOME($)	24,731	47,220	37,928	33,125	27,901
PHU_OWNED	35%	87%	61%	76%	47%
PHS_DIPLOMA	71%	90%	80%	81%	73%

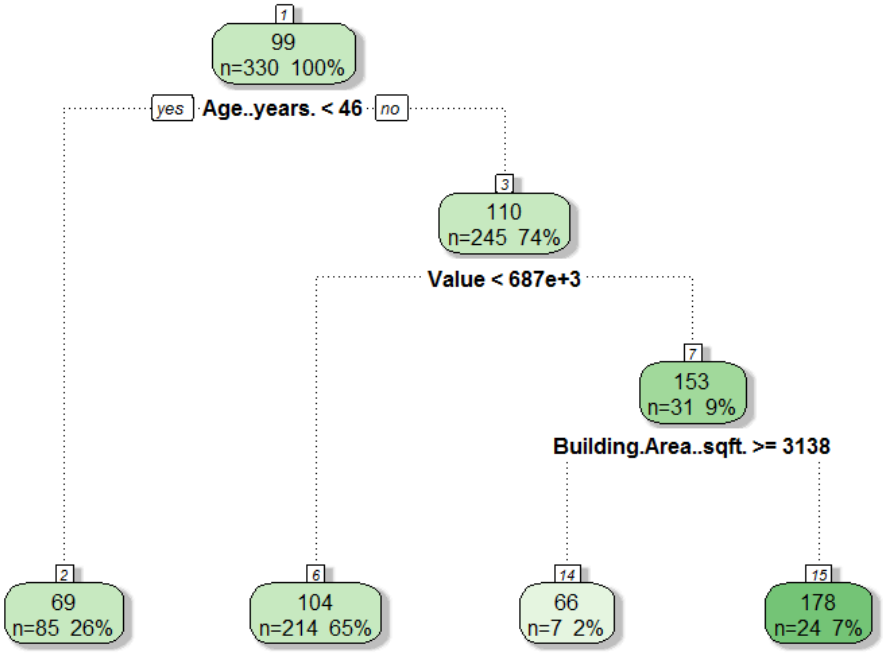

Fig. 4-9. An example of Random Forest regression tree

Among the 456 buildings included in the permit-issue-complete dataset, 342 are used to randomly generate 200 *CARTS* and the remaining 114 are used as the testing data. Fig. 4-10 compares the observed and simulated recovery trajectories which are generated using the testing dataset. It shows that, despite the bifurcation in the latter stages, the "statistical" simulated recovery compares well with the observed recovery and even performs better that the "updated" simulated recovery in Fig. 4-7b.

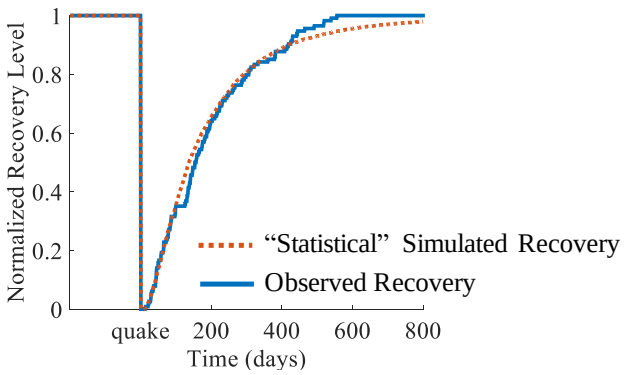

Fig. 4-10. Recovery curve comparing the predicted and observed recovery trajectories obtained from the test dataset (114 buildings)

A Random Forest regression model is also developed for the time-to-permit and repair time using the thirteen predictors and all 456 buildings in the permit-issue-completion dataset. The resulting statistical relationships between the time parameters and the various explanatory variables are used to formulate a generalized recovery model that can predict recovery trajectories for future earthquakes given the spatial distribution of building damage described by the HAZUS states. While the model will not be applicable to all scenarios, it can be used in cases where the affected region, earthquake and recovery typology are judged to be comparable to the 2014 South Napa consideration. In this study, the new model is used to generate a recovery trajectory for the 1470 buildings for which we have information on the damage state and the statistically significant predictors. Fig. 4-11 compares the simulated recovery trajectory for the dataset of 1470 buildings to the "statistical" simulated and observed trajectories for the 456 buildings in the time-to-permit dataset. The two simulation-based recovery curves for the complete and time-to-permit datasets overlap throughout the entire trajectory. However, the simulated recovery is slightly slower that the observed recovery.

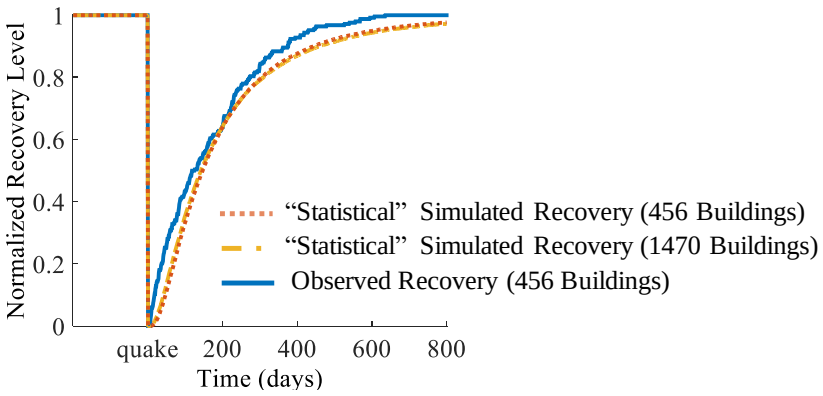

Fig. 4-11. Comparing observed and statistical recovery simulation for the permit-issue-complete (456 buildings) data subset the complete (1470 buildings) dataset

4.5 Replicating the Recovery Following the 2014 South Napa Earthquake using Simulation-Based Stochastic Process Models

The previous section represents a recovery model implicitly where the assumption exists that there are enough resources enabling all the buildings in the community to be repaired simultaneously and immediately (Fig. 4-12). However, the use of real inputs by recovery-related activities cannot exceed the volume of available resources. Examples of constraints of a physical or technical nature include the stock of labor of different activities, the access to finance, the capacity of machines and equipment ready for operation, and so on. This section will involve how we develop a stochastic simulation models explicitly which incorporates resource constraint.

Four recovery-related activities are considered in this framework: (1) Inspection, (2) Assessment, (3) Finance, and (4) Repair or Reconstruction. We will describe the inspection and repair or reconstruction process explicitly, and the other two-assessment and finance-processes implicitly. Fig. 4-13 shows the flow chart of objected-oriented design of this resource constraint recovery model. The inspection team will pick up buildings to be inspected in "Find nearby" algorithm. One neighborhood can have lots of buildings. The center building of the neighborhood is chosen as the benchmark. Based on the distance between this benchmark and each building, a list of ordered buildings is generated within the neighborhood which decides the sequence of inspection. One inspection team is responsible for one or more neighborhoods. The inspection team will not go to the next neighborhood until all the buildings in current neighborhood has been inspected. Not like the implicit model, the inspection team has the work hours. For example, the team can work 6 hours per day. If each building needs half an hour to

be inspected, the 13th building has to wait and start to be inspected on the second calendar day. t1 in the teams input is a list of neighborhoods which team 1 are responsible for.

Contractors work in a different way. First, contractors' work capacity is computed by multiplying the number of teams in this contractor and working hours per day. Second, the number of buildings each contractor is responsible for is computed based on the capacity and total number of buildings in this community. For example, there are three contractors A, B, C. The work capacity is 50 hours per day, 30 hours per day, 20 hours per day respectively. If the community has 1000 buildings, contractor A will be responsible for 500 buildings (1000*50/(50+30+20)). The contractor B and C will be responsible for 300 and 200 buildings. Third, a "dealing card" algorithm is utilized. Each time, we randomly select a building for the contractor with maximum capacity (In the previous example, contractor A will be assigned a building). Then select next building for other contractors (Contractor B and C will be assigned a building separately). When we go to the end of the contractor list, we go back to the first contractor who has the maximum capacity again. We repeat this procedure until one of the contractor has been assigned its require number of buildings. We delete this contractor in the contractor list and restart the "dealing card" algorithm with the contractors in the list. For example, when contractor C has been assigned 200 buildings, we will not consider contractor C any more. The 601th and 602th building will give to contractor A and B, then the 603th random building will give to contractor A, not C. Lastly, all contractors will start their repair or reconstruct buildings in the assigned sequence.

As for each building, all the four activities should be finished in order as shown in Fig. 4-12. The recovery path is constructed by randomly sampling the duration of each activity using their associated exponential distribution parameters as in section 4.2. However, the inspection and repair activities also need to consider the resource constraint and transfer the raw time to calendar time.

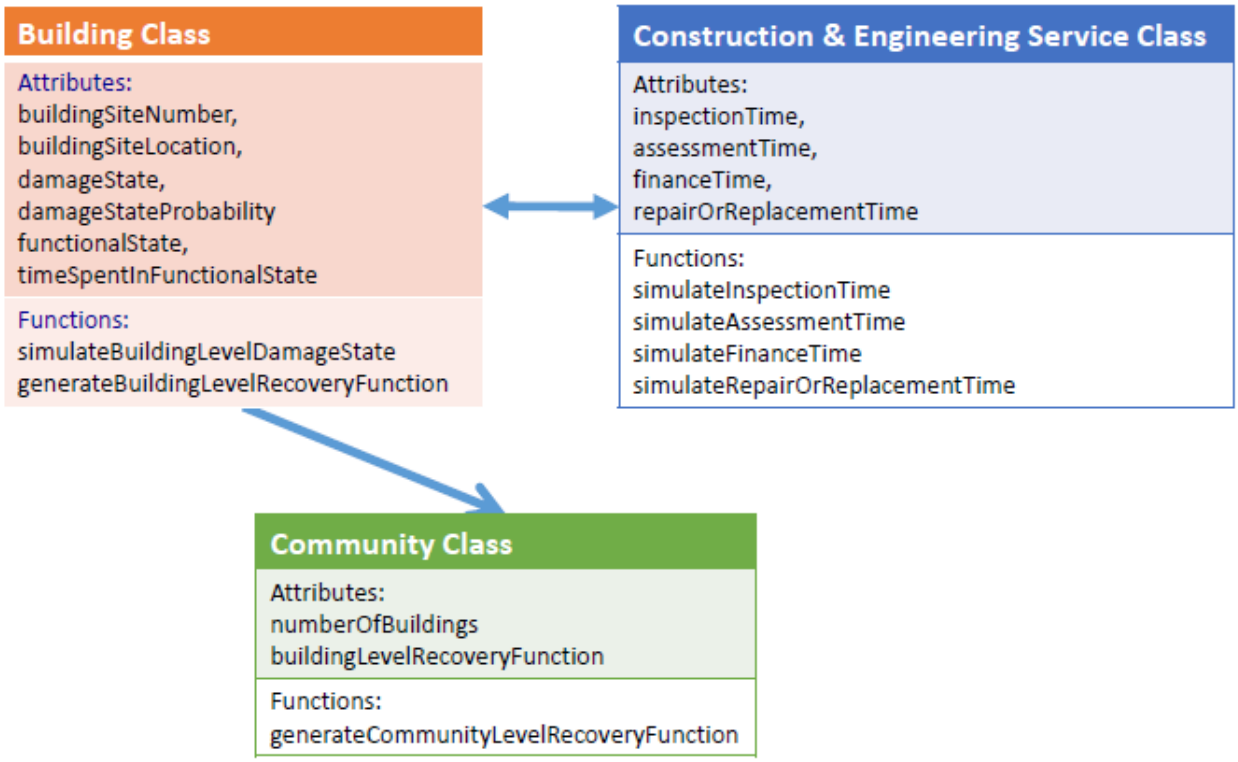

Fig. 4-12. Flow chart of Objected-Oriented classes for stochastic simulation model without resource constraint

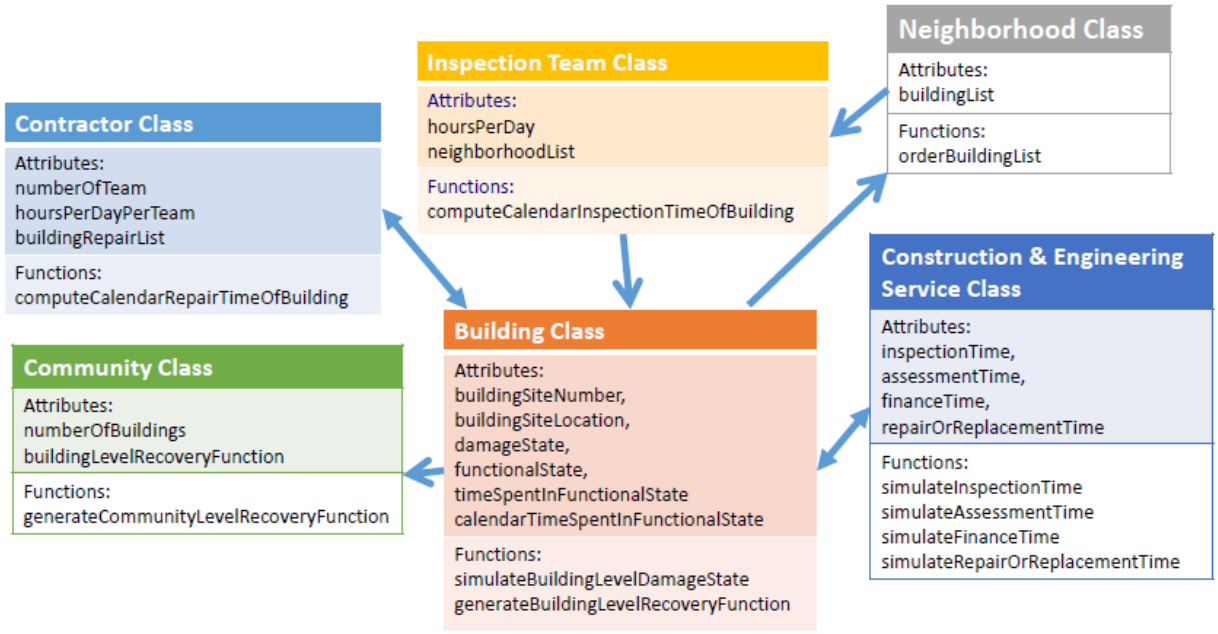

Fig. 4-13. Flow chart of Objected-Oriented classes for stochastic simulation model with resource constraint

The recovery simulation model in this section evaluates the available resources. Time parameters used for four recovery-related activities are shown in Table 4-3. The inspection time is assumed based on engineering judgement. The total time of the assessment and finance activities is equal to the median time-to-permit under each damage state from empirical Napa data. The repair time is calibrated by matching the simulated recovery curves to the observed recovery.

Table 4-3. Time Parameters Used in Resource Constraint Recovery Model

	Slight	**Moderate**	**Extensive**	**Complete**
Inspection	15min	30min	30min	15min
Assessment	20days	20days	40days	40days
Finance	30days	40days	60days	100days
Repair	500hrs	1000hrs	1380hrs	2760hrs

Fig. 4-14 shows how recovery trajectory will change when we add or remove resources. In the base case (green curve), there are three inspection teams A, B, C. Team A is responsible for central zone. Team B is responsible for eastern and northern zone. Team C is responsible for western and southern zone. The working hours for team A, B, C are 12, 10, and 10 hours per day. Twenty-five contractors are involved. Their capacity are 12 hours per day respectively. If we decrease the inspection work hours to 6, 5, 5 hours per day for team A, B, C, the recovery trajectory (pink curve) become faster and closer to the observed recovery (blue curve). However, if there are only twelve contractors available, the recovery become very slow (red curve). Thus, considering resource constraints in recovery model is necessary and meaningful.

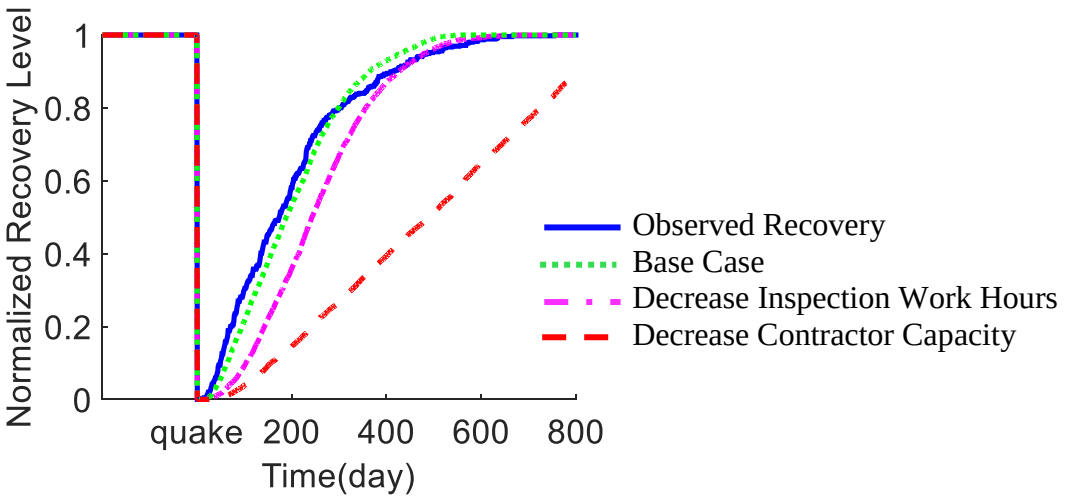

Fig. 4-14. Comparing observed and resource constraint stochastic simulation model for the permit-issue-complete (456 buildings) dataset

4.6 Summary and Conclusion

A stochastic process model is used to re-enact the recovery following the 2014 South Napa earthquake, focusing primarily on the reconstruction of damaged buildings. The objective of the study was to validate the simulation methodology and formulate a generalized model that can be used to generate recovery predictions for future earthquakes. The model was evaluated by performing a "blind" prediction, where none of the temporal data from the 2014 event was used. The simulation captures the uncertainty in the recovery trajectory, which is characterized by an empirical probability distribution of the recovery level (defined by mean and standard deviation) at any time point after the earthquake. The shape of the distribution (symmetric and bell-shaped) suggests that the normal distribution would be appropriate for describing the uncertainty in the recovery level conditioned on the time since the earthquake. The mean blind simulation curve captures the overall shape of the observed trajectory (sharp increase in the early stages and drops off in the latter part) but overpredicts the recovery level by as much as a factor of 2.8. The simulation is repeated with the building-level recovery disaggregated into the three recovery states and using the mean time-to-permit and repair time from the acquired dataset. This improves the simulated recovery curve, reducing the maximum error of the recovery level to a factor of 1.4.

The Random Forest algorithm is used to develop a statistical learning model that has the mean time-to-permit and repair time as the response variable and thirteen predictors related to the extent of damage, general characteristics of the building and property (e.g. age, occupancy, property value) and census-level sociodemographic variables (e.g. percentage of ethnic minorities). The building value, floor area, age, building damage and percentage of households in a community with at least a high school diploma, were found to be the strongest predictors of the time-to-permit and repair time. The statistical time parameters were used to develop a "generalized" recovery model and simulate the recovery trajectory for the 1470 damaged buildings. The results showed that the simulated recovery trajectory for the full dataset (1470 buildings) was slightly slower than observed recovery trajectory for the smaller subset of buildings used to develop the generalized model.

Post-earthquake recovery simulation is useful for quantifying and enhancing the seismic resilience of communities. By exploring trends for multiple "what-if" recovery-scenarios, different types of resilience-building interventions can be evaluated including pre- (e.g. seismic retrofit of infrastructure) and post-event (e.g. incentivize residents to remain in

affected community and rebuild) strategies. Pre-event measures such as seismic strength could be incorporated by incorporating damage simulation as part of the recovery model with differences in structural vulnerability embedded in the fragility functions. The recovery model can also incorporate post-event interventions (e.g. establishing mechanisms to support repair financing) by using statistical or anecdotal evidence of their effect on specific recovery time parameters (e.g. permit time, repair time).

Several areas of additional research are needed to enable widespread adoption of post-earthquake recovery models. The effect of lifeline damage on the recovery trajectory for the portfolio of damaged buildings was not considered in this study. While there has been some research work on infrastructure interdependencies, models that explicitly quantify the effect on post-earthquake recovery are still needed. Topographically explicitly models that capture the relative location of the systems being represented will also improve the predictive capability of recovery simulations. The "generalized" model was developed using data from a single event. As such, future applications of that model would need to be limited to scenarios where the target region, scale of damage and recovery typology are deemed similar to the 2014 South Napa earthquake. For example, the model presented in this paper cannot be used in cases where the effect of lifeline damage is prominent. Previous studies have used the fraction of demolished buildings (including collapses) to reflect the scale of damage. In the 2014 South Napa earthquake, less than 2% of the damaged buildings were demolished. Therefore, future applications of the "generalized" model should be limited to cases with similarly low rates of demolitions. Modelers should also consider that there may have been other external factors not considered in the current study, which could have also affected the recovery simulation. For example, observations from past events have shown that insurance coverage for earthquake damage have a major effect on the time to obtain financing and therefore, the overall recovery time. Moreover, interventions by local and federal authorities to provide financial assistance and other grassroots activities (e.g. an active social media campaign spurred business recovery) were not considered.

CHAPTER 5: Effect of Los Angeles Soft-Story Ordinance on the Post-Earthquake Housing Recovery of Impacted Residential Communities

This chapter is partly based on the following study:

Kang, H., Yi, Z., and Burton, H. V., (2018). "Effect of Los Angeles Soft-Story Ordinance on the Post-Earthquake Housing Recovery of Impacted Residential Communities," *Natural Hazards* (submitted).

Note that the building archetype development (Section 5.3.1), retrofit designs (Section 5.3.2), structural modeling (Section 5.3.3) and nonlinear response history analyses used to compute the building damage state fragilities (Section 5.4) was conducted by Zhengxiang Yi, who is a current PhD student at UCLA. The work related to the other parts of this chapter was done by the author of this dissertation (Hua Kang).

5.1 Introduction

5.1.1 Background on Disaster Housing Recovery

The physical damage to permanent residences caused by natural hazard events has cascading consequences that extend well into the recovery phase. Models that provide a quantitative link between the probable distribution of building damage and the ensuing recovery trajectory are important for several reasons. The information gleaned from such models can be used to inform the financial needs of a community following a hazard event and whether (and if so, how much) financial assistance is needed, identify subpopulations within the broader community that are likely to be acutely affected by infrastructure damage and develop what-if scenarios to understand the spectrum of possible consequences (Lindell and Prater, 2003). These models can also be used to evaluate policies that seek to mitigate specific vulnerabilities within the building stock, with the goal of enhancing community resilience.

Most of the prior research on disaster housing recovery has been empirically driven. By collecting and analyzing data on past events, these studies provide both qualitative and quantitative insights on the myriad of factors that affect housing recovery such as damage, tenure and social vulnerability (e.g. Comerio, 1998; Zhang and Peacock, 2009). However,

because of the general lack of longitudinal data describing disaster housing recovery, there is a growing recognition that computational models can be useful for augmenting empirical research (Miles et al. 2018).

Research to develop computational models of disaster housing recovery has seen significant growth (relatively speaking) within the past decade and a half. These models vary based on the adopted (or developed) conceptual frameworks, numerical methods, the nature of the input variables and the outcomes. Fig. 5-1 provides an overview of the numerical methods that have been used to model disaster housing recovery in prior studies. Linear (and generalized linear) regression models have been used to evaluate the effect of different factors (e.g. occupant tenure, neighborhood income) on the sequence of household movements, pace of recovery and household decisions. System dynamics models have been implemented to provide insights into the influence of labor supply on housing reconstruction and agent-based models have been shown to be useful for capturing micro-scale interactions (e.g. homeowner-homeowner, homeowner-insurance company). Due to the increasing number of open source software tools and programming libraries, discrete event simulation (DES) models have become the method of choice for some modelers. DES provides a customizable modular framework for representing multiple precedent-driven processes (e.g. building inspection, permitting, finance acquisition), resource constraints (e.g. number of available inspectors and contractors), and conditional event triggering. Disaster housing recovery has also been represented using stochastic process models such as Markov Chains. While much more research is needed to further advance the field of disaster housing recovery modeling, these recent developments have created new opportunities to evaluate the effect of real pre-event mitigation policies (planned or already implemented) on the resilience of residential communities.

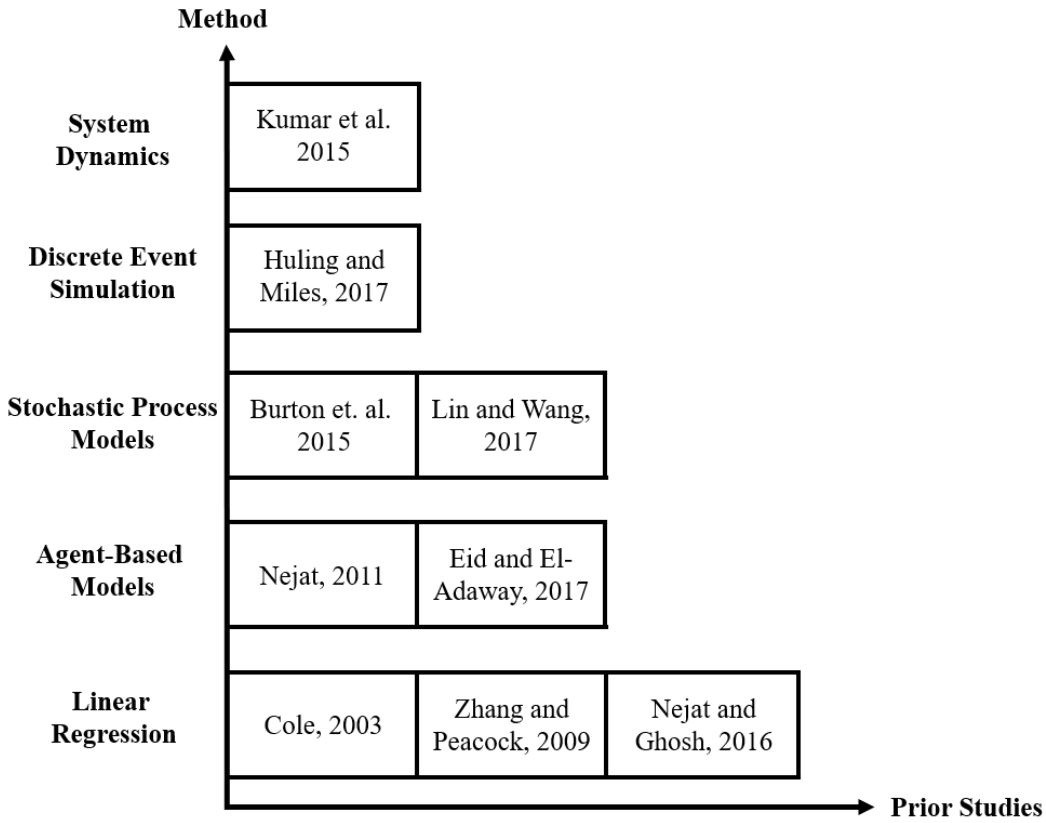

Fig. 5-1. Overview of prior studies and methods adopted to model disaster housing recovery

5.1.2 Overview of City of Los Angeles Soft, Weak, and Open-Front Wall Line Building Ordinance

In December 2014, the City of Los Angeles established the Resilience by Design (https://www.lamayor.org/resilience-design-building-stronger-los-angeles) initiative with the goal of enhancing the city's resilience by strengthening its social and economic functions. As part of that initiative, the Office of the Mayor worked with several domain-experts to develop tools and strategies to adapt to and recover from major disruptive events such as storms, earthquakes and economic recessions (LADBS, 2015). One of those initiatives, which was signed into law in October of 2015 (Ordinance No. 183983) and amended on January of 2016 (Ordinance No. 184081), mandated the seismic retrofit of Soft, Weak and Open Front (SWOF) woodframe buildings. SWOF buildings are identified as having either of the following: an exterior wall line that is (a) soft, with the stiffness being less than 70% of the stiffness of the wall immediately above, (b) weak, where the strength is less than 80% of the strength of the wall above or (b) open, having no vertical elements of the lateral-force resisting system (LFRS). The Los Angeles Department of Building and Safety (LADBS) estimates that there are 13,500 of these buildings in the city (Los Angeles Times, 2016). The Ordinance applies to

existing woodframe buildings for which the permit application for new construction was submitted prior to January 1, 1978 and a SWOF wall line exists in the first story. Residential buildings containing three dwelling units or less are exempt.

5.1.3 Objective of Current Study

The main objective of this study is to investigate the post-earthquake recovery-related benefits to the city of Los Angeles' residential communities that are derived from implementing the ordinance-mandated SWOF retrofits. The selected study region is comprised of approximately 8,000 residential buildings located in the neighborhoods of Koreatown, Westlake, Pico Union, Lomita and East Hollywood. These neighborhoods vary based on their sociodemographic profile, the distribution of single and multifamily residences and the fraction of the latter that have a soft story. Data on the number of stories, plan geometry and soft-story wall layout for the inventory is acquired using Google Street View. A set of SWOF and NonSWOF (buildings without soft-story) archetypes that capture the variation in the key structural characteristics of the inventory is then developed and the Ordinance retrofit procedure (LADBS, 2015) is applied to the former. The results from nonlinear analyses of structural models representing the existing SWOF and NonSWOF and retrofitted SWOF archetypes, are used to develop analytical building-level limit state fragility functions. The effect of the Ordinance retrofit on the recovery of livable housing following a hypothetical scenario earthquake is evaluated. The results from this study will provide useful insights into the extent to which a policy that was primarily targeted towards public safety (reducing collapse risk), has an impact on housing recovery.

5.2 Description of Study Region and Building Inventory

5.2.1 Demographics of Study Region

Five neighborhoods in the City of Los Angeles have been chosen for this study: Koreatown, East Hollywood, Westlake, Pico Union and Lomita. The relevant demographics of each neighborhood is summarized in Table 5-1 (http://maps.latimes.com/neighborhoods/). Four of the neighborhoods, –Koreatown, Westlake, Pico Union and East Hollywood– are in central LA and the fifth (Lomita) is located in the south bay. Koreatown and Westlake have similar land areas (approximately 7 square kilometers) and their population densities (approximately 17,000 people per square kilometer) are among the highest for the city of Los Angeles. The four central Los Angeles neighborhoods have a very high percentage of residents who occupy rental housing (more than 90%) and median income levels that are generally considered low

for the city of Los Angeles. For these same four neighborhoods, the median household size ranges from \2.7 to 3.3. Lomita has the smallest population density and median household size.

Table 5-1. Demographics of target neighborhoods

Neighborhood	Population	Land Area (km^2)	Percentage of Residents in Rental Housing	Median Household Size
Koreatown	124,281	7.0	93%	2.7
Westlake	117,756	7.0	95%	3.0
Pico Union	44,664	4.3	91%	3.3
East Hollywood	78,192	6.2	91%	3.0
Lomita	19,984	4.9	53%	2.5

5.2.2 Woodframe Residential Building Inventory

A set of woodframe building archetypes is developed based on a survey of all residences in the five target neighborhoods. Approximately 8,000 buildings were surveyed using Google Street View and relevant information including the latitude and longitude, number of stories, wall layout in the soft-story (only applies to SWOF buildings), plan geometry and type of dwelling (single versus multi-family dwellings). Non-residential buildings are not included in the survey because they are outside the scope of this study.

The details of the inventory for each neighborhood are summarized in Table 5-2. Westlake has the highest number of residential buildings followed by East Hollywood, Lomita, Koreatown and Pico Union. Koreatown has the highest percentage of multi-family dwellings (MFDs) (80%) and Lomita has the highest percentage of single-family dwellings (SFDs) (96%). This contrast is consistent with the relative fraction of renter-occupied homes noted earlier. Buildings with two and three stories comprise slightly more than half (54%) of the inventory and only 7% of all buildings have more than three stories. Among the 1-story buildings, which make up 39% of the entire inventory, 90% are SFDs. In Koreatown, 28% of all buildings and 35% of MFDs have SWOF wall lines. In Westlake and Pico, 9% of the inventory are SWOF buildings. Only 2% and 0.1% of the buildings in Pico Union and Lomita, respectively, have SWOF wall lines. A map showing the spatial distribution of residential buildings in the five neighborhoods is presented in Fig. 5-2. The SWOF buildings are highlighted in red. In East Hollywood, Koreatown and Pico Union, the residential buildings are located within two or three clusters. In Westlake and Lomita, the residential buildings are more dispersed throughout the neighborhood.

Table 5-2. Summary of building inventory

Neighborhood	No. of Buildings	Dwelling Type		Fraction of SWOF Buildings		No. of Stories		
		MFD[1]	SFD[2]	All[3]	MFD	1-Story	2-3 Stories	> 3-Stories
Koreatown	1,033	80%	20%	28%	35%	9%	66%	25%
Westlake	2,471	49%	51%	9%	18%	28%	64%	8%
Pico Union	715	53%	47%	2%	4%	25%	73%	2%
East Hollywood	2,081	50%	50%	9%	18%	48%	50%	2%
Lomita	1,600	4%	96%	0.1%	3%	71%	29%	0%

[1]MFD: multi-family dwelling

[2]SFD: single-family dwelling

[3]SFD + MFD

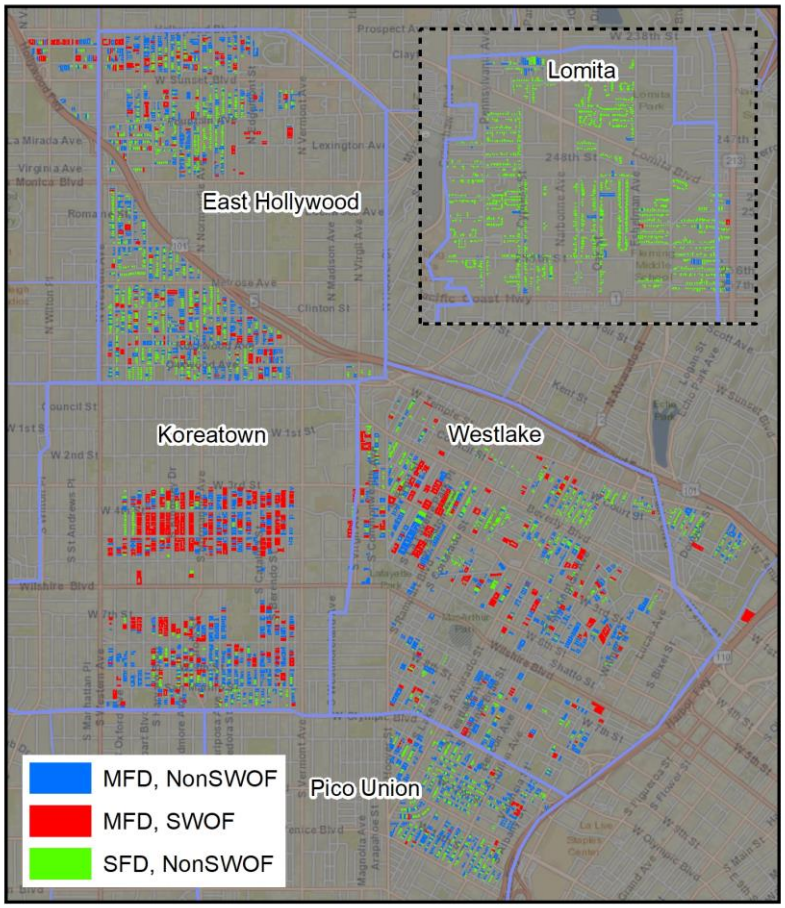

Fig. 5-2. Residential buildings in target neighborhood with SWOF, NonSWOF, SFD and MFD buildings identified

5.3 Development of Archetype Building and Structural Models

5.3.1 Description of Existing Woodframe Building Archetypes

This study is focused on quantifying the effect of differences in the seismic performance of existing and retrofitted SWOF buildings on post-earthquake recovery. Towards this end, capturing variations in the characteristics of SWOF buildings is the primary driver in the development of the archetypes.

The wall layout in the first story of SWOF woodframe buildings has strong implications to their seismic performance. From a survey of approximately 25% of the SWOF buildings on the Los Angeles Times list (http://graphics.latimes.com/soft-story-apartments-needing-retrofit/), four typical first-story wall layouts have been identified. Schematic isometric views of these typical wall layouts, which are identified as L1 through L4, are shown in Fig. 5-3. All four SWOF layouts have partially open first stories that include parking and an enclosed area with living, laundry or storage space. The SWOF layouts identified as L1 and L2 have one wall line that is completely open and two that are partially open. For L1, the completely open wall line is in the "short" direction whereas the "long" direction of L2 has the completely open wall line. L3 has a single completely open wall line that serves as the entrance to a parking garage that has walls on three sides. The parking area in L4 is located at the corner of the building where there are two partially open wall lines. The first-story wall layout of approximately one-third of the surveyed buildings (the ones that were clearly notable from Google Street View) was documented. Among those buildings, approximately 17%, 2%, 61% and 20% had layouts L1, L2, L3 and L4, respectively.

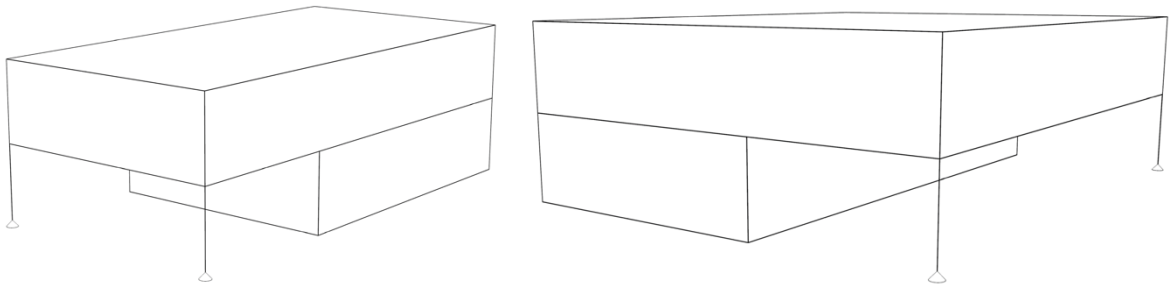

(a) (b)

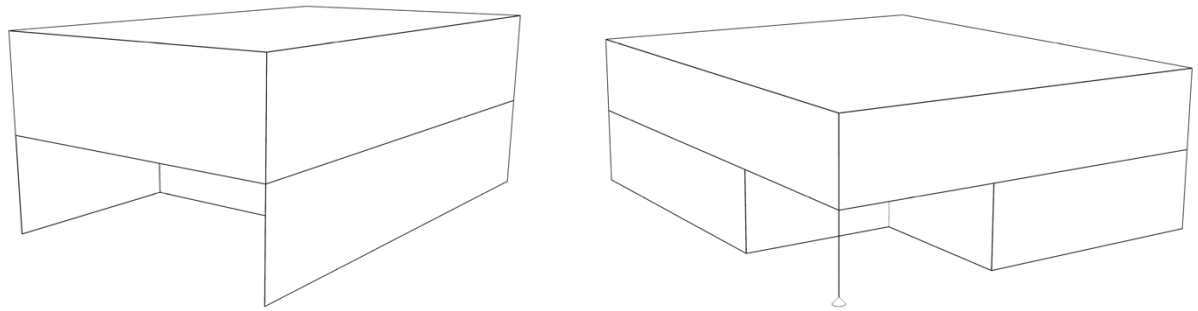

(c) (d)

Fig. 5-3. Typical SWOF woodframe building configurations identified in survey of target neighborhoods: (a) L1, (b) L2, (c) L3 and (d) L4

A total of twenty-one archetype buildings are developed and used to represent the inventory of residences in the target neighborhoods. The properties of each archetype are summarized in Table 5-3. There are sixteen multi-story and four 1-story MFDs and a single 1-story building is used to represent SFDs. The MFDs include archetypes with and without SWOF wall lines. In addition to the first-story SWOF layouts described earlier, variations in the number of stories are considered. Only 1-, 2- and 3-story buildings are included because they comprise approximately 93% of the inventory. The wall layout of the four typical 1st story plan configurations and the typical plan layout of the upper floors are shown in Appendix. The floor layouts (1st and upper) are configured with one, two- and three-bedroom apartments, such that the wall densities (total wall length normalized floor area), which range from 0.12 ft/ft^2 in the first story to 0.20 ft/ft^2 in the upper stories, are comparable to real buildings. The story heights for all archetypes is taken to be 9'-3". The exterior walls are taken to be constructed with 2 X 4 framing spaced at 16 inches on center (O.C.) with stucco (22 mm thick) on the outside and gypsum wallboard (GWB) (12 mm thick) on the inside. The interior partitions consist of GWB on both sides.

Table 5-3. Summary of building archetypes and their seismic weights and ASCE 7-10 estimated periods

Building ID	No. of Stories	Siesmic Weight (kips)	Code Period, $C_u T_a$ (s)
MFD-SWOF-L1-2S	2	284	0.25
MFD-SWOF-L2-2S		437	
MFD-SWOF-L3-2S		242	
MFD-SWOF-L4-2S		444	
MFD-SWOF-L1-3S	3	467	0.34
MFD-SWOF-L2-3S		709	
MFD-SWOF-L3-3S		394	
MFD-SWOF-L4-3S		716	
MFD-NonSWOF-L1-2S	2	298	0.25
MFD-NonSWOF-L2-2S		446	
MFD-NonSWOF-L3-2S		247	
MFD-NonSWOF-L4-2S		446	
MFD-NonSWOF-L1-3S	3	482	0.34
MFD-NonSWOF-L2-3S		719	
MFD-NonSWOF-L3-3S		399	
MFD-NonSWOF-L4-3S		719	
MFD-L1-1S	1	114	0.15
MFD-L2-1S		174	
MFD-L3-1S		95	
MFD-L4-1S		174	
SFD-1S	1	34	0.15

5.3.2 Summary of SWOF Retrofit Designs

The SWOF retrofits are developed based on an S_{MS} = 2.2g, which approximately corresponds to the median value for the sites of the surveyed buildings. The corresponding S_{M1} = 1.2 g. Risk Category II, importance factor *I = 1.0* and soil site class *D* is assumed for all archetypes. The seismic weight of each building is computed using 35 psf as the typical floor dead load, 25 psf for roof dead loads, 10 psf for the weight of the interior partitions and 15 psf for the exterior wall weight per square foot of wall (LADBS, 2015). Details of the seismic weight and empirical period (ASCE 7-10 Equation 12.8-7) of each archetype are summarized in Table 5-3.

The engineering requirements for retrofitting of SWOF buildings in accordance with the Ordinance are outlined in the Structural Design Guidelines prepared by LADBS (LADBS, 2015; SEAOSC, 2017). The design forces used to retrofit the SWOF wall lines are based on 75% of the design base shear obtained from the ASCE 7-16 (ASCE, 2016) standard. The R-Factor used to design the strengthening elements must be less than or equal to that of the existing lateral force resisting elements in the story above but does not need to be less than 3.5.

The story drift limit is based on the smaller of the allowable deformation compatible with all vertical load resisting elements and 2.5%. More details on the SWOF retrofit requirements can be found in LADBS (2015) and SEAOSC (2017).

The ordinary moment frames (OMFs) used for the SWOF retrofit designs are placed in the center of the open wall line. The beam and column size for the frame used in each SWOF archetype is summarized in Appendix A. The bay width for all OMFs is taken to be 15'-0". The force demands used to design these elements are computed using a seismic response modification coefficient and deflection amplification factors of R = 3.5 and C_D = 3.0, respectively, which is consistent with stucco and gypsum wall board serving as the lateral force resisting elements in the upper stories (LADBS, 2015).

5.3.3 Structural Modeling

Three-dimensional numerical models of the existing and retrofitted buildings cases are developed in OpenSees (McKenna, 1997). The wood panels are idealized using a two-node link element with a horizontal spring that captures the force-deformation behavior of the panel. The two nodes are located at the top and bottom of each panel at mid-length. The Pinching4 material (Lowes et al. 2004) is used to model the nonlinear response of the panels. To obtain the Pinching4 parameters for each panel used in the retrofitted and unretrofitted SWOF buildings, a calibration was performed using the hysteretic response of the 10-parameter SAWS material as the benchmark. The SAWS-based hysteretic response is obtained from the CASHEW program (Folz and Filiatrault, 2001) using the CUREE-Caltech loading protocol (Krawinkler et al. 2001). The Pinching4 material parameters are selected such that the hysteretic response under the CUREE-Caltech loading protocol is comparable to the SAWS response.

The *OMF* beams and columns are modeled using elastic elements with concentrated plastic hinges that incorporate the Modified Ibarra-Krawinkler deterioration model (Ibarra et al. 2005). The model parameters for the hinges are obtained from the empirical equations developed by Lignos and Krawinkler (2013). Nine leaning columns (one in each corner, one at mid-length of each exterior wall line and one at the center of mass) are used to capture the spatial distribution of masses and P-Δ effects. A rigid diaphragm constraint is applied at all suspended floor levels.

5.4 Building Limit State Fragilities

A scenario-based assessment of the spatial distribution of building damage is included as part of the recovery modeling framework. To support the damage assessment, limit state fragility curves are developed for each archetype building through nonlinear response history analyses of the associated structural models. The four building performance limit states for woodframe structures identified by Jennings (2015) are adopted for the scenario-based damage assessments. The description and associated structural demand (story drift ratio) limit of each damage state, which is summarized in Table 5-4, are based on observations from experiments on woodframe buildings (Jennings, 2015). The drift limits shown in Table 5-4 are based on the mean values suggested by Jennings. The "demolition" limit state, which was not explicitly defined by Jennings, is also adopted and a demand threshold corresponding to a residual story drift ratio of 0.01 (FEMA, 2012) is used. For the purpose of establishing the recovery activities (see Section 5.6 for details), buildings in the "complete" damage state and those exceeding the 0.01 residual drift demand threshold are assumed to be demolished and rebuilt.

Limit state fragility curves are developed for each archetype building by conducting incremental dynamic analyses (IDAs) with bi-directional loading using the far-field record set of 22 component pairs of the ground motions specified in the FEMA P695 (FEMA, 2009). The ground motions are scaled such that the geometric mean of each record-pair matches the target spectral acceleration level. Two analyses are conducted for each record-pair by switching their orthogonal directions resulting in a total of 44 collapse intensities. The method of moments is applied to obtain the median $Sa_{T_1}(g)$ (denoted as $\hat{S}a$ hereafter) and lognormal standard deviation (dispersion) of each limit state based on the respective drift limits. Fragility curves for the "slight" and "complete" limit states are shown in Fig. 5-4 for the existing and retrofitted MFD-SWOF-L1-2S and MFD-SWOF-L1-3S archetypes. It is observed that the performance enhancement provided by the Ordinance retrofit is generally higher for the more extreme limit states. Fig. 5-4a shows that the ratio between $\hat{S}a$ corresponding the retrofitted (dashed lines) and existing (solid lines) MFD-SWOF-L1-2S is 1.07 for the "slight" damage state compared to 1.3 for "complete". This is consistent with the fact that the Ordinance retrofit is specifically targeted towards mitigating the risk of collapse. Higher performance levels such as immediate occupancy are not considered. Comparing the fragility curves in Fig. 5-4a and Fig. 5-4b, it is observed that, across all limit states, the 3-story archetype derives a greater benefit from the Ordinance retrofit. The ratio between $\hat{S}a$ corresponding the retrofitted and existing MFD-SWOF-L1-3S is 1.34 for the "slight" damage state, which is 25% higher than the corresponding

ratio for MFD-SWOF-L1-2S. A similar difference is observed for the "complete" state, where the ratio between $\hat{S}a$ corresponding the retrofitted and existing MFD-SWOF-L1-3S is 1.55, which is 20% higher than the corresponding ratio for MFD-SWOF-L1-2S. The $\hat{S}a$ for all archetypes (existing and retrofitted) is summarized in Table 5-5 and the record-to-record dispersion values ranged from 0.28 to 0.51. However, a single dispersion value of 0.6, which incorporates record-to-record and modeling uncertainties, is used for all archetypes (FEMA, 2009).

Table 5-4. Woodframe building damage state descriptions and story drift ratio limits (Jennings, 2015)

Damage State	Description	Story Drift Limit
No Damage	Structure can be immediately occupied, no repairs required.	0.003
Slight	Structure can be immediately occupied, minor drywall repairs required.	0.012
Moderate	Shelter-in-place allowed, drywall replacement required.	0.028
Severe	Shelter-in-place prohibited, structural damage incurred.	0.055
Complete	Structure is not safe for entry, must be reconstructed.	0.090

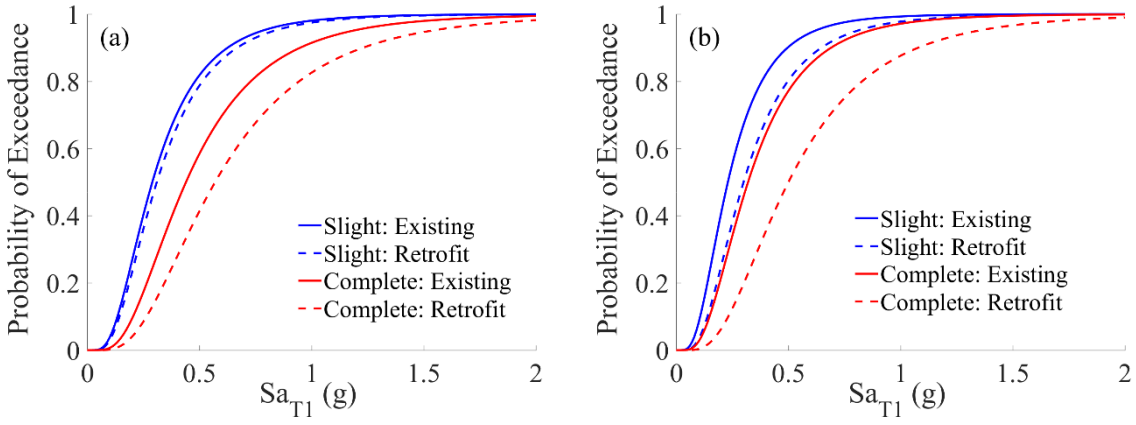

Fig. 5-4. Limit state fragility functions for the existing and retrofitted (a) MFD-SWOF-L1-2S and (b) MFD-SWOF-L1-3S buildings

Table 5-5. $\widehat{Sa}$ corresponding to limit state fragility curves for the existing and SWOF retrofitted archetypes

Building ID	Slight		Moderate		Severe		Complete		Demolition	
	Existing	Retrofit	Existing	Retrofit	Existing	Retrofit	Existing	Retrofit	Existing	Retrofit
MFD-SWOF-L1-2S	0.29	0.31	0.41	0.49	0.44	0.56	0.44	0.57	0.74	1.03
MFD-SWOF-L2-2S	0.24	0.27	0.34	0.43	0.35	0.54	0.36	0.54	0.61	1.05
MFD-SWOF-L3-2S	0.52	0.57	0.74	0.83	0.81	0.92	0.81	0.92	0.75	0.92
MFD-SWOF-L4-2S	0.31	0.32	0.45	0.48	0.47	0.52	0.47	0.53	0.75	0.81
MFD-SWOF-L1-3S	0.23	0.30	0.30	0.44	0.32	0.49	0.32	0.50	0.57	0.85
MFD-SWOF-L2-3S	0.18	0.26	0.26	0.41	0.26	0.47	0.26	0.47	0.49	0.83
MFD-SWOF-L3-3S	0.41	0.47	0.57	0.66	0.60	0.70	0.61	0.70	0.59	0.73
MFD-SWOF-L4-3S	0.25	0.28	0.34	0.39	0.35	0.41	0.35	0.42	0.61	0.67
MFD-NonSWOF-L1-2S	0.32	NA	0.45	NA	0.47	NA	0.48	NA	0.81	NA
MFD-NonSWOF-L2-2S	0.32		0.45		0.48		0.48		0.78	
MFD-NonSWOF-L3-2S	0.54		0.75		0.80		0.80		0.84	
MFD-NonSWOF-L4-2S	0.32		0.45		0.48		0.48		0.78	
MFD-NonSWOF-L1-3S	0.28	NA	0.38	NA	0.39	NA	0.39	NA	0.69	NA
MFD-NonSWOF-L2-3S	0.25		0.35		0.37		0.37		0.64	
MFD-NonSWOF-L3-3S	0.44		0.61		0.63		0.63		0.70	
MFD-NonSWOF-L4-3S	0.25		0.35		0.37		0.37		0.63	
MFD-L1-1S	0.65	NA	0.85	NA	0.90	NA	0.90	NA	1.56	NA
MFD-L2-1S	0.67		0.85		0.91		0.91		1.59	
MFD-L3-1S	1.15		1.45		1.55		1.55		1.81	
MFD-L4-1S	0.67		0.85		0.91		0.91		1.57	
SFD-1S	0.69	NA	0.89	NA	0.99	NA	0.99	NA	1.68	NA

5.5 Scenario Earthquake and Damage Assessment

The simulated ShakeOut rupture (Jones et al. 2008) event is used as the scenario earthquake for the current study. Graves et al. (2008) used broadband physics-based simulations of fault rupture and seismic wave propagation to generate the ground motion histories for that scenario at a large number of Southern California sites. The Sa for each building site in the target region is computed using the simulated records and the overall distribution for the entire inventory is shown in Fig. 5-5. The median value is 0.22g and the 90% confidence interval is between 0.11g and 0.32g.

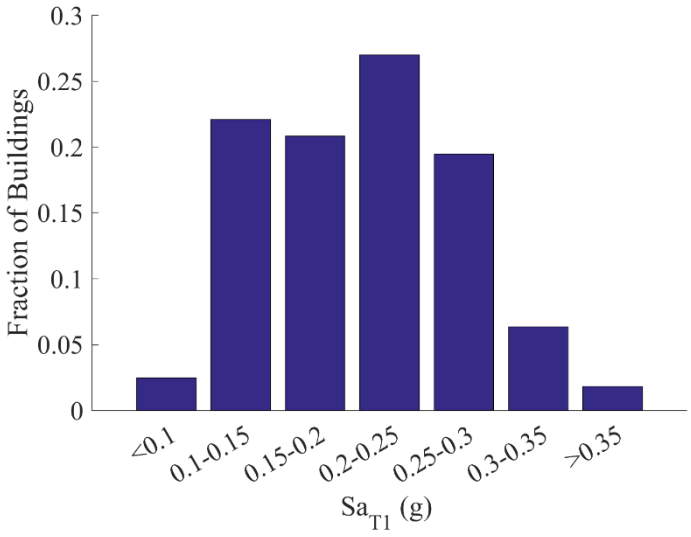

Fig. 5-5. Distribution of $\boldsymbol{Sa}$ values at target building sites for the ShakeOut scenario

The simulated $Sa's$ at each building site are combined with the damage fragility parameters shown in Table 5-5 to generate realizations of building damage, which are described using the damage states listed in Table 5-4,. After computing the discrete probability of being in each damage state conditioned on the Sa, Monte Carlo simulation is applied to generate 1,000 realizations of damage for each building. Two inventory cases are considered: the first has all existing (SWOF and NonSWOF) buildings and the second has existing NonSWOF buildings and retrofitted SWOF buildings. The distribution of simulated damage for the existing and retrofitted inventories are shown in Fig. 5-6. The bar charts are disaggregated (based on the color scheme) to show the fraction of NonSWOF (existing only) and existing and retrofitted SWOF buildings. The distribution of damage is shown in terms of the fraction of buildings in each damage state (Fig. 5-6a) and the fraction of residents occupying buildings within each damage state (Fig. 5-6b). The occupancy of a typical single-family residence is taken to be the same as the neighborhood-based median household sizes provided in Table 1. For multi-family residences, the per-building occupancy is computed to be consistent with the total population for each neighborhood shown in Table 1 and the assumed SFD household size.

Fig. 5-6a and Fig. 5-6b show that the impact of the SWOF retrofit increases with the severity of damage, which is consistent with the results from the building-specific fragility functions shown in Fig. 5-4. The SWOF retrofit reduces the fraction of buildings in the "complete/demolished" damage state by about 21%. When only the SWOF buildings are considered, the fraction of buildings in the "complete/demolished" state is reduced by 59%. In

contrast, the SWOF retrofit reduces the fraction of buildings with "slight" damage by 2.7%, which is significantly less than the "complete/demolished" state reduction. The reduction for the "slight" damage state is about the same when only SWOF buildings are considered.

The distribution of impacts changes dramatically when described in terms of the affected residents. For the existing inventory case, only 73% of occupants are in "undamaged" buildings even though 89% of all buildings are undamaged. On the other extreme, while only 5.2% of buildings in the existing inventory are in the "complete" state, 13.5% of all residents are housed in these buildings. The Ordinance retrofit reduces the fraction of occupants in all "complete" state buildings by 30% whereas the fraction of "complete" state SWOF buildings is reduced by 77%. The difference between the impact of the Ordinance retrofit on residents and residences is because the overwhelming majority of the population resides in MFDs, which tend to be more vulnerable compared to SFDs. This also highlights the importance of earthquake risk mitigation policies for residential buildings located in dense urban centers such as Los Angeles.

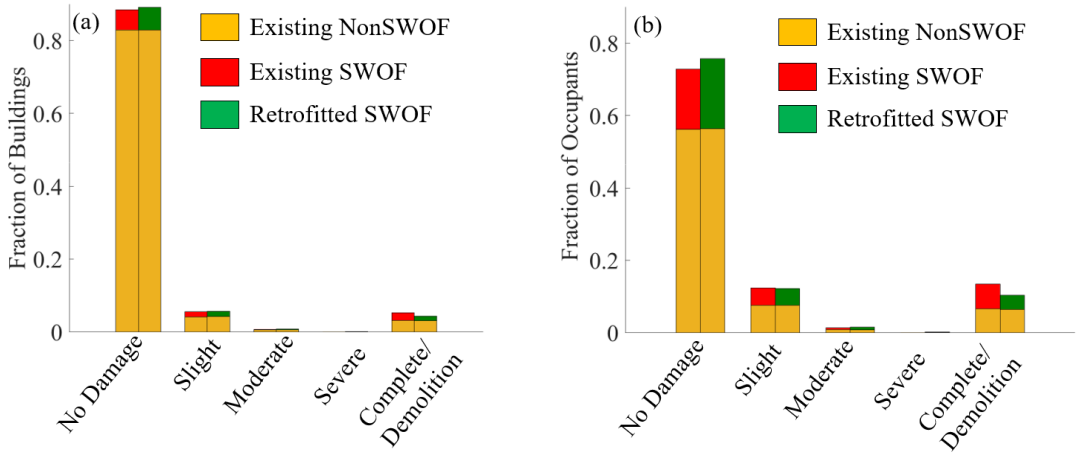

Fig. 5-6. Distribution of damage to all (SWOF and NonSWOF) existing and retrofitted buildings for ShakeOut scenario based on (a) buildings and (b) occupancy

5.6 Modeling Post-Earthquake Recovery Using Discrete-Time State-Based Models

5.6.1 Methodology

The discrete-time state based stochastic (DTSB) process (or Markov Chain) model, which has been adopted in several prior studies (e.g. Burton et al. 2018; Lin and Wang, 2017), is used to represent the recovery trajectory of earthquake-damaged buildings. The DTSB model

conceptualizes post-earthquake recovery as occurring in sequential and non-overlapping stages or discrete states. A recovery path describes the discrete states that are used to model the trajectory and the time spent in each state. The uncertainty in the state duration is considered by computing the probability of transitioning to the next (higher) state at regular increments in time. The realization of a given state is achieved by sampling from that discrete probability distribution. The recovery states utilized herein are based on the activities that are needed to restore building functionality, which include (1) post-earthquake inspection (*Insp*), (2) acquisition of financing for repairs (*Fin*), (3) permitting (*Perm*) and (4) repair, demolition and reconstruction (*Rep*).

Statistical analysis of "time-to-permit" and "repair time" data for buildings damaged by the 2014 South Napa earthquake revealed that the exponential (used herein) and lognormal distributions are appropriate probabilistic models for representing the state transitions (Kang and Burton, 2018). As part of the current study, the correlation between the time-to-permit and repair time was computed using the same dataset and found to be 0.07. This result justifies the use of the DTSB recovery model, which assumes that the sequential state durations are statistically independent.

The recovery trajectories for the target neighborhoods are described in terms of the state of the building and the occupancy of the residence. The "building-state" trajectories capture differences in the level of initial damage and the completion of the various recovery activities (e.g. inspection, financing). The recovery level for an individual building can take on discrete values between 0 and 1. Immediately following the earthquake (i.e. time = 0), the building recovery level is taken to be 0.75, 0.50, 0.25 and 0 for the "slight", "moderate", "severe" and "complete or demolition" damage states, respectively. Each of the recovery activities (*Insp*, *Fin*, *Perm* and *Rep*) is assumed to transition the building towards fully recovery (level 1) in equal increments. For instance, a building that is in the "complete or demolition" state will be at recovery level 0 immediately following the earthquake. The recovery level for the same building will increase in 0.25 increments after the completion of each activity. Whereas, a building that is in the "severe" state immediately following the earthquake will begin at a recovery level of 0.25, and will increase by 0.1875 after each successive recovery activity is completed. It is assumed that 95% of buildings in the "slight" damage state do not a require permit for repairs. For the "moderate" damage state buildings, it is assumed that 45% will require permits. These assumptions are based on an analysis of the 2014 South Napa earthquake dataset assembled by Burton and Kang (2018), where 6% and 42% of the green and yellow-

tagged buildings, respectively, required building permits to complete repairs. For buildings not requiring a permit, only three activities (*Insp*, *Fin*, and *Rep*) are needed to bring about full recovery.

For the "building-occupancy" trajectories, only two discrete recovery levels are considered: 1 for a building that is occupied and 0 for a building that is vacated. While buildings that are in the "slight" and "moderate" damage states are expected to be safe to occupy, 5% and 25% probabilities of post-earthquake evacuation, respectively, are assumed to account for the possibility that the residents choose to vacate for other reasons (e.g. utility disruption, level of surrounding damage). For the "severe", "demolition" or "complete" states, the buildings are assumed to be unsafe to occupy and always vacated. Reoccupancy of any building that is evacuated following an earthquake is assumed to occur after the repair, demolition or reconstruction activities are complete.

The state durations for the DTSB recovery model include the time to inspection, T_{Insp}, time to acquire financing for repairs, T_{Fin}, time to obtain a permit, T_{Perm}, and repair time, T_{Rep}. As noted earlier, these durations are modeled using the exponential distribution and their mean values are summarized in Table 5-6. Three sources of data are used as the basis of the mean state durations, which are based on the condition of the building immediately following the earthquake. The primary data source is the study by Comerio and Bleacher (2010), which compiled a dataset on the recovery time of approximately 5,000 single- and multi-family buildings affected by the 1994 Northridge earthquake. The recovery times in this study are further disaggregated based on whether buildings needed to be repaired or demolished and replaced. The average recovery time for repaired red-tagged buildings was 16 and 22 months for MFDs and SFDs, respectively. For the red-tagged buildings that were demolished and reconstructed, the average recovery time was 38 and 28 months for single- and multi-family residences respectively. Note that these values represent the time from the occurrence of the earthquake to complete recovery and includes the total duration of all recovery activities (*Insp*, *Fin*, *Perm* and *Rep*). The mean recovery time for yellow-tagged multi-family buildings was approximately 12 months. No information on the recovery time for yellow-tagged single-family buildings was provided.

To incorporate the findings from Comerio and Bleacher in the current study, buildings in the "complete", "demolition" and "severe" damage states are assumed to be red-tagged where the former two will require "demolition and reconstruction" and the other "repairs". All

buildings in the "moderate" damage state are assumed yellow tagged, require repairs and the ratio of recovery time for SFDs and MFDs is taken to be the same as the "red-tagged and repaired" case (1.375). Since the Comerio and Bleacher study reported no information on green-tagged buildings (assumed for "slight" damage herein), findings from the 2014 South Napa earthquake (second data source) are incorporated, where ratio of the average recovery time for green- and yellow-tagged buildings was found to be 0.88. This ensemble of information and assumptions is the basis for the total recovery time ($T_{Insp} + T_{Fin} + T_{Perm} + T_{Rep}$) associated with each damage state and residence type (single- and multi-family) shown in Table 5-6.

Given the recovery time for each residence type and damage state, the next step is to determine the appropriate disaggregation among the different state durations ($T_{Insp}, T_{Fin}, T_{Perm}$ and T_{Rep}). A study by Trifunac and Todorovska (1997) reported that most of the tagging after the 1994 Northridge earthquake was completed within the first two months. Therefore, the mean inspection time, $\mu_{T\,Insp}$, is taken to be 30 days for all damage states and both resident types. From the 2014 South Napa earthquake data, the average permit time was computed to be 117%, 77% and 53% of the repair time for green-, yellow- and red-tagged buildings. This information was used to disaggregate the time from tagging to full recovery (based on the Northridge data) into the "permit" (time from tagging to permit acquisition) and repair time (time from permit acquisition to recovery). However, this "permit time" is different from T_{Perm} in this study, since the former is equal to $T_{Fin} + T_{Perm}$. Further disaggregation of the "permit" time into T_{Fin} and T_{Perm} is informed by the REDi guideline (third data source) (Almufti and Willford, 2013), where the ratio of T_{Fin} to $T_{Fin} + T_{Perm}$ is obtained.

Table 5-6. Mean state-durations used in discrete-time state-based recovery model (Comerio and Bleacher, 2010; Kang and Burton, 2018; Almufti and Wilford 2013)

Recovery Activity	Slight		Moderate		Severe		Demolition/Complete	
	SFD	MFD	SFD	MFD	SFD	MFD	SFD	MFD
Inspection	30	30	30	30	30	30	30	30
Financing	90	70	80	60	80	60	80	60
Permit	150	100	140	100	140	100	300	220
Repair	200	140	290	200	410	290	730	530
All	**470**	**340**	**540**	**390**	**660**	**480**	**1140**	**840**

5.6.2 Probabilistic Description of Recovery-Outcomes

The primary uncertainties embedded in the modeled recovery trajectories are the building damage conditioned on the shaking intensity and the state-transition conditioned on the time elapsed after the earthquake. The uncertainty in the immediate post-earthquake occupancy of buildings in the "slight" and "moderate" damage states is also implicitly considered by assigning a probability of evacuation for each of these conditions. This section uses some sample results from building- and neighborhood-level assessments to highlight the effect of these uncertain parameters.

Fig. 5-7 shows the temporal distribution of the in-recovery-state probabilities for multifamily buildings with slight (Fig. 5-7a) and complete/demolition (Fig. 5-7b) damage. Both plots show the in-state probabilities for the activities in the later stages of the recovery increase with time and vice versa. The in-state probability for the *Insp* and *Recovered* states are always 0 and 1 at the start and completion of the recovery process, respectively. Because of the lower mean activity durations, the in-state probability for penultimate recovery states (i.e. *Recovered*) is always higher for the less severe damage state. For instance, the probability of full recovery 800 days following the earthquake is approximately 1.0 for the multifamily building with slight damage compared to 0.75 for the same building in the complete/demolition state. The neighborhood- and community-level recovery trajectories are obtained using a Monte Carlo simulation process, whereby the time-dependent state of each building is sampled from the distributions like the ones shown in Fig. 5-7.

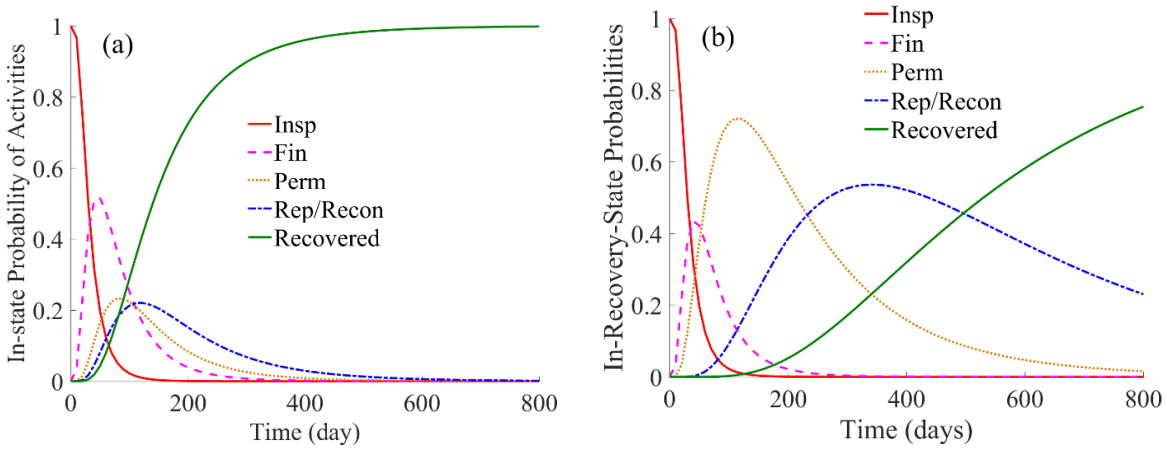

Fig. 5-7. Temporal distribution of in-recovery-state probabilities for a multifamily building with (a) slight and (d) complete/demolish damage

Several probabilistic metrics can be used to describe post-earthquake recovery outcomes at the neighborhood or community scale. Fig. 5-8 shows occupancy- (Fig. 5-8a) and building-based (Fig. 5-8b) "recovery clouds" for the existing inventory case of Koreatown. Recall that this neighborhood has the highest percentage of SWOF buildings (28% of all residential buildings and 35% of MFDs). The term "recovery cloud" is adopted because it shows the full range of possible trajectories when the various sources of uncertainty are combined. Monte Carlo simulation is employed, whereby a single recovery curve realization is generated by sampling (a) the damage state of each building (none, slight, moderate, severe, demolished or complete) conditioned on their respective shaking intensities (Sa), (b) the occupancy state of "slight" and "moderate" damage buildings and (c) the state-transitions conditioned on the time elapsed following the earthquake. In Fig. 5-8, each grey line represents a single recovery realization and the black line represent the central tendency (in this case mean). All recovery outcomes presented in the current study are based on 1000 realizations.

For the occupancy-based recovery cloud (Fig. 5-8a), the vertical axis represents the fraction of neighborhood residents in occupied buildings (or occupancy rate). The vertical axis of the plot shown in Fig. 5-8b represents the aggregated state of the buildings in the neighborhood. Recall that, for a given damage state, the recovery level of an individual building is increased by the same increment after each activity is completed. Therefore, the recovery trajectories shown in Fig. 5-8b capture the changes in the physical state of the buildings, which is only affected by the *Rep/Recon* activity, as well as the completion of the activities that lead up to *Rep/Recon* (*Insp*, *Fin* and *Perm*). An alternative approach would be to limit the trajectories shown in Fig. 5-8b to the physical state of the inventory. In that case, a single increment would be used for each building, which transitions it from the immediate post-earthquake level (0, 0.25, 0.50, 0.75 or 1.0 depending on the damage state) to a recovery level of 1.0 after all activities are completed. However, this approach would provide a very limited view of the overall progression of building recovery.

There are a couple of distinct differences in the recovery-clouds shown in Fig. 5-8 that warrant further discussion. The first is the lag between the building- and occupancy-based trajectories, where the recovery for the latter is much slower. As discussed earlier, the adopted building-state model transitions the through incrementally higher recovery levels even for the activities leading up to *Rep/Recon*. However, for the occupancy-based trajectories, a single transition occurs from 0 to 1 after all recovery activities are completed. Using these two approaches, the model is able to capture the lag between the progression towards building

repair and reconstruction and occupancy. The second major difference between the occupancy- and building- based recovery clouds is the much smaller dispersion in the latter. This can be explained by comparing the variance in the individual-building recovery levels used in the two models. For the occupancy-based recovery, the variance between the two utilized recovery levels (0 and 1) is 0.5; whereas, the variance between the five recovery levels used for the building-based recovery (0, 0.25, 0.50, 0.75 and 1.0) is approximately 0.16. A comparable dispersion between the two metrics can be obtained by setting the immediate-post-earthquake recovery level for all damaged buildings to be 0. However, this approach would negate the effect of the different building damage states on the initial loss.

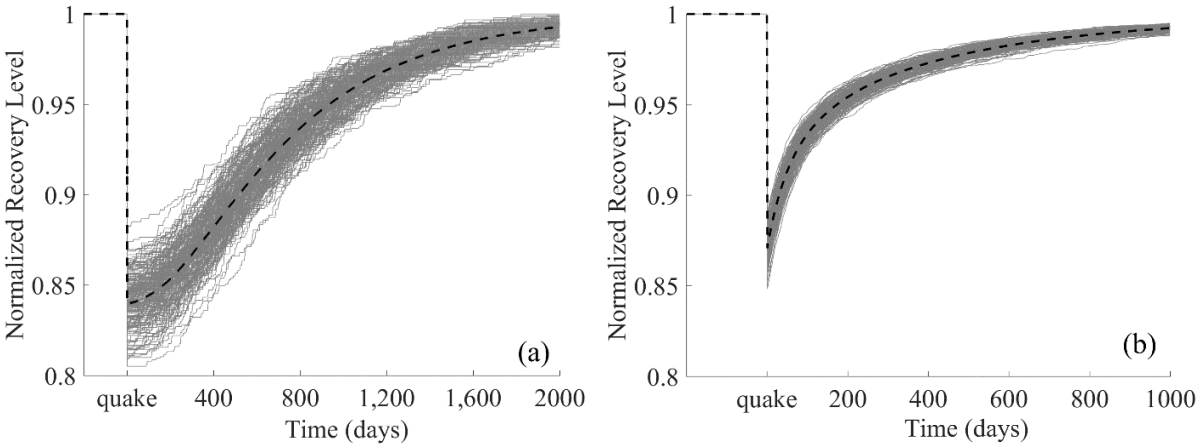

Fig. 5-8. (a) Occupancy- and (b) building-based recovery clouds for Koreatown existing inventory case

The effect of the uncertainty in the building damage state conditioned on the shaking intensity can be isolated by examining the probability distribution of the normalized occupancy level immediately following the scenario earthquake ($t = 0$). This empirical probability density function (PDF) is shown in Fig. 5-9a where the mean and coefficient of variation of the occupancy rate are computed to be 0.84 and 0.02, respectively. The shape of the empirical distribution indicates that the normal distribution would be a good probability model for the occupancy rate conditioned on the time elapsed since the earthquake. This is confirmed by performing the two-sample Kolmogorov-Smirnov (KS) test (Massey Jr 1951) where a *p-value* greater than 0.05 was obtained when the null hypothesis is that the occupancy rate conditioned on T follows a normal distribution. The empirical and theoretical cumulative distribution function (CDF) is shown in Fig. 5-9b. It can be observed that the median immediate post-earthquake occupancy rate is 0.84 and the probability that the initial loss of occupancy exceeds 10% is essentially zero.

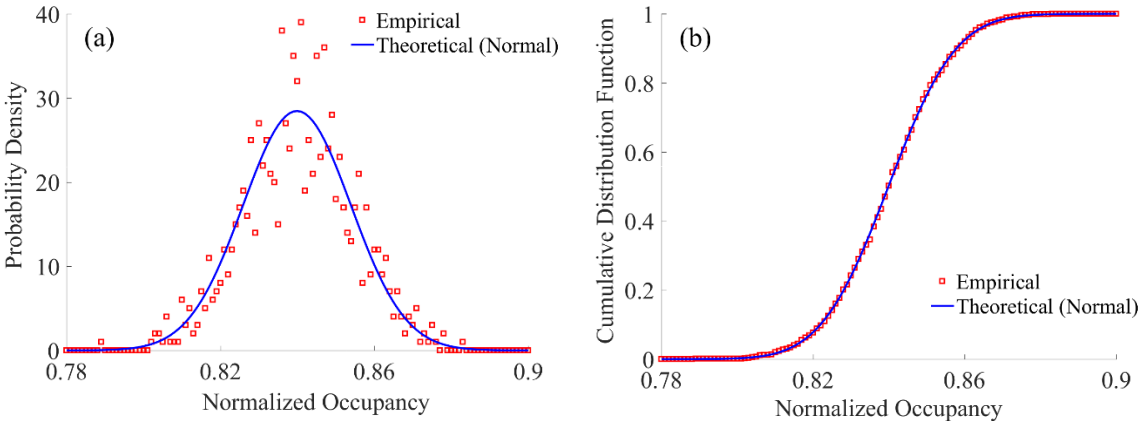

Fig. 5-9. Empirical and theoretical (normal) (a) probability density and (b) cumulative distribution functions of the normalized occupancy in Koreatown immediately following the scenario earthquake

The National Institute of Standards and Technology (NIST) Community Resilience Planning Guide for Buildings and Infrastructure Systems (NIST 2015a, NIST 2015b) established a framework for setting recovery-based performance targets for building clusters. The targets are described in the terms of the desired recovery times for some percentage of elements in a cluster (Table 9-12 of NIST, 2015a). The ability of a residential neighborhood or community to achieve these targets can be probabilistically evaluated by examining the distribution of the time to restore a predefined occupancy rate. Fig. 5-10 shows the probability distribution for the time it takes Koreatown to achieve a 95% occupancy rate ($T_{95\%}$). The results of a KS-test showed that $T_{95\%}$ can also be modeled using a normal distribution. Therefore, both the empirical and normal PDF (Fig. 5-10a) and CDF Fig. 5-10b) are shown. The mean and coefficient of variation of $T_{95\%}$ is computed as 932 and 0.1, respectively. The CDF shown in Fig. 5-10b can be used to obtain the probability of meeting recovery targets based on 95% occupancy rate. For example, the probability that Koreatown achieves this level of occupancy within a 2-year period is approximately 2%. However, if the target duration is increased to 30 months, the probability of $T_{95\%}$ increases to 42%.

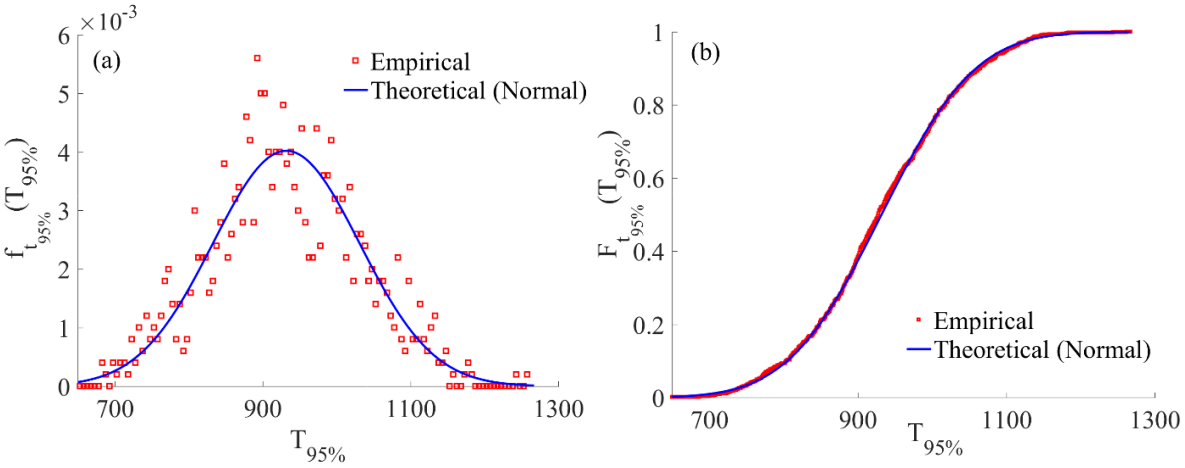

Fig. 5-10. (a) Probability density and (b) cumulative distribution functions (empirical and theoretical) for $\boldsymbol{T_{95\%}}$

5.6.3 Effect of LA Ordinance Retrofit on Post-Earthquake Recovery Trajectories

The effect of the LA Ordinance retrofit on the post-earthquake recovery of the target neighborhoods is assessed by comparing the probabilistic distribution of trajectories for the existing and retrofitted inventory cases in addition to the various overall performance metrics. The occupancy- and building-state-based recovery outcomes are quantified at the "entire housing stock" and neighborhood scales. Fig. 5-11a compares the mean recovery of occupancy for the existing and retrofit cases considering all neighborhoods. It shows that the Ordinance retrofit reduces the mean initial loss of occupancy by approximately 25% and the mean $T_{95\%}$ is reduced by 14%. It is worth noting that if the metric is changed to the time to restore 90% occupancy i.e. $T_{90\%}$, the impact of the Ordinance retrofit becomes much more significant, where $T_{90\%}$ is reduced by approximately 64%. Fig. 5-11b compares the $T_{95\%}$ CDF for the existing and retrofitted inventory when all neighborhoods are considered. It shows that the probability of achieving a hypothetical target of $T_{95\%} = 2$ years increases from a fraction of 1% for the existing case to approximately 42% when the Ordinance retrofit is applied.

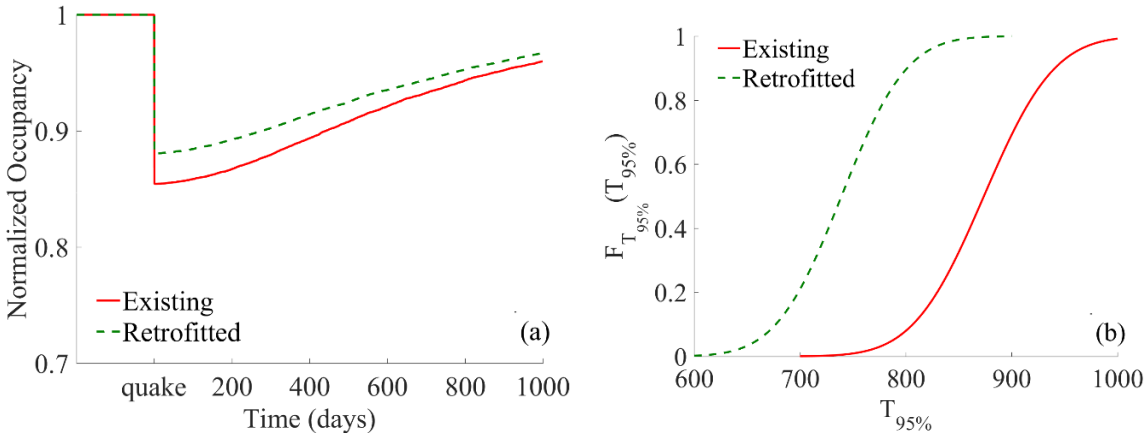

Fig. 5-11. Effect of SWOF retrofit on (a) mean recovery of occupancy and (b) the CDF for $\boldsymbol{T_{95\%}}$ considering all neighborhoods

Table 5-7 summarizes the building- and occupancy-based recovery performance for the existing and retrofitted inventory cases. In addition to the entire community, the recovery outcome for individual neighborhoods is shown. It can be observed from Table 5-7 that, for both the existing and retrofitted case, the impact on housing occupancy is much greater than the impact to the buildings themselves. For example, the mean $T_{95\%}$ for the existing buildings considering all neighborhoods is 42 days compared to 872 days for occupancy-based recovery. This observation can be explained by comparing the percentage of SWOF buildings in the inventory (9%) to the fraction of residents who live in SWOF buildings (29%). Koreatown, which has the highest percentage of SWOF buildings (28%), derives much greater recovery-related benefits from the Ordinance retrofit compared to the other neighborhoods. For example, the retrofit reduces the initial loss of occupancy in Koreatown by is 45% compared to 25% when considering all neighborhoods. Moreover, the Ordinance retrofit reduces $T_{95\%}$ in Koreatown by 60% compared to 14% when considering all neighborhoods. Lastly, the impact of the scenario earthquake on Lomita (existing and retrofitted cases) in terms of building damage and occupancy is minimal. Recall that SWOF buildings make up less than 1% of the Lomita inventory.

Table 5-7. Summary of recovery performance metrics

Recovery Case		Mean Time to 95% Recovery (Days)		Mean Initial Loss (%)	
		Building	**Occupancy**	**Building**	**Occupancy**
All Neighborhoods	Existing	42	872	7	15
	Retrofit	26	766	6	12
Koreatown	Existing	173	1049	13	16
	Retrofit	111	658	11	11
Lomita	Existing	NA	NA	less than 1%	1
	Retrofit	NA	NA	less than 1%	less than 1%
Westlake	Existing	76	947	9	16
	Retrofit	52	857	8	13
Pico Union	Existing	48	720	7	11
	Retrofit	48	647	7	10
East Hollywood	Existing	51	848	7	13
	Retrofit	29	771	6	12

5.7 Summary and Conclusion

An evaluation of the post-earthquake recovery-related benefits of the Los Angeles Soft Story Ordinance is presented in this paper. The Ordinance mandates the retrofit of multifamily woodframe residential buildings with soft, weak and open-front (SWOF) wall lines. Five Los Angeles neighborhoods are considered included Koreatown, Westlake, Pico Union, Lomita and East Hollywood. Among these five neighborhoods, there are variations in the population density, presence of SWOF buildings and percentage of single-family and multi-family dwellings. The results from a building-specific survey performed using Google Street view informed the development of a set of archetype buildings that are representative of the target inventory. The structural properties considered in the archetype development include the presence (or absence) of a soft story, number of stories and for the SWOF buildings, the wall configuration in the soft 1st story.

Incremental dynamic analyses (IDAs) was performed on nonlinear structural models developed for each archetype. The results from the IDAs was used to develop analytical fragility functions for each archetype, which links ground shaking intensity to building-level damage states. The fragility functions were used to perform a scenario-based damage assessment using shaking intensities generated from the simulated ShakeOut rupture scenario. Two inventory cases were considered: one with the existing SWOF and non-SWOF (buildings

without SWOF wall lines) and another with existing non-SWOF and SWOF buildings retrofitted in accordance with the Ordinance. The distribution of damage was quantified in terms of the fraction of buildings in each damage state as well as the fraction of residents occupying each damage state. The results showed that the adverse damage-related impacts of the scenario earthquake was more significant for the latter. For the existing inventory, 13.5% of all residents occupy buildings that suffered "complete" damage or "demolition" even though only 5.2% of the buildings are in these two states. The Ordinance retrofit reduced fraction of occupants in "complete/demolition" damage state buildings by 30%. If only SWOF buildings are considered the reduction increases to 77%. Both the fragility analyses and scenario-based damage assessment show that the effect of the Ordinance retrofit is much less significant for the less severe damage states. For instance, when the SWOF retrofit is applied, the fraction of buildings in the "slight" damage state is reduced by approximately 3%.

Post-earthquake building-level recovery is modeled as a discrete-time state-based stochastic process where trajectories are quantified based on housing occupancy and the state of the building. Recovery states are defined based on the activity needed to restore building functionality including post-earthquake inspection, acquisition of building permits (when necessary) and financing for repairs and repair, demolition and reconstruction. In addition to the building damage state conditioned on the earthquake shaking intensity, the uncertainty in the recovery state conditioned on the time elapsed after the earthquake is considered. The effect of the Ordinance retrofit on post-earthquake recovery outcomes varied based on the considered metric. For example, the Ordinance retrofit reduces the mean initial loss of occupancy by approximately 25%. However, if the mean time to achieve 95% ($T_{95\%}$) occupancy is used as the recovery metric, the reduction is 14%. If the 90% is used as the conditioning occupancy level, the reduction in the mean duration as a result of the Ordinance retrofit increases to 64%. Recovery goals can also be quantified based on the probability that a specified target occupancy level is achieved within a predefined period. When the CDF of $T_{95\%}$ for the existing and Ordinance-retrofitted inventory was compared, the probability of achieving a hypothetical target of two years was found to be a fraction of 1% and 42%, respectively.

5.8 Appendix

The appendix is used to provide details of the plan layout and retrofit designs for the archetype buildings. The blue lines shown in Fig. 5-12 show the location of the retrofit elements, which

are 15’-0” long ordinary moment frames placed at the center of the open wall lines. The frame sizes used in the retrofit are summarized in Table 5-8.

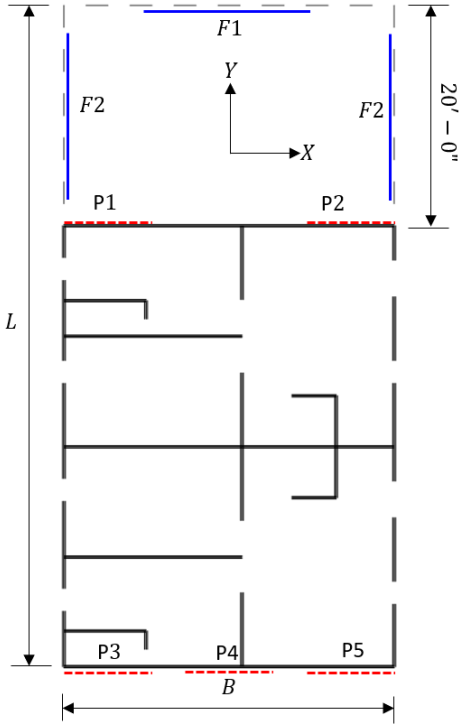

(a)

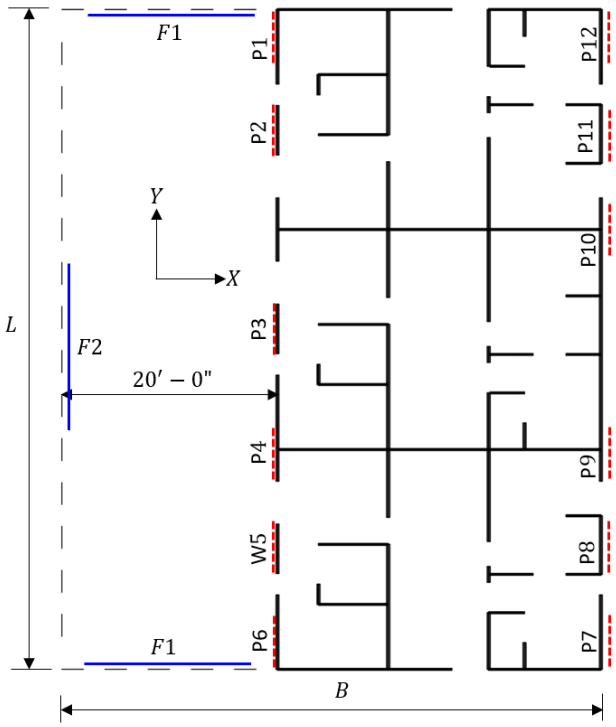

(b)

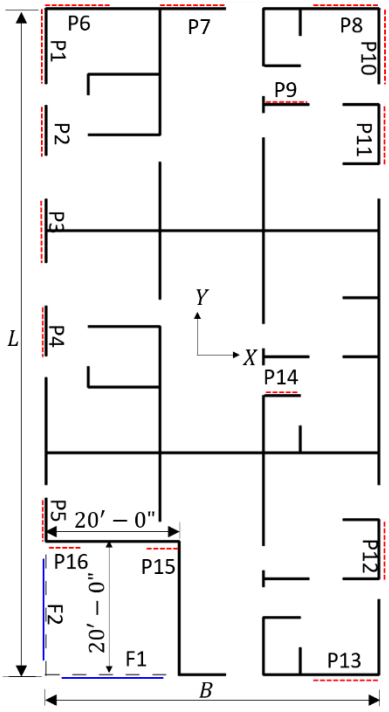

(c)

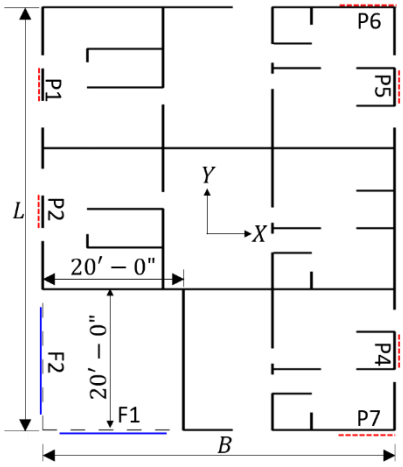

(d)

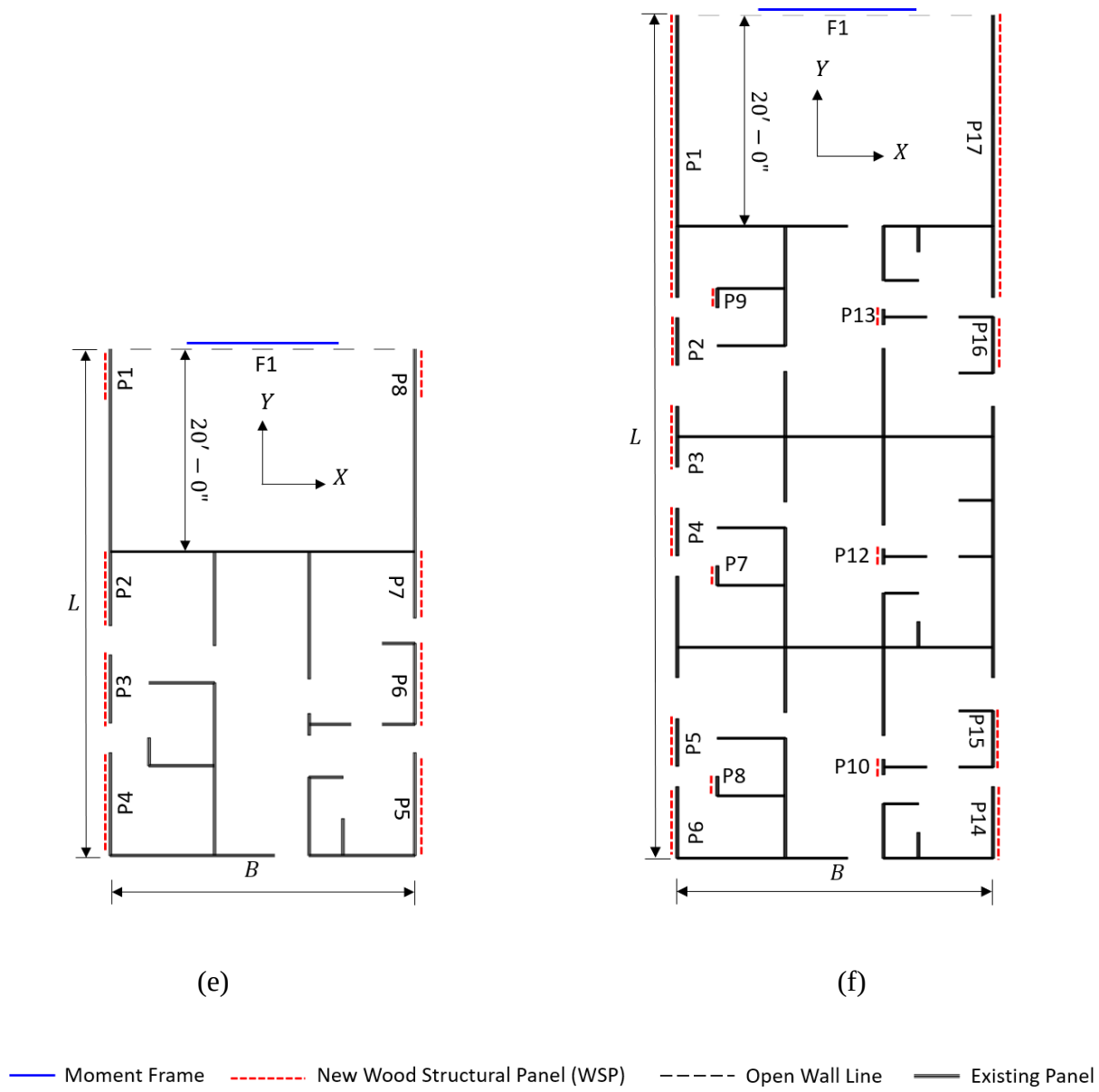

Fig. 5-12. First floor plan showing wall layouts and locations of retrofit elements including moment frames and wood structural panels (WSPs): (a) L1 $(\boldsymbol{L = 100; b = 30})$, (b) L2 $(\boldsymbol{L = 100; b = 50})$, (c) L3 $(\boldsymbol{L = 80; b = 30})$ and (d) L4 $(\boldsymbol{L = 100; b = 50})$

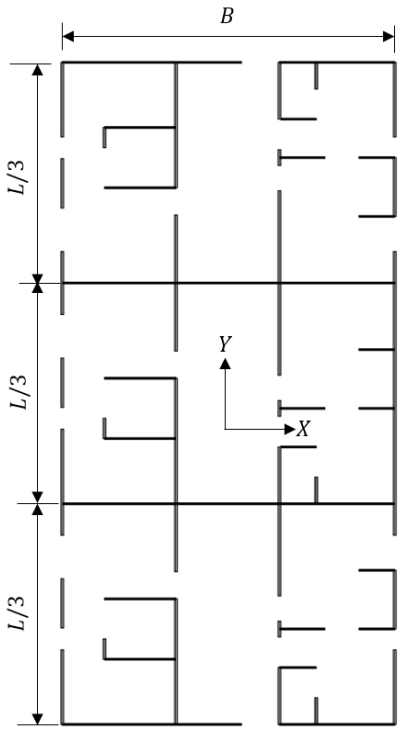

Fig. 5-13. Plan configuration for upper floors of SWOF MFDs and all floors of NonSWOF MFDs

Table 5-8. Ordinance retrofit frame sizes

Building ID	Basic Ordinance			
	F1		F2	
	Beam	Column	Beam	Column
MFD-SWOF-L1-2S	W8x10	W10x15	W8x10	W10x15
MFD-SWOF-L2-2S	W8x13	W10x22	W10x15	W10x22
MFD-SWOF-L3-2S	W8x10	W10x15	W10x22	W10x39
MFD-SWOF-L4-2S	W8x13	W10x22	W10x33	W10x54
MFD-SWOF-L1-3S	W8x10	W10x17		
MFD-SWOF-L2-3S	W8x13	W10x22		
MFD-SWOF-L3-3S	W8x10	W8x15	W8x10	W8x15
MFD-SWOF-L4-3S	W8x10	W10x15	W8x10	W10x15

CHAPTER 6: Modeling Post-Earthquake Decisions of Owner and Renters of Residential Buildings

This chapter is partly based on the following publication:

Burton, H. V., Miles, S. B., and Kang, H. (2018). "Integrating performance based engineering and urban simulation to model post-earthquake housing recovery," *Earthquake Spectra* (accepted for publication).

6.1 Introduction

Household decisions play a major role in disaster recovery of residential communities. Decisions such as whether to remain in their community and rebuild or temporarily or permanently relocate affect the spatiotemporal processes involved in housing recovery. As such, characterizing the uncertainty in post-disaster decision-outcomes of affected households is central to modeling the recovery of residential communities. Two alternative methods can be explored to model household decision making (Burton and Kang, 2017). The first is utility-based theoretical models where the statement that a household will always make the rational decision that maximizes its utility is assumed. The other approach uses empirically-based utility functions in which statistical models are employed to establish the discrete probability distribution of the various decision outcomes. Using the results of an online or face-to-face survey, a multinomial logistical regression model can be developed in which the decision outcomes are dependent variables and the drivers of those decisions are the independent variables.

This chapter starts with a review of the existing literature on modeling decisions using survey method. The only three studies (Nejat et al, 2011, 2012, 2016; Binder et al 2015) on decision-modeling in the specific context of disaster recovery with household as a decision-maker (as far as we know) are presented in this review. While not directly specific to recovery, four other studies more broadly related to disaster risk management (Davidson. 2014; Dong et al. 2015), electronic commerce (Kim et al. 2007) and weather prediction (Morss et al. 2010) are included because of the relevance of the applied decision models to the current research. An overview of the framework that is adopted in the current research is then presented including the elements of the decision-making process in the context of disaster housing recovery, a general discussion on utility-based choice theory and key assumptions. The chapter

continues with the formulation of theoretical and empirical decision-models for predicting post-disaster household decision-outcomes. The theoretical model section presents utility-based choice theory where multi-attribute utility theory is used. The empirical model section discusses how to develop decision making models based on empirical data. A case study using a survey of Los Angeles households is conducted to demonstrate the above approach. A summary of the survey design, including proposing a hypothesis, constructing and defining the relevant independent and dependent variables, choosing a representative sample, and estimating the sample size is presented. To follow, we describe how the data is collected and the survey is conducted. In addition, a multilevel statistical analysis is implemented. In the result section, a description of the study region and the main decision outcomes in the sample are presented. The chapter concludes with the general discussion of theoretical and empirical decision-models for predicting post-disaster household decision-outcomes in Los Angeles County.

6.2 Literature Review

6.2.1 Post-Disaster Household Decision-Making Theoretical Model

Nejat et al. (2011, 2012) used agent-based modeling to represent the post-disaster dynamic interactions among homeowners and between homeowners and insurance companies. These two types of interactions are modeled to influence homeowners' decisions regarding whether to repair, sell or abandon damaged property, which in turn affects the overall recovery trajectory of their community. The temporal behavior of agents (homeowners and insurance companies) are represented using both theoretical and empirical models (the empirical models will be reviewed in the later section 5.2.3). In the theoretical model, interactions among homeowners were represented as rational agents seeking to maximize their utility, which is a function of the gains/losses associated with specific post-event actions. The theoretical model for the homeowner-insurer bargaining process is based on a game. The homeowner-homeowner and homeowner-insurance interaction models are placed in a Multi-domain Multi-agent system to represent the behavior of individual neighborhoods or communities. In the spatial domain, the relative location of entities drives interactions. For example, homeowner decisions are also affected by their location relative to commercial properties, educational institutions and essential lifelines. In the organizational domain, interactions are based on the social dynamics among homeowners and between homeowners and insurance companies.

6.2.2 Other Studies on Modeling Decision-Making in the Context of Disasters

Davidson (2014) developed a regional natural disaster risk management model that is directed towards representing the interaction of stakeholders' decisions when insurance strategies and retrofit are considered simultaneously under different policy configurations. Four agents are included in the model: homeowners, insurers, reinsurers and government. Homeowners' decisions are related to whether or not to purchase insurance choosing among a set of alternative retrofit options. Insurers' decisions are related to the premiums to charge based on the level of risk and how much of the risk is transferred to reinsurers. Reinsurers decide on the price of reinsurance and the government makes decisions related to policy-constraints on the insurer and homeowners. Utility-based models are used to quantify the relative benefit of the possible decision-outcomes for each stakeholder. Genetic algorithms are then used to determine the policy-level decision that maximizes combined profit of all stakeholders over a specified time horizon.

In contrast to the Nejat et al. and Davidson model, where utility value is described and computed in terms of monetary value, Dong et al (2015) used a single, global sustainability performance measure to quantify the social, economic and environmental life cycle seismic impacts and determine the optimal retrofit strategy for a bridge. Multi-Attribute Utility Theory (MAUT) is used to combine the three metrics into a single utility value that describes the overall desirability of each retrofit strategy. First, marginal utility functions are developed for each metric including the cost of bridge retrofit. The utility values associated with each metric are then combined using the Weighted Sum Method (Stewart, 1996) to obtain a single multi-attribute utility. The maximization of this utility served as the basis for selecting the optimum retrofit scheme.

Utility-based theoretical decision theory has been implemented in three of the four studies presented in this section. Nejat et al. modeled the decisions of homeowners based on maximizing their utility, Davidson used utility theory to model stakeholders' decisions with the goal of establishing policies that maximize total profit and Dong et al. used MAUT to develop optimal retrofit strategies for bridge networks based on a global performance metric that incorporates social, economic and environmental life cycle impacts.

6.2.3 Post-Disaster Household Decision-Making Empirical Model

Nejat and Damnjanovic (2011, 2012) also developed an empirical household-interaction model based on the results of experiments that are designed to mimic the conditions following a real disaster. The conditions include the availability of infrastructure and severity damage, the availability of funds and the cost of reconstruction. 80 students from the civil engineering department at Texas A&M University were involved as the participants in the experimental study. The choices were to reconstruct immediately or wait for 6 months and decide according to the observations from neighbors' actions. Multinomial logistic regression model was used to predict the probability of alternatives which is described in Equation 6.1.

$$log\left(\frac{P(Y=j)}{P(Y=k)}\right)=\sum_{i}\beta_{i,j}x_i \tag{6.1}$$

where $log\left(\frac{P(Y=j)}{P(Y=k)}\right)$ is the log-odds of decision outcome j over outcome k, x_i is explanatory variable i and β_i is the regression coefficient for explanatory variable i.The empirical model for the homeowner-insurer bargaining process is also based on an experiment. Participants were divided into two groups (insurers and homeowners/clients), and were asked to provide offer and accept/reject the offer. 77 students participated in the experiment where 6 students acted as insurer, and each of them was responsible for 10 to 12 clients. An empirical model presenting a payoff structure for players was formed. Different statistical analysis methods were used for parameter estimation for the empirical model, such as Maximum Likelihood Estimation (MLE). The homeowner-homeowner and homeowner-insurance interaction models are placed in a Multi-domain Multi-agent system to represent the behavior of individual neighborhoods or communities. In the spatial domain, the relative location of entities drove the interactions. For example, homeowner decisions are also affected by their location relative to commercial properties, educational institutions and essential lifelines. In the organizational domain, interactions are based on the social dynamics among homeowners and between homeowners and insurance companies.

In a later study, Nejat and Ghosh (2016) used linear regression to predict post-disaster household-level decisions (rebuild or repair damaged houses; wait and stay in temporary housing; relocate) and their impact on community-level recovery. Data related to a wide range of internal and external attributes (demographic, socioeconomic, exposure parameters, external signals and spatial activities) was collected in Staten Island, New York after Hurricane Sandy

(2012). Two faculty members and three students from Texas Tech University conducted face-to-face interviews. Two sampling methods were adopted: (1) door-to-door surveying, which mainly focused on heavily damaged areas. First, a single address was randomly chosen as the benchmark within predefined locations per member. Secondly, households around the benchmark were asked to participate in the survey. If a home was not approachable, they would go to its neighbors and choose this one as new benchmark. The unapproachable home was marked for at most two follow-ups for the next day; (2) surveying people staying at designated shelters. 126 surveys of occupied homes and temporary shelters were conducted. Categorical housing recovery decisions (repair or wait/relocate) were used as the dependent variable. The Least Absolute Shrinkage and Selector Operator (LASSO) method (Tibshirani, 1996) was used to perform the regression. The LASSO method is often used in multi-variate regression when there is multicollinearity in the data representing the explanatory variables. Multicollinearity, which refers to the presence of strong correlations among predictor variables, can lead to inaccurate estimates of regression coefficients, inflated standard errors and deflated partial t-test values in the regression coefficients. The LASSO estimates can be acquired by equation 6.2.

$$l_c(\beta_0, \beta) = \sum_{i=1}^{n} [y_i(\beta_0 + x_i^{'}\beta) - \log(1 + e^{\beta_0 + x_i^{'}\beta})] - \lambda \sum_{k=1}^{p} |\beta_k| \quad (6.2)$$

where $l_c(\beta_0, \beta)$ is the log-likelihood function under LASSO constraints, y_i is the i^{th} response from a sample where $Y_i = 1$ is one if the homeowner decides to rebuild or repair his/her current residence, and $Y_i = 0$ if one decides to wait or relocate, $x_i^{'} = (x_{1i}, x_{2i}, ..., x_{pi})$ is the i^{th} row of predictor matrix, p is dimension of predictors which equals to 23, $\beta = (\beta_1, \beta_2, ..., \beta_p)^T$ is the vector of regression coefficients, β_0 is the intercept, λ is Lagrangian multiplier which can only be positive and controls the regularization. Of the 23 predictor variables considered in the regression model, the availability of insurance, tenure or place attachment, and availability of funding from external resources such as federal, state, local, and charities, were found to be statistically significant. The authors used anecdotal evidence from previous disasters (Comerio, 1998 and Wu et. al 2004) to validate the results obtained from their prediction model.

Binder et al (2015) investigated the relationship between community resilience and the relocation decision (pursue a buyout program or not) in disaster-affected communities. The home buyout program is a policy tool to facilitate the permanent relocation of residents out of

areas with high disaster risk. Data was collected from residents in Oakwood Beach and Rockaway Park, both working-class communities in New York City, which were heavily damaged after Hurricane Sandy in 2012. Two types of measures were used in this study: (1) quantitative measures via survey, which focused on analyzing the role community resilience in the buyout decision, (2) qualitative measures via interviews, which were designed to expand on the findings from the quantitative data. 23 individuals participated in both the survey and interview, 150 individuals only participated in the survey and 5 only participated in an interview. Survey participants were recruited in a similar way to the Nejat and Ghosh (2016) study i.e. door-to-door surveys and surveying at local community. The overall response rate was 34.8% (146 out of 419) across both neighborhoods. Interviews were organized through the surveying process. Interview participants were selected based on their interest as well as the balance distribution in terms of age and gender. Each participant received a gift card in the amount of $20. Multiple imputation (MI) procedures were used first to impute missing values in the initial dataset. T-tests and Chi-square tests were utilized to analyze and compare the data across communities. Logistic regression was implemented to evaluate the influence of resilience in the buyout decision. The participants' decision outcome (accept or reject the buyout program) was the dependent variable. Independent variables are resilience related including the length of time in current residence in years, exposure index, disaster management, transformative potential, connection and caring, resources, etc. Qualitative data including responses to open-ended survey questions and interviews was also analyzed. The results demonstrated that community resilience lead to opposite responses on the buyout decision. History of disasters, local culture norms, and sense of place play an important role on these responses.

6.2.4 General Decision-Making Empirical Model

Kim et al (2007) developed a decision-making model in the context of electronic commerce to test the role of trust, perceived risk, and their antecedents. Internet consumer purchasing behavior data (whether or not to purchase a product online) was collected via a Web survey. The undergraduate students were chosen to participate in the study voluntarily for extra credit. Two rounds Web-based surveys were conducted as the following: (1) pre-purchase round, in which students were instructed to go through the entire store but without the final "buy" decision. In this round, students were asked to give the preference to the product that they most wanted to buy and was least inclined to buy. Therefore, the collected data was related to antecedents of trust and perceived risk, trust, perceived risk, and perceived benefit, (2) in the

post-purchase round, students were asked to purchase their preferred products. Data related to the actual purchase decision were recorded. In addition, the demographic characteristics of respondents including age, gender, education level, household income, products purchased, money spent on purchase, frequency of Internet purchases in last year, number of years using the Internet, and experience on computer and the Internet were investigated. 468 of 512 responses were usable and complete. Partial Least Squares (PLS) Structural Equation Modeling technique with bootstrapping were used to test the model and analyze the data. Decisions were used as the dependent variables. The BENEFIT and RISK which can be reflected by convenience, saving money, saving time etc were selected as formative indicators and the others were used as reflective indicators. The results show that trust and risk are important in consumers' purchasing decision.

Morss et al (2010) employed the results from decision scenario questions asked in a nationwide US survey to test the use of weather forecasts in decision-making. Two sets of decision questions were asked to respondents. The first set of questions were related to the respondents' probabilistic threshold for taking action to defend the uncertainty in heavy weather. The potential weather conditions were described in term of the probability of rain or temperature below freezing. For the questions, the respondents had to give "yes or no" answers to protective decisions in a scenario. The scenario included monetary losses. The data was collected in 2006 via the Internet. A survey sampling company was used for the data collection. The respondents were required to be representative of the US population reachable online. Moreover, the sample had the same sociodemographic characteristic distribution to the US population. 1465 of 1520 completed surveys were useable. The data was analyzed using MATLAB and SAS. Multiple non-parametric significance tests were employed. For example, the Wilcoxon rank-sum test was used to test whether two independent samples of observations have the same underlying distribution. The Kruskal-Wallis test was used when three or more independent samples are involved. Person chi-square was used to test whether the frequency distributions of two or more samples come from identical populations. Logistic regression was used to model the exam respondents' binary decision as a function of probabilistic forecast, decision scenario and cost of protection.

Decision-making survey-based models has been applied not only in disaster recovery but also to more broad research areas. Even though the applications are different, the method are similar and the current survey will be conducted using the following procedure: (1) propose a hypothesis or specific objectives, (2) declare and construct all related independent variables,

(3) design a comprehensive survey, and (4) conduct a multilevel statistical analysis. The objective is to model households' preferences for multiple informed decisions in the context of disaster recovery. Households in Los Angeles were surveyed. The questionnaire includes different earthquake-related scenarios. Moreover, the relations between the attractiveness of an alternative and a set of exogenous and endogenous characteristics related to the household and the community in which it resides are investigated.

6.3 Decision Modeling Framework

A conceptual framework for integrating household decision-making into a post-earthquake recovery model is presented in this section, where "the household" is taken to be synonymous with the decision-maker. We will also describe how the probabilistic descriptions of the recovery-based residential building limit states discussed in the previous section can be incorporated into the decision model. The main steps needed to formulate the model include (1) defining the possible alternative courses of actions that are available to the household in the wake of earthquake damage, (2) specifying the attributes associated with each alternative and (3) using an appropriate decision rule to make a choice among the available alternatives (Ben-Akiva and Lerman 1985). It is worth noting that the current study is concerned with descriptive decision theory, which seeks to assess the most likely decision-outcome based on an assumed set of rules that govern the behavior of the decision-maker. This contrasts with normative or prescriptive decision theory, which seeks to identify the ideal choice for a decision-maker who is assumed to be fully rational (Bell and Raiffa 1988).

Faced with damage to property and their surrounding environments, the household must decide on an appropriate course of action. Fig. 6-1 shows an event tree with some examples of possible recovery actions (A_1 through A_4) for a single-family home conditioned on the extent of damage, as measured by the recovery-based building performance limit states described in the previous section. Each of these actions has strong implications to recovery at the household, neighborhood and community levels. For example, the actions and time-to-recovery for a single-family residence where the household chooses to repair and reoccupy their home following an earthquake will be different from the case where the house is sold without conducting repairs. Likewise, a home that is abandoned will have a different recovery trajectory than the previous two.

The attractiveness of an alternative is determined based on a set of exogenous and endogenous attributes related to the household and the community in which it resides.

Examples of endogenous attributes include household income, education, tenure and the value of the residence. Attributes that are universal to the community such as the extent of ambient damage and the existence of organizational structures to manage the recovery are considered exogenous (Nejat and Ghosh 2016). Attributes can be deterministic or defined by some probability distribution. Generic attributes are invariant with respect to the alternatives (e.g. income and educational level) and alternative-specific attributes can vary from one alternative to the next (Koppelman et al. 2006). Earthquake-related expenditures will differ between alternatives and are therefore considered an alternative-specific attribute. For instance, the cost associated with temporary relocation and sheltering-in-place will be different.

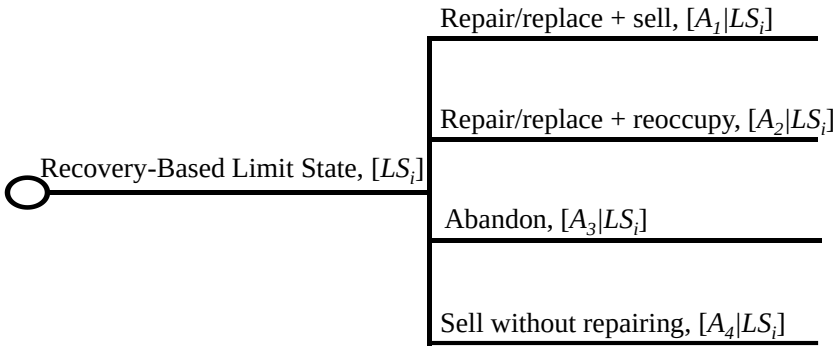

Fig. 6-1. Event tree showing examples of alternative post-earthquake actions for single-family residential building owners

Decision models can be categorized based decision rules used to process the relevant information and evaluate the available options. In this study, utility-based decision rules are considered, which are part of a broader classification of rational discrete choice models, in which the decision-maker (or household) is assumed to have rational preferences that are constrained by the von Neumann-Morgenstern axioms (Von Neumann and Morgenstern 2007). A utility value is a measure or indicator of the preference of a decision-maker (Varian and Repcheck 2010). In utility-based decision models, utility values are obtained for each alternative and is used as the basis of the final decision-outcome. These utility values are computed from empirical or theoretical utility functions. Theoretical utility functions are prescribed based on knowledge of the risk preference of the decision-maker and typically do not rely on data. Although data may be used to test the validity of the theoretical projections. Concave utility functions are generally used for risk-averse decision makers and convex functions are used for risk-seeking decision makers (Hillson and Murray-Webster 2007). Risk-neutral individuals are represented by using linear utility functions. The parameters that define theoretical utility functions can be obtained by calibration to observed decisions (Kesete et al.

2014) or by "curve fitting" using an assumed attribute (e.g. minimum and maximum) and corresponding utility values (Dong et al. 2015). For empirical utilities, a basic functional form is assumed and the model parameters are estimated using statistical tools.

Utility-based models can also be categorized based on the treatment of uncertainty. In deterministic choice utility-based models, the uncertainty in the utility value is not considered and the utility maximization rule is applied, whereby the decision-outcome is taken to be the alternative that maximizes that utility value. In probabilistic choice utility-based models, the final decision is described in terms of the probabilities of choosing each alternative rather than predicting that the decision-maker will choose an alternative with certainty (Koppelman et al. 2006). Two types of models, deterministic theoretical and probabilistic empirical, are described in the following sub-sections where the metrics used to quantify the relative value of each decision-outcome include: (1) minimizing the net earthquake-related household expenditure and (2) minimizing the "social consequence" experienced by the household due to the earthquake. Multi-attribute (theoretical and empirical) utility functions are used to combine the economic and social impact metrics into a single performance measure.

6.3.1 Deterministic Theoretical Utility-Based Decision Models

When a deterministic theoretical utility-based decision model is used, the household is assumed to make the choice that maximizes a multi-attribute utility function. The utility function captures the desirability of each alternative in terms of the combined earthquake-related expenditure and social impact. The uncertainty in the extent of damage caused by the earthquake is considered by selecting the option that maximizes the sum of the expected multi-attribute utilities over all possible building performance states.

$$Max\left\{\sum_{i=1}^{n_{rbls}} P\left(RBLS_i\right)\cdot U\left(x\right)_{LS_i,A_1}, \sum_{i=1}^{n_{rbls}} P\left(RBLS_i\right)\cdot U\left(x\right)_{LS_i,A_2}, ..., \sum_{i=1}^{n_{rbls}} P\left(RBLS_i\right)\cdot U\left(x\right)_{LS_i,A_{n_{alt}}}\right\} \quad (6.3)$$

where $U\left(x\right)_{LS_i,A_j}$ is the utility value associated with limit state LS_i and alternative action A_j, n_{alt} is the number of alternative actions and $P\left(RBLS_i\right)$ is the probability of recovery-based limit state i, which can be obtained from Equation 3.2. Equation 6.3 assumes that (1) after repair/replacement, the property value returns to the pre-earthquake value, (2) the property value after damage is equal to the pre-earthquake value minus the cost of repairing/replacing the damaged residence and (3) if the property is sold, the price is taken to be based on the exact property value.

The sub-attributes used to compute the earthquake-related net expenditure include (1) the repair cost associated with a particular damage state, C_{LS_i}, (2) the cost of purchasing a new residence, C_{NR}, (3) the service fee for selling the current residence, SF, (4) the value of the insurance reimbursement (if home is insured) conditioned on the recovery-based limit state, IR_{LS_i} and (5) the property value of the current resident, C_{CR}. The net expenditure for each alternative, x, is computed based on the relevant costs and reimbursements.

$$x = \begin{cases} C_{LS_i} - IR_{LS_i} - C_{CR} + SF + C_{NR} & for\ A_1 \\ C_{LS_i} - IR_{LS_i} & for\ A_2 \\ C_{NR} - IR_{LS_i} & for\ A_3 \\ C_{NR} - IR_{LS_i} - C_{CR} + SF + C_{LS_i} & for\ A_4 \end{cases} \tag{6.4}$$

For alternative A_1, where the homeowner chooses to repair/replace and sell the old residence, the expenditures include the repair costs, the cost of purchasing a new residence and the fee for selling the old residence. The incoming funds associated with A_1 include the selling price of the house and, the insurance payout (where applicable). For the second alternative, A_2, the homeowner reoccupies the residence after it is repaired and the net expenditure is based on the cost of repairs and the insurance payout. In the case of A_3, the household chooses to abandon the residence and the net expenditure is based on the cost of a new residence and the insurance payout. For A_4, the residence is sold without repairing it and the net expenditure is the same as A_1. The utility function associated with each attribute is established using an exponential form that is representative of a risk-averse decision-maker (Dong et al. 2015). However, it should be noted that other types of utility functions (e.g. linear) could also be used.

$$U(x) = a + b \cdot e^{-cx} \tag{6.5}$$

As noted earlier, the constants a, b and c can be obtained through calibration to observed trends in the post-earthquake decision-making of households or through curve fitting using assumed data points. For example, two data points can be obtained by relating the maximum and minimum earthquake related expenditure to utility values of 0 and 1 respectively. Additionally, the expenditure corresponding to a utility value of 0.5 can be assumed. A curve can be fitted using these three points and the parameters associated with the closed form function shown in Equation 5 can be obtained. Note that the value of the constant b should be positive, which corresponds to a reduction in the utility value as the net expenditure increases.

The social consequence utility function is used to incorporate the earthquake-related inconvenience that is experienced by the household as defined by three sub-attributes: personal time spent, distance traveled and level of "comfort" (based on available utilities) associated with each option. The sub-attributes (e.g., time to move in, etc.) are analyzed separately using the utility function represented in Equation 5 for each one. Once the utility values for the sub-attributes are computed, they are combined using the weighted sum method (Stewart, 1996).

$$U_{soc}(x) = w_T U_T(x) + w_D U_D(x) + w_C U_C(x) \tag{6.6}$$

where $U_T(x)$, $U_D(x)$ and $U_C(x)$ are the utilities associated with time, distance and comfort respectively and w_T, w_D, and w_C are the weighting factors applied to the time, distance and comfort utilities respectively. The weighted sum method is also used to combine the expenditure and social consequence utility values.

$$U(x) = w_{soc} U_{soc}(x) + w_{\exp} U_{\exp}(x) \tag{6.7}$$

where $U_{soc}(x)$ and $U_{\exp}(x)$ are the utilities associated with the social and economic impacts respectively and w_{soc}, and $w_{\exp}$ are the weighting factors applied to the social and economic impacts utilities respectively. Weighting factors can be assumed based on observed trends of post-earthquake decision-making of households or by polling actual decision makers (Dong et al. 2015).

6.3.2 Probabilistic Empirical Utility-Based Decision Models

As noted earlier, probability choice theory seeks to incorporate the uncertainty associated with the perception of the alternatives of the decision-maker and the internal mechanics of his or her decision-making process. This uncertainty arises because of the modeler's lack of knowledge and can therefore be categorized as an epistemic uncertainty. The decision-outcome is described in terms of the probability of choosing each alternative, which captures the difference between the estimated utility values and the actual values used by the decision-maker. This difference is represented by disaggregating the utility value into the component observed by the modeler and an unknown component, which is represented by a random error. Equation 8 is used to define a linear probabilistic utility function in which the parameters can be obtained from statistical analysis of empirical data obtained from surveys of households that have experienced a real or simulated earthquake (Gale 1976).

$$U_{i,k} = \beta_{1,k} X_{1,i} + \beta_{2,k} X_{2,i} + \ldots\ldots\ldots + \beta_{n_{att},k} X_{n_{att},i} + \varepsilon_{i,k} \tag{6.8}$$

where $U_{i,k}$ and $\{\beta\}_k \lfloor X \rfloor_i$ are the actual and estimated utility values, respectively, based on observation i (individual surveyed) and alternative k, $\beta_{j,k}$ is the regression coefficient for predictor (attribute) $(X_{j,i})$, n_{att} is the total number of attributes, and $\varepsilon_{i,k}$ is the random error representing the unknown utility, which is taken to have identical and independent distributions (Type I Extreme Value) across all individuals and alternatives. Note that the utility in Equation 8 is a latent variable and its value is never known by the modeler. The discrete probability distribution for the set of alternatives can be obtained using a multinomial logit model, which is a classification method that is useful for problems with multiple categorically distributed dependent variables.

$$P(A_k) = \frac{e^{\{\beta\}_k \lfloor X \rfloor_i}}{\sum_{k=1}^{n_{alt}} e^{\{\beta\}_k \lfloor X \rfloor_i}} \tag{6.9}$$

where $P(A_k)$ is the probability of choosing alternative k given the set of attributes associated with observation i, $\lfloor X \rfloor_i$. Using the set of predictors and alternatives from the survey data, the maximum likelihood estimator (MLE) can be used to obtain the regression coefficients corresponding to the best choice based on the highest actual utility value. MLE produces the set of coefficients that maximizes the probability of the observed choices. Given a new set of attributes, the logit model shown in Equation 9 and the MLE coefficients, the discrete probability distribution for the set of alternatives can be computed.

6.4 Survey to Develop a Probabilistic Empirical Utility-Based Model of Post-Earthquake Household Decision-Making

Objective: To determine households' preferences for a series of decisions related to post-earthquake recovery of residential buildings, and assess the relationsship between the attractiveness of an alternative and a set of exogenous and endogenous characteristics related to the household and the community in which it resides.

Design and Setting: Structured interviews were conducted between September, 2017 and August, 2018 by undergraduate students at UCLA. Households' demographics and socioeconomics, building physical information, and decision-making were assessed in a cross-sectional survey.

Participants: 42 homeowners and 54 renters in Los Angeles County selected using a stratified random sample.

Measurements: 20 different earthquake-related scenarios were given and asked for a decision for each individual. Multinomial logistic regression model was used to evaluate a priori hypotheses test of whether decisions were associated with predictors acquired in survey. This model was also employed in a case study on five Los Angeles neighborhoods.

Main Results: 1606 of 1680 (95.6%) homeowner responses were useable. 1052 of 1080 (97.4%) renter surveys were useable. Overall, 56%, 21%, and 23% of the homeowners made the decision to reoccupy and repair (if necessary/possible), repair and sell, and sell without repairing, respectively. Similarly, 16%, 46%, and 38% of the renters chose to reoccupy during/after repairs (if necessary/possible), temporarily relocate and permanently relocate. Households in neighborhoods characterized by a high-level income was associated with greater individual likelihood of staying in the original neighborhood. The same case happened for those with more belonging sense of their community.

6.4.1 Declare Variables

Based on the above hypothesis, this study uses the following decision options and independent variables. The variables used in this study include demographic characteristics, socio-economic factors, and earthquake impact to the building and neighborhood.

For each scenario, the homeowner must choose from the following three decision outcomes:

1. Reoccupy their home after making the necessary repairs.
2. Sell their home after making the necessary repairs.
3. Sell their home without making repairs.

Similarly, renters need to select one of the three choices below for each scenario:

1. Reoccupy residence while the building is being repaired (assuming it is safe to occupy).
2. Relocate Temporarily while the building is being repaired (even if it is safe to occupy).
3. Relocate Permanently.

Eight predictors are used in this study: (1) sense of community, (2) number of years living in the neighborhood, (3) earthquake insurance (only applies to homeowners), (4)

occupier's income, (5) physical damage to residence, (6) loss of utilities, (7) building access, and (8) neighborhood evacuation.

The "sense of community" is the number the following services that the participants consider part of their neighborhoods: church, school, gym, job, grocery store, restaurant, theater, bank, and public transportation. Earthquake insurance is a categorical variable indicating whether the homeowners have the insurance or not. Occupiers' income is private information so the data was acquired at the census level from https://www.census.gov/. When considering direct earthquake impact, we provided participants different scenarios responding to various levels of damage involving access to buildings and lifelines, building damage, and neighborhood damage. Participants were asked to choose a decision for each scenario. Lifelines include power, water, and sewerage system. The loss of access is quantified based on the time needed to enter the building, or fully recover the lifelines. The neighborhood damage is measured by percentage of neighborhood vacancy. Initially, four different classes are given to each of variable and three classes to neighborhood vacancy (Table 6-1). This resulted in 3072 ($=4^5 \times 3$) scenarios. In order to decrease the number of scenarios, some simplification rules were implemented.

Table 6-1. Direct variables classification included in the dataset

Class	0	1	2	3
Neighborhood Evacuation(N)	0	50%	100%	
Physical Damage to Residence(R)	None	Minor	Moderate	Extensive
Access to Power(P)	0	24 hrs	2 weeks	3 months
Access to Water(W)	0	24 hrs	2 weeks	3 months
Access to Sewerage(S)	0	24 hrs	2 weeks	3 months
Access to Building(B)	0	1 month	3 months	6 months

Rule 1. Delete all impossible scenarios. For example, if the access to the building and all lifeline systems are allowed immediately after disaster, it is impossible that 50% or 100% neighbors move out of their original community. Also, 0% of neighborhood vacancy with 3 months to the access to the water system will never happen.

Rule 2. Combine power, water, and sewerage into one lifeline system. In other words, the time to access to the power and water system is assumed to be the same as that for sewerage, or we assume only the worst case is considered. For example, in the questionnaire, one scenario can

be described as "The access to power, and/or water, and/or sewerage is allowed within 1 week". This one scenario actually includes 7 cases which is elaborated in the below equation.

$$(P_0,W_0,S_1)=(P_0,W_1,S_0)=(P_1,W_0,S_0)=(P_1,W_1,S_0)=(P_1,W_0,S_1)=(P_0,W_1,S_1)=(P_1,W_1,S_1) \quad (6.10)$$

Using this type of combination, the number of scenarios (3072) goes down to the 192 ($=4^3 \times 3$).

Rule 3. Delete all "repeated" scenarios. Thinking of a situation where the time to access the building is 6 months, repair time and access time to lifeline can be ignored. The reason is that whether the repair time is 1 week, or 1 month, or 3 months, households have to wait for 6 months to live in their houses. In this case, we only keep one scenario and delete the other "repeated" scenarios.

After applying three rules above, 20 scenarios were left, which are listed in the Appendix Questionnaire section. The appendix only shows the questionnaire for homeowners. The renters' questionnaire is the same as that for homeowners except not having earthquake insurance and with different decision choices.

6.4.2 Design Survey

Los Angeles County is chosen as the study region. The final objective is to investigate the households' (both owners and renters) decision-making for all of Los Angeles County. However, gathering information from every single member of that particular population would be exceedingly laborious. Instead, a representative sample is employed to reflect the larger entity. The representative sample in this study is selected according to "income" level. The 20^{th}, 60^{th}, 80^{th} percentile of the household income in the Los Angeles County is below \$18.8k, between \$18.8-\$108.1k, and above \$108.1k respectively (http://statisticalatlas.com/place/California/Los-Angeles/Household-Income). Based on the total population characteristics distributions, three income levels are utilized: low (40%), middle (40%) and high (20%) income. Ideally, the sample should keep the same income distribution.

The size of the sample is important to the model development. A larger sample size can yield more accurate results but costs more. The sample size is determined based on the population size, margin of error and confidence level etc. (Krejcie and Morgan 1970). The margin of error, which determines the confidence interval, indicates how much higher or lower

the responses to survey questions are expected to be if you had asked the entire population. In this study, the total population of Los Angeles County is 10,163,507 (US Census Bureau). Owner-occupied housing rate is 45.7%. 95% confidence level is adopted. 42 owner sample size and 54 renter sample size give 15% and 13% margin of error respectively.

The surveys were conducted by students and faculty of UCLA. Respondents were interviewed using a structured questionnaire that assessed the demographic, socioeconomic, and earthquake impacts to the building and neighborhood. 42 homeowners and 54 renters participated. Participants answered a variety of questions related to different assumed scenarios. Each owner answered 40 questions (w/ and w/o earthquake insurance). Each renter only answered 20 questions. Among owners, 1606 out of 1680 observations are valid. Thus, the response rate is approximately 95.6%. Renters' response rate is 97.4%. All procedures and instruments received approval from Institutional Review Board at University of California, Los Angeles.

6.4.3 Conduct Statistical Analysis

As shown in questionnaire (Appendix), 20 questions related to damage conditions were asked. Each question corresponds to a combination of variables that describe the damage status. The first variable is the neighborhood evacuation level. The variable takes three values: "None" stands for 0; "Almost Half" stands for 0.5; and "Almost All" stands for 1. The second variable is the physical damage to residence. When estimating the model, the damage states are translated to the number of months used to fully repair the building: "None" represents 0 days; "Minor" represents 5 days, "Moderate" represents 120 days; "Extensive" represents 360 days and "Complete" represents 720 days. When two states are presented, one of them will be randomly chosen for estimation. The third variable is the time of utility loss, measured in days. For example, "3 months" will be treated as 90 days. As there are six basic levels of utility loss (0 day, 1 day, 14 days, 30 days, 90 days, and 180 days), if the condition is "< 1 month", one of the three levels that satisfy the requirement (0 day, 1 day, and 14 days) will be randomly selected. The fourth variable is the number of months it takes to access the building after the earthquake. The level can be 0, 1, 3, or 6 months. Similar to the time of utility loss, if the condition is "< 3 months", either 0 or 1 month will be selected with equal probability. Finally, for the owner's data, an additional dummy variable that indicates whether the individual has insurance or not is included, which doubles the number of damage conditions. Other variables that are used to model the individual's choice include the individual's sense of community, the

number of years the individual has lived in the neighborhood, and the individual's annual income. A different model is developed for homeowners and renters.

A multinomial logistic model is used to estimate the individual's preference where Choice 1 is used as the baseline.

For the owners, the model assumes

$$\ln\left(\frac{\text{Prob}(Choice_i=2)}{\text{Prob}(Choice_i=1)}\right) = \beta_{20} + \beta_{21}SEN_i + \beta_{22}YR_i + \beta_{23}NE_i + \beta_{24}DM_i + \beta_{25}UL_i + \beta_{26}AC_i + \beta_{27}I_i + \beta_{28}INS_i \quad (6.11)$$

$$\ln\left(\frac{\text{Prob}(Choice_i=3)}{\text{Prob}(Choice_i=1)}\right) = \beta_{30} + \beta_{31}SEN_i + \beta_{32}YR_i + \beta_{33}NE_i + \beta_{34}DM_i + \beta_{35}UL_i + \beta_{36}AC_i + \beta_{37}I_i + \beta_{38}INS_i \quad (6.12)$$

For the renters, the model assumes

$$\ln\left(\frac{\text{Prob}(Choice_i=2)}{\text{Prob}(Choice_i=1)}\right) = \beta_{20} + \beta_{21}SEN_i + \beta_{22}YR_i + \beta_{23}NE_i + \beta_{24}DM_i + \beta_{25}UL_i + \beta_{26}AC_i + \beta_{27}I_i \quad (6.13)$$

$$\ln\left(\frac{\text{Prob}(Choice_i=3)}{\text{Prob}(Choice_i=1)}\right) = \beta_{30} + \beta_{31}SEN_i + \beta_{32}YR_i + \beta_{33}NE_i + \beta_{34}DM_i + \beta_{35}UL_i + \beta_{36}AC_i + \beta_{37}I_i \quad (6.14)$$

where

- SEN_i is the individual's sense of community.
- YR_i is the number of years the individual has lived in the neighborhood.
- NE_i is the neighborhood evacuation level.
- DM_i is the state of physical damage to residence.
- UL_i is the time of utility loss.
- AC_i is the number of months it takes to access the building.
- I_i is the individual's annual income.
- INS_i is the insurance indicator variable.

It is worth noting that only owner models have the variable INS_i indicating whether the individual has insurance or not.

The model predicts that the probabilities of choosing options 1, 2, and 3, for the renters, are

$$\text{Prob}(Choice_i = 1) = \frac{1}{1+\sum_{j=2}^{3}\exp(\beta_{j0}+\beta_{j1}SEN_i+\beta_{j2}YR_i+\beta_{j3}NE_i+\beta_{j4}DM_i+\beta_{j5}UL_i+\beta_{j6}Ac_i+\beta_{j7}I_i)} \quad (6.15)$$

$$\text{Prob}(Choice_i = 2) = \frac{\exp(\beta_{20}+\beta_{21}SEN_i+\beta_{22}YR_i+\beta_{23}NE_i+\beta_{24}DM_i+\beta_{25}UL_i+\beta_{26}Ac_i+\beta_{27}I_i)}{1+\sum_{j=2}^{3}\exp(\beta_{j0}+\beta_{j1}SEN_i+\beta_{j2}YR_i+\beta_{j3}NE_i+\beta_{j4}DM_i+\beta_{j5}UL_i+\beta_{j6}Ac_i+\beta_{j7}I_i)} \quad (6.16)$$

$$\text{Prob}(Choice_i = 3) = \frac{\exp(\beta_{30}+\beta_{31}SEN_i+\beta_{32}YR_i+\beta_{33}NE_i+\beta_{34}DM_i+\beta_{35}UL_i+\beta_{36}Ac_i+\beta_{37}I_i)}{1+\sum_{j=2}^{3}\exp(\beta_{j0}+\beta_{j1}SEN_i+\beta_{j2}YR_i+\beta_{j3}NE_i+\beta_{j4}DM_i+\beta_{j5}UL_i+\beta_{j6}Ac_i+\beta_{j7}I_i)} \quad (6.17)$$

And the corresponding probabilities, for the owners, are

$$\text{Prob}(Choice_i = 1) = \frac{1}{1+\sum_{j=2}^{3}\exp(\beta_{j0}+\beta_{j1}SEN_i+\beta_{j2}YR_i+\beta_{j3}NE_i+\beta_{j4}DM_i+\beta_{j5}UL_i+\beta_{j6}Ac_i+\beta_{j7}I_i+\beta_{j8}INS_i)} \quad (6.18)$$

$$\text{Prob}(Choice_i = 2) = \frac{\exp(\beta_{20}+\beta_{21}SEN_i+\beta_{22}YR_i+\beta_{23}NE_i+\beta_{24}DM_i+\beta_{25}UL_i+\beta_{26}Ac_i+\beta_{27}I_i+\beta_{28}INS_i)}{1+\sum_{j=2}^{3}\exp(\beta_{j0}+\beta_{j1}SEN_i+\beta_{j2}YR_i+\beta_{j3}NE_i+\beta_{j4}DM_i+\beta_{j5}UL_i+\beta_{j6}Ac_i+\beta_{j7}I_i+\beta_{j8}INS_i)} \quad (6.19)$$

$$\text{Prob}(Choice_i = 3) = \frac{\exp(\beta_{30}+\beta_{31}SEN_i+\beta_{32}YR_i+\beta_{33}NE_i+\beta_{34}DM_i+\beta_{35}UL_i+\beta_{36}Ac_i+\beta_{37}I_i+\beta_{38}INS_i)}{1+\sum_{j=2}^{3}\exp(\beta_{j0}+\beta_{j1}SEN_i+\beta_{j2}YR_i+\beta_{j3}NE_i+\beta_{j4}DM_i+\beta_{j5}UL_i+\beta_{j6}Ac_i+\beta_{j7}I_i+\beta_{j8}INS_i)} \quad (6.20)$$

Maximum Likelihood Estimation is used to estimate the parameters βs.

6.4.4 Estimation Result

Sample Characteristics Analysis

We received 42 questionnaires from owner-occupied households and 54 questionnaires from renter-occupied households. There is one renter who didn't report the zip code, and the final sample contains 42 homeowners and 53 renters. Fig. 6-2 shows the histograms of the sense of community for the homeowners and the renters. The median and mean sense of community for the owners are 4.00 and 4.45 out of 9, while the median and mean sense of community for the renters are 5.00 and 5.18 out of 9. Although the sample size of the renters is larger, there is no clear difference in the distribution of the sense of community between the two samples.

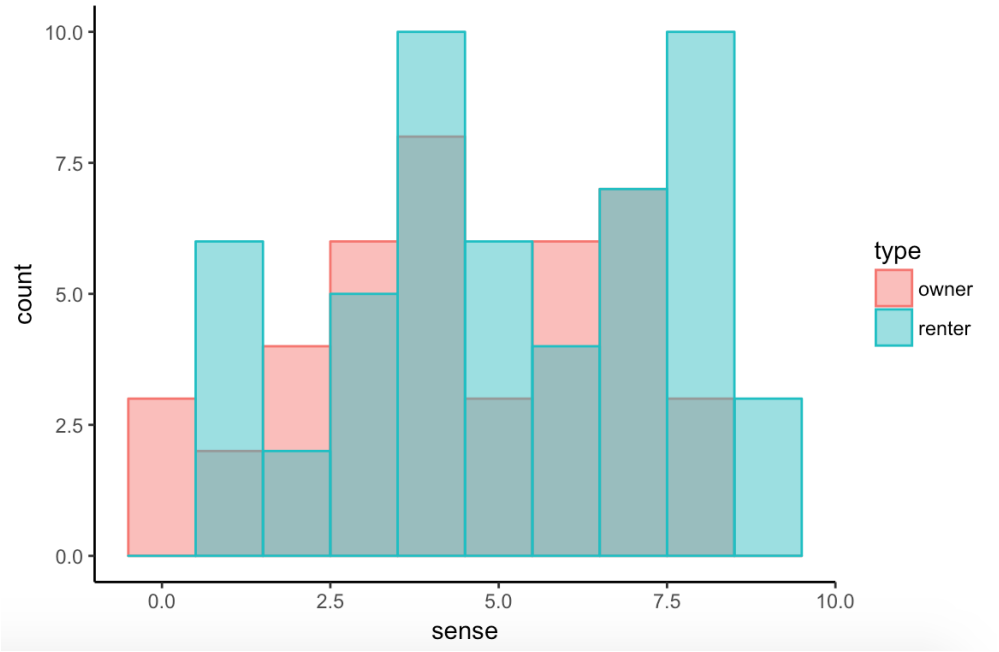

Fig. 6-2. Histogram of sense of community

Fig. 6-3 shows the histograms of the number of years the homeowners and the renters have lived in the neighborhoods. The median and mean for homeowners are 8.00 and 8.34, while the median and mean for renters are 3.00 and 4.84. 79% of the renters lived in their neighborhood for no more than 5 years. The corresponding share for the owners is 50%.

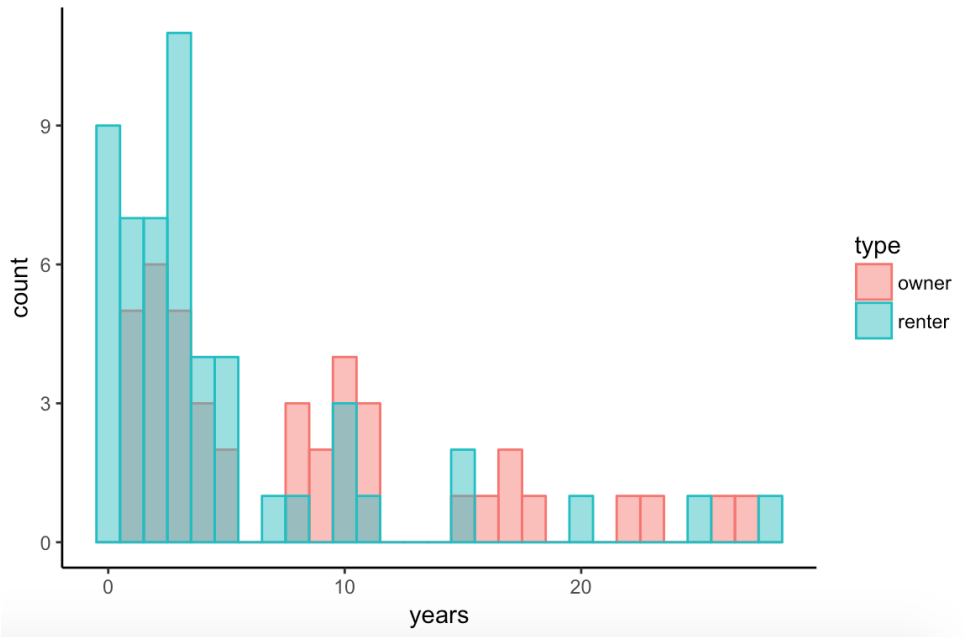

Fig. 6-3. Histogram of living years

Fig. 6-4 shows the histograms of the annual incomes of the neighborhoods where the homeowners and the renters live. The median and the mean incomes of the neighborhoods where the owners live are 72,653 and 75,543, whereas the median and the mean incomes of the neighborhoods where the renters live are 60,965 and 57,982. The histograms suggest that most of the renters in the sample live in relatively lower income neighborhoods, while the neighborhoods of the homeowners have a wider range of classes. Among them, the homeowners' sample income distributions are 5%, 71%, and 24% for low, middle, and high income. The renters' sample income distributions are 19%, 79%, and 2% for low, middle and high incomes.

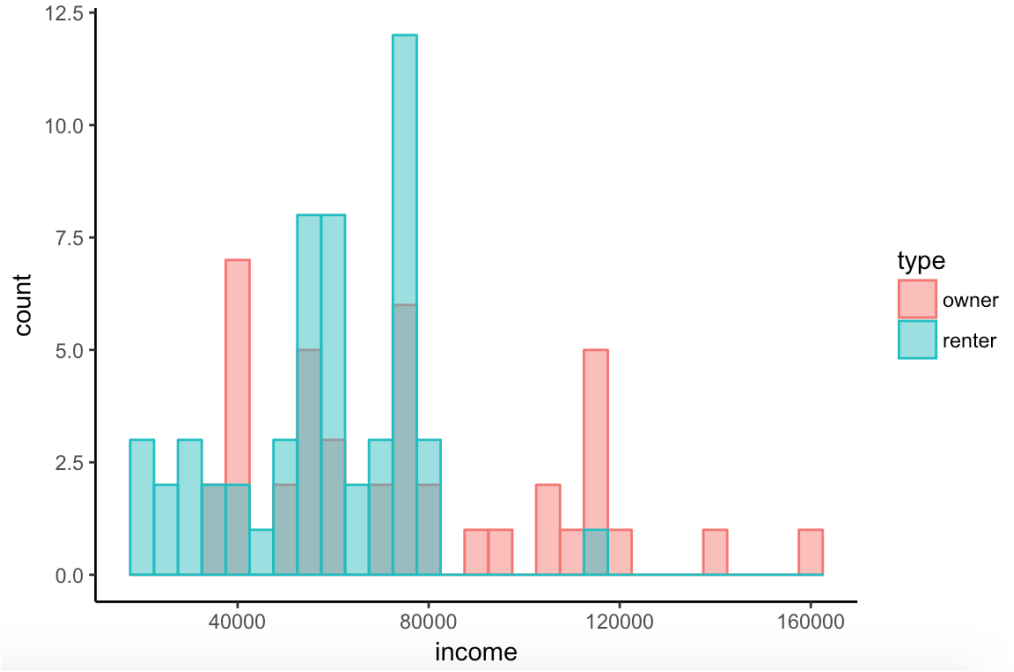

Fig. 6-4. Histogram of annual income

Fig. 6-5 summarizes the choices made by the homeowners under the 20 conditions listed in the questionnaires. The left side of the figure shows the proportions of the individuals, without earthquake insurance, choosing to reoccupy, to repair and sell the building, and to sell the building directly. The right side of the figure shows the corresponding proportions of the individuals choosing the three options with earthquake insurance. Vertical comparisons suggest that as the damage condition becomes more severe (from 1 to 20), a higher proportion of the respondents choose to sell their houses, and a lower proportion choose to reoccupy. Horizontal comparisons between the left and the right sides of the figure show that, under the same damage condition, while the fraction of people choosing to sell their houses are similar, a higher proportion of the residents tend to repair the buildings before selling them.

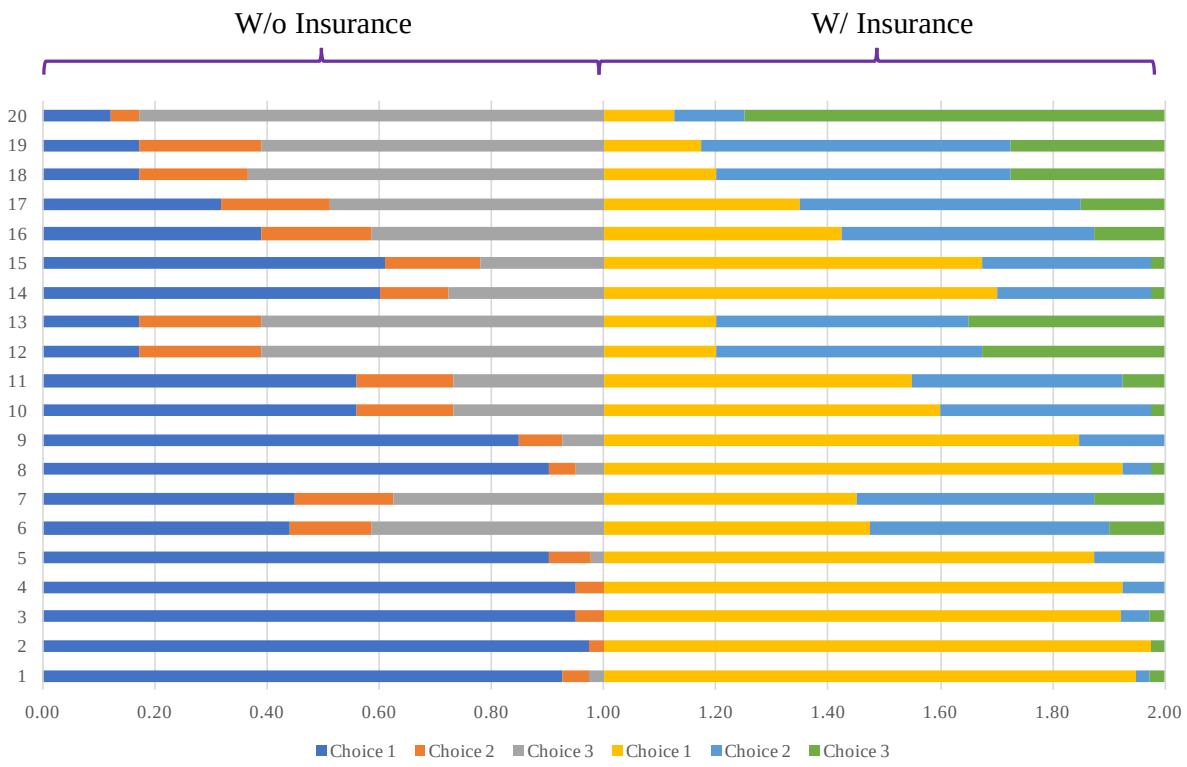

Fig. 6-5. Choice distribution for owners

Fig. 6-6 shows the fraction of the renters choosing to reoccupy, to relocate temporarily, and to relocate permanently under the twenty conditions listed in the questionnaire. Similar to the patterns of the homeowners' choices, as the damage conditions become more severe (from 1 to 20), more people choose to relocate rather than to reoccupy directly.

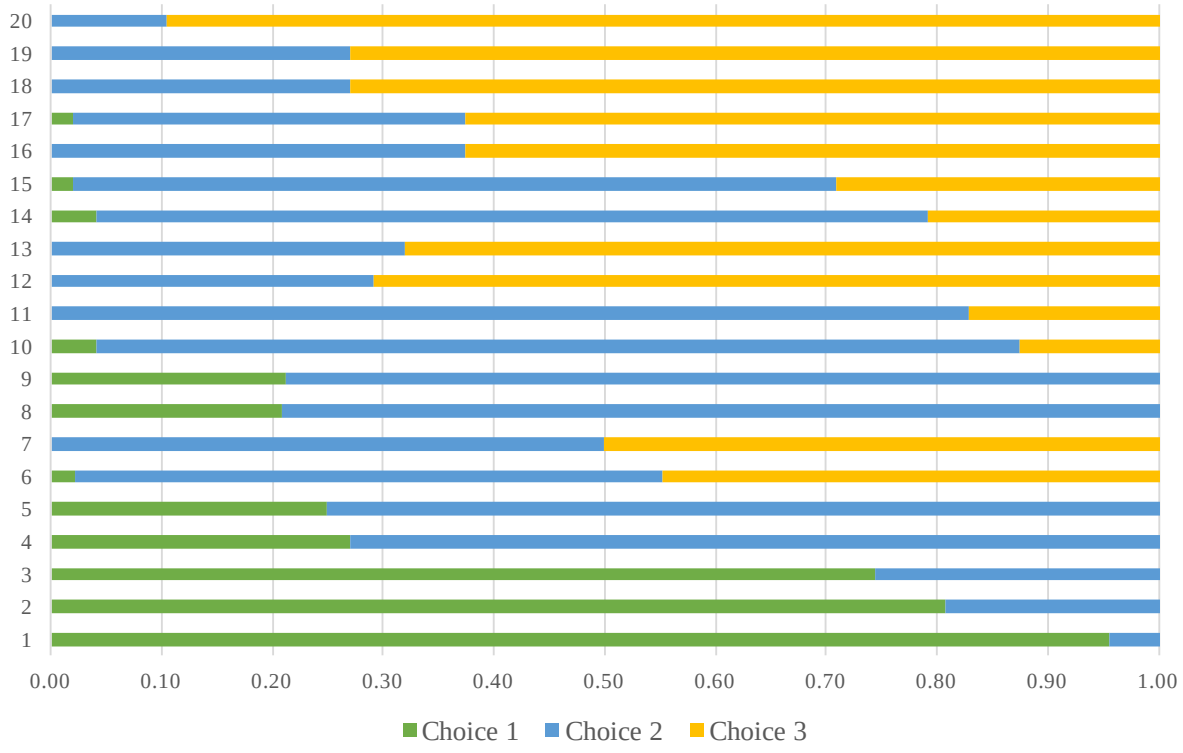

Fig. 6-6. Choice distribution for renters

Estimation Analysis

The data is randomly partitioned into a training set of 70% of the observations and a testing set of 30% of the observations. The training set is used to estimate the parameters, and the testing set is used to compare predictions and observed choices to judge the model accuracy. The goodness of fit was examined. Moreover, cross validation with full dataset is applied to guarantee the goodness of fit. The accuracy of the owner and renter model is 68% and 65%, respectively.

Table 6-2. Confusion matrix and statistics for owners

	Reference		
Prediction	**1**	**2**	**3**
1	237	54	39
2	14	32	13
3	21	14	56

Table 6-3. Confusion matrix and statistics for renters

	Reference		
Prediction	**1**	**2**	**3**
1	33	14	1
2	16	103	51
3	1	27	68

The estimation results are given by the following tables *(*Table 6-4, Table 6-5*).* The result of the statistical significance test is expressed in the form of a p-value. A p-value of 5% is used as the acceptable margin. If the p-value obtained from the hypothesis test falls below 5%, then the null hypothesis is false, the regression coefficient is greater than zero and the predictor is statistically significant. The coefficient can show the effect of each predictor. A larger coefficient stands for larger effect. The negative coefficient means people would like to keep the baseline decision. The positive coefficient indicates that people would like to change their decision from baseline to the current decision. In this study, the baseline decision is always the first choice.

Table 6-4. Parameter estimates for owners

	Choice 2				Choice 3			
	Coefficient	**Std. Errors**	**P-value**		**Coefficient**	**Std. Errors**	**P-value**	
INS	0.63	0.15	1.47E-05	***	-1.15	0.17	2.78E-12	***
SEN	0.03	0.03	3.73E-01		0.02	0.03	5.75E-01	
YR	-0.05	0.01	8.86E-06	***	-0.06	0.01	6.53E-07	***
NE	1.17	0.26	7.41E-06	***	1.17	0.29	4.47E-05	***
DM	0.12	0.02	1.22E-11	***	0.20	0.02	0.00E+00	***
UL	0.38	0.08	3.34E-06	***	0.47	0.09	6.54E-08	***
AC	0.33	0.04	2.22E-16	***	0.43	0.04	0.00E+00	***
I	-0.44	0.17	1.08E-02	***	-0.54	0.19	4.18E-03	***

Table 6-5. Parameter estimates for renters

	Choice 2				Choice 3			
	Coefficient	**Std. Errors**	**P-value**		**Coefficient**	**Std. Errors**	**P-value**	
SEN	-0.01	0.04	8.64E-01		-0.06	0.05	2.50E-01	
YR	0.02	0.02	2.68E-01		-0.04	0.02	6.40E-02	*
NE	-0.74	0.42	7.70E-02	*	0.00	0.49	9.96E-01	
DM	0.69	0.21	1.00E-03	***	0.89	0.21	2.95E-05	***
UL	1.20	0.49	1.50E-02	**	1.23	0.50	1.28E-02	**
AC	0.37	0.39	3.43E-01		0.67	0.39	8.50E-02	*
I	-0.41	0.28	1.33E-01		-0.06	0.33	8.59E-01	

Note: *** if p-value < 0.01, ** if p-value < 0.05, * if p-value < 0.1.

Several findings can be drawn from the estimation results. First, all the predictors except for sense of community shows statistical significance for owners. For renters, the number of years in the current residence, neighborhood vacancy, damage to physical residence, utility loss, and access to building show significance. It is reasonable that as homeowners, when facing earthquake, they will consider more factors compared to renters. Second, having insurance, homeowners would like to sell with repair rather than reoccupy and repair, they have the least priority to sell without repair. Third, the more years they live in the community, the less likely they will leave the community. However, the sense of community (the number of selected items they would consider part of their neighborhood) does not have a strong association with the decision to stay or leave. The renters having more of a sense of belonging choose to reoccupy than relocate permanently. Fourth, the building damage variable has a positive coefficient which demonstrates that a more severe condition would lead both owners and renters to relocate. Utility loss has the most critical effect on the decisions of renters. Owners care about the time to access to the building rather than building damage. The opposite is true for renters. Fifth, higher income increases the chance that both the owners and renters' chance to stay in the neighborhood. Lastly, a higher fraction of the neighbors leaving the neighborhood makes the individual more likely to move.

6.5 Integrating Household Decision-Making into Stochastic Simulation Model

6.5.1 Conceptual Framework

Household decision-making is incorporated in the stochastic simulation model by defining a set of probabilistically characterized decision paths at the individual building-level based on 1) the possible decision outcomes of the building owner and occupiers and functioning states immediately following an event, 2) the activities needed to restore occupancy and functionality given the condition of the building immediately following the event, and 3) the possible decision outcomes of the building owner and occupiers at various time intervals during recovery.

If decision-making is not incorporated in the model, the relationship between the recovery-based damage states and post-event actions is assumed deterministic and there is a single recovery path. The decision model is integrated with the stochastic process model by defining a unique recovery path for each of the possible decision-outcomes of the building owner and occupier. These recovery paths will differ based on the ensuing recovery activities and time spent in the various functioning states. Fig. 6-7 shows a conceptual illustration of such

decision paths for a single building represented using three functioning states. The discrete probability distribution for the possible paths to recovery are obtained using the probabilistic empirical utility-based decision models described earlier. Therefore, in addition to the uncertainty in the damage state and time spent in each functioning state, the uncertainty in the path to recovery, which is represented in the decision-model, is incorporated in the stochastic simulation model.

Note that functioning states shown in Fig. 6-7 are not intended to be exhaustive. Additional states will need to be defined in order to consider the uncertainty in the action that will be undertaken by the household immediately following the earthquake and during the recovery process. Examples of other relevant functioning states not shown in Fig. 6-7 include, the building is safe with some loss of functionality but unoccupied (e.g. occupants decide to leave because of disruption in utility services) and the building is fully functional but unoccupied (for reasons unrelated the state of the building itself).

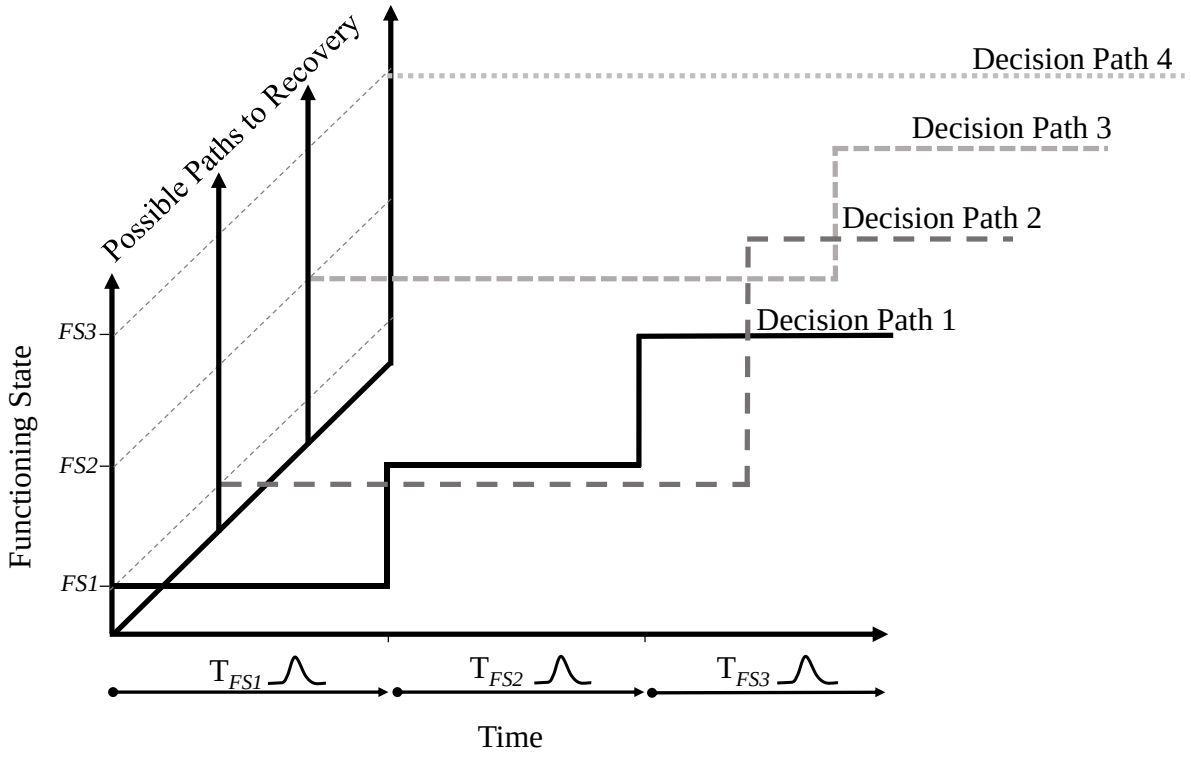

Fig. 6-7. Partial conceptual representation of recovery decision and event paths possible for an individual household conditioned on the immediate post-earthquake limit state of their building.

6.5.2 Application to Two Los Angeles County Neighborhoods (Koreatown and Lomita)

In this section, the decision model is incorporated in developing recovery trajectories for two Los Angeles County neighborhood. Two key things: (1) for the decision-making model, the output is the probability of each choice for owners and renters and the input is damage to the building, lifeline, sense of community, and characteristics of household; (2) for the recovery model, the output is the community level trajectory and the input is recovery path for each decision and the output from the decision-making model. For the decision-making model, the multinomial logistic regression model was obtained in section 6.4. The building damage can be acquired from fragility functions in chapter 5. No lifeline damage is assumed. The sense of community is randomly sampled from a uniform distribution. Applying those predictors to multinomial logistic models, the probability of each choice can be computed. Fig. 6-8 presents the recovery path for owners when decision making is considered. If the owner chooses to sell his or her house, a selling time is added to the path. Also, the house has to be vacated during all activities. It is worth noting that the house is occupied if it is safe when people choose to repair and reoccupy. Fig. 6-9 describes the recovery path for renters. As long as renters relocate (temporally or permanently), the building will be vacated. The time parameters used are the same ones as those in Chapter 5.

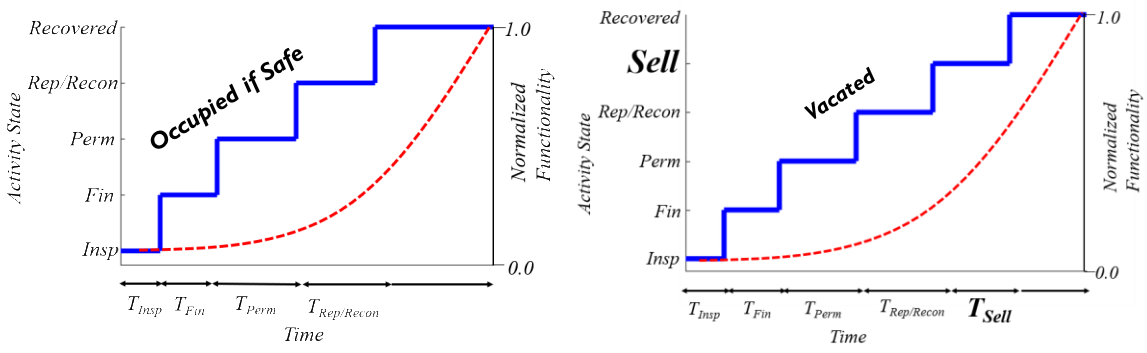

(a) (b)

Fig. 6-8. Recovery path of owners for (a) choice 1: repair and reoccupy, and (b) choice 2&3: sell with & without repair

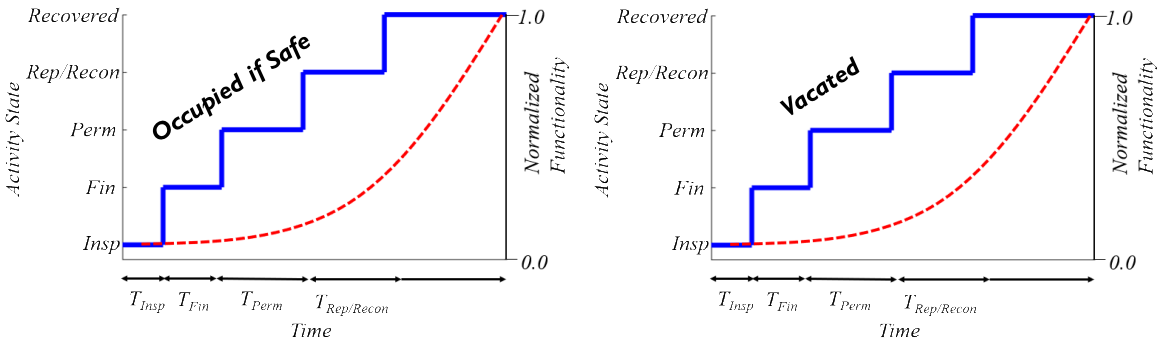

(a) (b)

Fig. 6-9. Recovery path of renters for (a) choice 1: reoccupy, and (b) choice 2&3: relocate temporally & permanently

As noted in Chapter 5, the Los Angeles case study included five neighborhoods: Koreatown, Westlake, Pico Union, East Hollywood, and Lomita. In this section, only Koreatown and Lomita are considered as they are very different and can be used to highlight the effect of decision-making. Koreatown has 93% of rental housing while Lomita only has 50%. Koreatown has 28% soft story building while Lomita almost has no soft story. Moreover, household income in Lomita is much higher than Koreatown. Fig. 6-10. presents the decision-making result which brings some interesting findings. More severe damage leads owners to sell their buildings, renters relocate temporally or permanently. Owners/Renters with high income would like to repair and reoccupy.

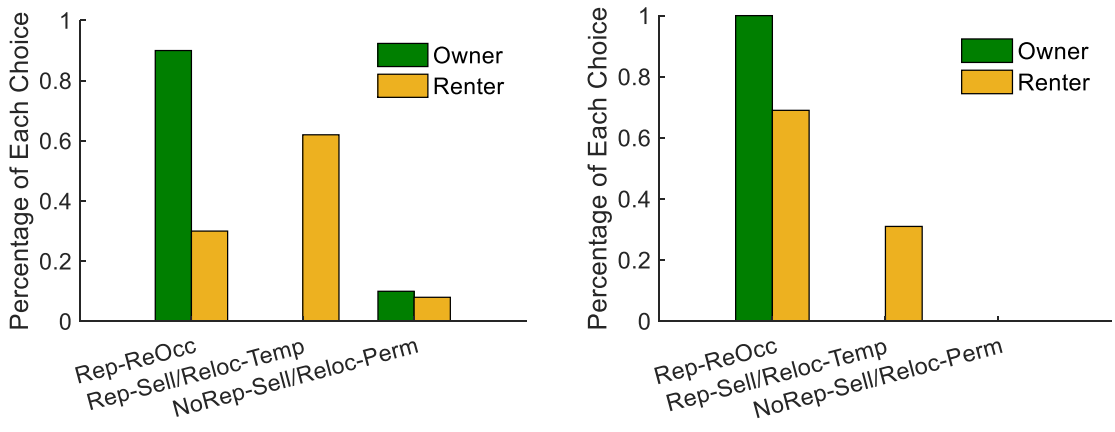

(a) (b)

Fig. 6-10. Decision-Making result for (a) Koreatown, and (b) Lomita

The sensitivity analysis is conducted on various sell/vacant time. **Error! Reference s ource not found.** shows the recovery result considering the decision-making models. After incorporating decision-making part, the pace of the recovery decreases. Furthermore, increasing the selling and vacant time will slower the pace of recovery.

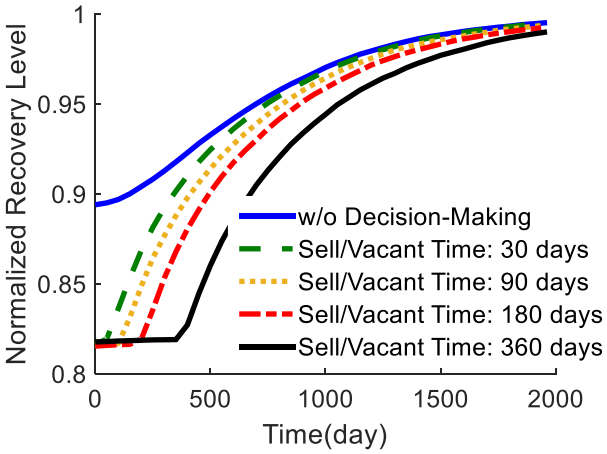

Fig. 6-11. Effect of sell/cacant time on post-earthquake recovery

Fig. 6-12 demonstrates an almost linear relationship between selling/vacant time and mean time to achieve 95% recovery.

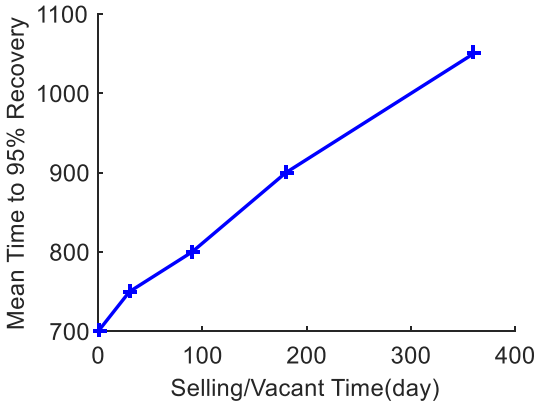

Fig. 6-12. Relationship between selling/vacant time and mean time to achieve 95% recovery

6.6 Summary and Conclusion

The uncertainty in the decision-outcomes of households affected by the disaster can be captured using theoretical or empirical utility models. Theoretical models are based on maximizing the utility of the relevant stakeholders and empirical models are established based on the results of controlled surveys. Given the immediate post-earthquake state of a building and the probabilistic characterization of possible decision outcomes, a characteristic recovery

path is established, which defines the discrete functioning states (or activities) needed to bring about recovery and the time spent in each state. This study showed that characteristics of the household and buildings are associated with likelihood of different post-earthquake decisions. This study adds to the growing literature that suggests the importance of sense of community, household income, damage of lifelines, physical buildings, and time to enter the building on resilience. The sensitivity of various selling and vacant time to the pace of recovery is also investigated. The results of such a study is relevant to national efforts such as the Rockefeller Foundation's 100 Resilient Cities, which will bring attention to mounting issues related urban disaster resilience and provide information and tools to understand and act upon the necessary solution alternatives

CHAPTER 7: Conclusion, Limitations and Future Work

7.1 Overview

The primary objective of the study is to present an overall framework for quantifying the seismic resilience of residential communities, which integrates probabilistic building performance assessment, household decision-making and socioeconomic vulnerability. Two case studies were performed to validate the framework: 2014 South Napa Earthquake and Los Angeles Ordinance. The proposed recovery model can provide an effective way to engage key stakeholders from government, industry and other groups, who are concerned with enhancing disaster recovery of residential communities. More specifically, the model can be used to assist policy-makers, municipal governments and planners in understanding the possible interdependencies, interventions, and tradeoffs associated with housing recovery. The interdisciplinary scope of the proposed framework will provide a unique opportunity for collaboration and constructive exchanges between disaster researchers from different fields, including structural engineering, urban planning, geography and sociology.

7.2 Findings

7.2.1 Chapter 2: Modeling post-disaster restoration of socio-technical systems: a state of the art review

A comprehensive review of methods to simulate disaster recovery is presented. Five main types of models are described and compared to assess the time-dependent effects of hazard events on the built environment. Empirically-based statistical model is the most straight forward method where data from previous disaster is employed to fit recovery curve or to study trends on building characteristics. Agent-based model models recovery process as a dynamic system of interacting agents so that individual entities that may speed or constraint the pace of disaster recovery process and their interdependencies inherent between key agents can be investigated. Stochastic simulation model performs a sampling-based computational simulation that keeps track of recovery process with random increments over any time interval. Therefore, this method is complemented with stochastic process and Monte-Carlo simulation. Discrete event simulation (DES) model assumes each event occurs at a particular instant in time and changes the state of the system. Contrasting to continuous simulation, no change is allowed between

consecutive events. Network Models use a series of links that connect a supply node and multiple demand nodes as the neuron-like units to optimize system.

7.2.2 Chapter 4: Stochastic Process Models of Post-Earthquake Recovery

Post-earthquake recovery models can be used as decision-support tools for pre-event planning. However, due to a lack of available data, there have been very few opportunities to validate and/or calibrate these models. This chapter describes the use of building damage, permitting and repair data from the 2014 South Napa Earthquake, to evaluate a stochastic process simulation post-earthquake recovery model. Damage data was obtained for 1470 buildings and permitting and repair-time data was obtained for a subset (456) of those buildings. A "blind" simulation is shown to adequately capture the shape of the recovery trajectory despite overpredicting the overall pace of the recovery. Using the mean time-to-permit and repair time from the acquired dataset significantly improves the accuracy of the recovery simulation. A generalized simulation model is formulated by establishing statistical relationships between key time parameters and endogenous and exogenous factors that have been shown to influence the pace of recovery.

7.2.3 Chapter 5: Effect of Los Angeles Soft-Story ordinance on the post-earthquake housing recovery of impacted residential communities

Post-earthquake recovery models can be used quantify the resilience-related benefits of policies intended to mitigate building seismic risk. An assessment of the effect of the Los Angeles Soft-Story Ordinance on the post-earthquake housing recovery of residential communities is presented herein. An inventory of 8,000 buildings located in five Los Angeles neighborhoods is considered. The neighborhoods vary based on the percentage of soft-story buildings, population density and the fraction of renter- versus owner-occupied residences. Archetype buildings that are representative of the target inventory are developed based on a building-by-building survey performed using Google Street View. Variations in the number of stories and presence and layout of soft-first story are considered in the development of the archetypes. Analytical building level damage fragility curves are developed using the results nonlinear analyses of structural models representing each archetype. A scenario-based damage assessment is performed using shaking intensities generated from the Southern California ShakeOut scenario and a discrete-time state-based stochastic process model is used represent post-earthquake recovery. The quantified effect of the Ordinance retrofit varied based on the considered recovery metric. For instance, the initial loss of occupancy for the entire inventory

is reduced by 25%. However, if the time to restore 90% occupancy is used as the recovery performance metric, the Ordinance retrofit leads to a 64% reduction.

7.2.4 Chapter 6: Modeling post-earthquake decisions of owners and renters of residential buildings

In this chapter, the spatiotemporal likelihoods and influences of homeowners' decisions whether to repair, reoccupy, sell, or abandon damaged homes is explicitly investigated based on building and neighborhood conditions, socio-demographic factors and lifeline services. Two alternative approaches to accounting for the uncertainty in the decision-outcomes of households affected by the disaster is presented. The first approach uses a purely theoretical model in which the household decision is assumed to be based on achieving the maximum utility. In the second approach, a statistical model is formulated based on the results of surveys in which participants are asked to choose from alternative courses of action based on a lived or simulated earthquake scenario. Structured interviews were conducted in Los Angeles City. 20 different earthquake-related scenarios were given and asked for a decision for each individual. Multinomial logistic regression model examined a priori hypotheses testing whether decisions was associated with predictors acquired in survey. 1067 among 1120 (95%) are valid responses for homeowners. 952 among 980 (97%) are valid responses for renters. Homeowners with earthquake insurance prefer selling with repair rather than reoccupy, and have the least priority of sell without repairing. Both homeowners and renters would like to leave their community when facing more severe damaged situation. Among all scenarios, the effects on physical damage to residence, building access, loss of utilities and neighborhood evacuation decrease respectively. Future prospective work designed to integrate household decision-making into a post-earthquake recovery model may guide government, policy-maker and urban planning efforts aimed at improving community resiliency.

7.3 Limitations and future work

- The main focus of the current study is to formulate a comprehensive framework for post-earthquake recovery and show its viability through application to a set of regions and scenarios. It is important to note that the findings of the present study in terms of the potential seismic resilience and recovery that a building can experience are limited to residential buildings. More studies with a variety of buildings, ground motions and sites with different characteristics are needed to quantify the impact of earthquakes on post-earthquake recovery performance more broadly.

- The main purpose of this study was to demonstrate the viability of the discussed approach for static recovery process i.e. recovery paths and decisions don't change over time. Bayesian methods can be applied to improve the current modeled post-earthquake recovery using "real-time" data to update predictions over time.
- The validation study was conducted for a single event (2014 South Napa earthquake). More datasets are needed to create a truly generalized model that can be applied to different recovery contexts (e.g. urban versus rural regions, different scales of damage etc.).
- The effect of disruption to lifelines and other sectors of the economy (e.g. business) was implicitly considered in this study by using temporal parameters that are based on prior recovery events. Future research could focus on integrating the methods developed as part of this work into multi-sector (e.g. housing and businesses) recovery models that explicitly represent lifeline functionality disruption and restoration.
- For the decision-models developed in the current study, homeowner and renter choices are fixed immediately following the earthquake. However, it is possible for residents to change their decision during the course of the recovery process. Future work on household decision making in the context of post-earthquake recovery should incorporate these dynamic conditions.

Appendix

POST-EARTHQUAKE DECISION-MAKING QUESTIONNAIRE

This survey is part of a research project funded by the National Science Foundation (CMMI grant # 1538747) entitled "Modeling Post-Earthquake Recovery of Residential Communities". The overall goal of the research is to develop engineering tools and methods that can be used to inform policies and planning for earthquake resilient communities. To help us achieve this goal, we are asking the survey participants to answer a series of questions related to their likely decision-making after a major earthquake. The survey has approved by the UCLA Institutional Review Board and no information related to your personal identity is needed.

Your zip code: _____

Sense of Neighborhood:

To what degree do you feel a sense of belonging to your current neighborhood?

1. None 2. Some 3. High

Circle the item shown below that you would consider part of your neighborhood?

1. Church 2. School 3. Gym
4. Job 5. Grocery store 6. Restaurant
7. Theater 8. Bank 9. Public Transportation

How long have you been a resident of your current community? _____

There are two tables of questions below. Each question/row presents a unique earthquake damage or socioeconomic impact scenario, which is described in terms of the following impact categories: (a) the extent to which your neighborhood is vacated because of earthquake damage, (b) the physical damage to your residence, (c) availability of utilities (water, sewer and power) after the event and (d) loss of access to your residence. Guidelines for interpreting the impact categories are shown below.

Guidelines for Interpreting Earthquake Impact Categories:

Neighborhood evacuation: The percentage of homes in your neighborhood that have been vacated as a result of earthquake damage.

Physical damage to residence:

- **None:** Little or no damage to your house.
- **Minor:** Small cracks in walls (repair involves patching and painting), doors (useable without repairs) and windows (glass needs to be replaced) and chimney (can be patched).
- **Moderate:** Large cracks walls (repairs involve patching and painting) and doors (small repairs needed), broken windows (glass and frame needs to be replaced) and cracked chimneys (can be repaired by replacing individual blocks).
- **Extensive:** Major damage to walls (entire wall needs to be replaced) and doors (need to be re-built or replaced). The building has a permanent lean. Chimney has toppled. Partial collapse of "room-over-garage" and large cracks in foundations.

Loss of utilities: The time it takes for power, and/or water, and/or sewerage system in your house to be restored.

Building access: The time it takes for your building to be accessible. Inaccessibility may be a result of damage nearby roads and bridges or safety concerns during repairs.

For each scenario, select (check the box) from one of three decision options:

1. **Reoccupy** your residence after making the necessary repairs
2. **Sell** your home **after** making the necessary **repairs**
3. **Sell** your home **without (w/o)** making **repairs**

Also note that you will need to provide two answers for each scenario. One assuming you have earthquake insurance (left three columns) and another assuming you do not have earthquake insurance (right three columns).

No.	Neighborhood Evacuation	Physical Damage to Residence	Loss of Utilities	Building Access	You have earthquake insurance			You do NOT have earthquake insurance		
					Reoccupy	Sell w/ Repair	Sell w/o Repair	Reoccupy	Sell w/ Repair	Sell w/o Repair
1	**Almost Half**	None	None	Immediate	☐	☐	☐	☐	☐	☐
2	None	None	**24hrs**	Immediate	☐	☐	☐	☐	☐	☐
3	*Almost Half*	None	**24hrs**	Immediate	☐	☐	☐	☐	☐	☐
4	None	Minor or None	**2 weeks**	Immediate	☐	☐	☐	☐	☐	☐
5	*Almost Half*	Minor or None	**2 weeks**	Immediate	☐	☐	☐	☐	☐	☐
6	*Almost Half*	Moderate or Lower	**3months**	<3 months	☐	☐	☐	☐	☐	☐
7	*Almost All*	Moderate or Lower	**3months**	< 3 months	☐	☐	☐	☐	☐	☐
8	None	**Minor**	<2 weeks	Immediate	☐	☐	☐	☐	☐	☐

9	*Almost Half*	**Minor**	<2 weeks	Immediate	☐	☐	☐	☐	☐	☐
10	*Almost Half*	**Moderate**	< 1 month	Immediate	☐	☐	☐	☐	☐	☐
11	*Almost All*	**Moderate**	< 1 month	Immediate	☐	☐	☐	☐	☐	☐
12	*Almost Half*	**Extensive**	< 3 months	<3 months	☐	☐	☐	☐	☐	☐
13	*Almost All*	**Extensive**	< 3 months	< 3months	☐	☐	☐	☐	☐	☐
14	*Almost Half*	Moderate or Lower	< 1 month	**1 month**	☐	☐	☐	☐	☐	☐
15	*Almost All*	Moderate or Lower	< 1 month	**1 month**	☐	☐	☐	☐	☐	☐
16	*Almost Half*	Moderate or Lower	< 3 months	**3 months**	☐	☐	☐	☐	☐	☐
17	*Almost All*	Moderate or Lower	< 3 months	**3 months**	☐	☐	☐	☐	☐	☐
18	*Almost Half*	Extensive or Lower	<6 months	**6 months**	☐	☐	☐	☐	☐	☐
19	*Almost All*	Extensive or Lower	< 6 months	**6 months**	☐	☐	☐	☐	☐	☐
20	**Your building is not repairable and has to be demolished.**				☐	☐	☐	☐	☐	☐

References

Almufti, I. and Willford, M., 2013. REDi Rating System - Resilience-based Earthquake Design Initiative for the Next Generation of Buildings.

Akaike, H., 1998. Information theory and an extension of the maximum likelihood principle. In *Selected Papers of Hirotugu Akaike* (pp. 199–213). incollection, Springer.

Applied Technology Council, 1995. *Procedures for Post-earthquake building safety evaluation procedures, ATC-20,* Redwood City, CA.

ASCE, 2016. ASCE/SEI 7-16 Minimum Design Loads for Buildings and Other Structures. Reston, Virginia.

Balakrishnan, N., 1991. Handbook of the Logistic Distribution. Marcel Dekker, Inc. ISBN 978-0-8247-8587-1.

Ballantyne, D. B., and Taylor, C., 1990. Earthquake Loss Estimation Modeling of the Seattle Water System Using a Deterministic Approach, *In Lifeline Earthquake Engineering*, pp. 747-760.

Bell, D. E., and Raiffa, H., 1988. *Decision making: Descriptive, normative, and prescriptive interactions.* Cambridge University Press.

Ben-Akiva, M. E., and Lerman, S. R., 1985. *Discrete choice analysis: theory and application to travel demand (Vol. 9)*. MIT press.

Binder, S. B., Baker, C. K., and Barile, J. P., 2015. Rebuild or relocate? Resilience and postdisaster decision-making after Hurricane Sandy, *American journal of community psychology*, 56(1-2), 180-196.

Bocchini, P., and Frangopol, D. M., 2012. Restoration of bridge networks after an earthquake: multicriteria intervention optimization. *Earthquake Spectra*, *28*(2), 426–455. article.

Brink, S., Davidson, R. A., and Tabucchi, T. H. P., 2009. Estimated durations of post-earthquake water service interruptions in Los Angeles. *Proceedings of TCLEE*, 539–550. article.

Bruneau, M., Chang, S. E., Eguchi, R. T., Lee, G. C., O'Rourke, T. D., Reinhorn, A. M., … Von Winterfeldt, D., 2003. A Framework to Quantitatively Assess and Enhance the Seismic Resilience of Communities. *Earthquake Spectra*, *19*(4), 733–752. http://doi.org/10.1193/1.1623497

Burton, H. V., Deierlein, G., Lallemant, D., and Lin, T., 2015. Framework for incorporating probabilistic building performance in the assessment of community seismic resilience, *Journal of Structural Engineering*, 142(8), C4015007.

Burton, H. V., Kang, H., 2017. Towards the seismic resilience of residential communities: a conceptual framework and case study, *Proceedings of the 16th World Conference on Earthquake Engineering*, Santiago, Chile.

Burton, H. V., Miles, S.B. and Kang, H., 2018. "Integrating performance based engineering and urban simulation to model post-earthquake housing recovery," *Earthquake Spectra* (accepted for publication).

Çağnan, Z., Davidson, R., and Guikema, S., 2004. Post-earthquake restoration modeling of electric power systems. *Proceedings of the 13th World Conference on Earthquake Engineering*, Vancouver, British Columbia.

Çağnan, Z., Davidson, R. A., and Guikema, S. D., 2006. Post-earthquake restoration planning for Los Angeles electric power, *Earthquake Spectra*, 22(3), 589-608.

Çağnan, Z., and Davidson, R. A., 2007. Discrete event simulation of the post-earthquake restoration process for electric power systems, *International Journal of Risk Assessment and Management*, 7(8), 1138-1156.

Chang, S. E., Eguchi, R. T., and Seligson, H. A., 1996. Estimation of the economic impact of multiple lifeline disruption: Memphis light, gas and water division case study.

Chang, S. E., Shinozuka, M., and Svekla, W., 1999. Modeling post-disaster urban lifeline restoration, In *Optimizing Post-Earthquake Lifeline System Reliability*, pp. 602–611.

Cimellaro, G. P., Reinhorn, A. M., and Bruneau, M., 2010. Framework for analytical quantification of disaster resilience, *Engineering Structures*, 32(11), 3639–3649.

Cole, P. M. S., 2003. An empirical examination of the housing recovery process following a disaster, Ph.D. dissertation, Texas A & M University, College Station.

Comerio, M. C., 1998. *Disaster hits home: New policy for urban housing recovery*. book, Univ of California Press.

Comerio, M. C., 2006. Estimating downtime in loss modeling, *Earthquake Spectra*, 22(2), 349-365.

Comerio, M. C., and Blecher, H. E., 2010. Estimating downtime from data on residential buildings after the Northridge and Loma Prieta Earthquakes, *Earthquake Spectra*, 26(4), 951-965.

Council, A. T., Scawthorn, C., Khater, M., Rojahn, C., and Cluff, L. S., 1991. *Seismic Vulnerability and Impact of Disruption of Lifelines in the Conterminous United States*. book, Applied Technology Council.

Davidson, R. A., and Cagnan, Z., 2007. Discrete event simulation of the post-earthquake restoration process for electric power systems. *International Journal of Risk Assessment and Management*, *7*(8), 1138–1156. http://doi.org/10.1504/IJRAM.2007.015298

Dong, Y., Frangopol, D. M., and Sabatino, S., 2015. Optimizing bridge network retrofit planning based on cost-benefit evaluation and multi-attribute utility associated with sustainability, *Earthquake Spectra*, 31(4), 2255-2280.

Decò, A., Bocchini, P., and Frangopol, D. M., 2013. A probabilistic approach for the prediction of seismic resilience of bridges, *Earthquake Engineering & Structural Dynamics*, 42(10), 1469–1487.

Didier, M., Sun, L., Ghosh, S., and Stojadinovic, B., 2015. Post-earthquake recovery of a community and its electrical power supply system, *Proceedings of the 5th international conference on computational methods in structural dynamics and earthquake engineering*, Crete, Greece.

Earthquake Engineering Research Institute (EERI), 2014. EERI Special Earthquake Report, M6.0 South Napa Earthquake of August 24, 2014, available at http://www.eqclearinghouse.org/2014-08-24-south-napa/preliminaryreports/ (last accessed 19 January 2017).

Eid, M. S., and El-Adaway, I. H., 2017. Sustainable disaster recovery: multiagent-based model for integrating environmental vulnerability into decision-making processes of the associated stakeholders. Journal of Urban Planning and Development, 143(1).

Elliott, J. R., 2014. Natural hazards and residential mobility: General patterns and racially unequal outcomes in the United States, *Social Forces*, 93(40, 1723-1747.

Folz, B., and Filiatrault, A., 2001. Cyclic analysis of wood shear walls. *Journal of Structural Engineering*, 127(4), 433-441.

FEMA P695, Quantification of building seismic performance factors, Applied Technology Council, Redwood City, CA, 2009.

Federal Emergency Management Agency (FEMA), 2003. *HAZUS MR4 Technical Manual, Multi-hazard Loss Estimation Methodology*, Washington, D.C..

Federal Emergency Management Agency (FEMA), 2012. *Seismic Performance Assessment of Buildings. FEMA P58-1*, Redwood City, CA.

Federal Emergency Management Agency (FEMA), 2015. *Performance of Buildings and Nonstructural Components in the 2014 South Napa Earthquake. FEMA P-1024,* Washington, D.C.

Gale, D., 1976. The linear exchange model, *Journal of Mathematical Economics*, 3(2), 205-209.

Geis, D. E., 1996. Creating sustainable and disaster resistant communities: Elements of change natural hazards and global change. In *Creating sustainable and disaster resistant communities: Elements of change natural hazards and global change*. incollection, US The Aspen Global Change Institute.

Geotechnical Extreme Events Reconnaissance (GEER) Association, 2014. *Geotechnical engineering reconnaissance of the August 24, 2014 M6 South Napa earthquake. GEER Association Report No. GEER-0*37.

Gilbert, N., 2008. Agent-based models (quantitative applications in the social sciences). *Series, 7*, 2006. article.

Gilbert, S. W., 2010. Disaster resilience: A guide to the literature. *NIST Special Publication, 1117*. article.

Graves, R. W., Aagaard, B. T., Hudnut, K. W., Star, L. M., Stewart, J. P., and Jordan, T. H., 2008. Broadband simulations for Mw 7.8 southern San Andreas earthquakes: Ground motion sensitivity to rupture speed. Geophysical Research Letters, 35(22).

Grinberger, A. Y., and Felsenstein, D., 2014. Bouncing back or bouncing forward? Simulating urban resilience. *Proceedings of the Institution of Civil Engineers-Urban Design and Planning*, 167(3), 115–124.

Grinberger, A. Y., Lichter, M., and Felsenstein, D., 2015. Simulating urban resilience: Disasters, dynamics and (synthetic) data. In *Planning Support Systems and Smart Cities*, pp. 99–119.

Grinberger, A. Y., and Felsenstein, D., 2016. Dynamic agent based simulation of welfare effects of urban disasters. Computers, *Environment and Urban Systems*, 59, 129–141.

Grinberger, A. Y., and Felsenstein, D., 2017. A Tale of Two Earthquakes: Dynamic Agent-Based Simulation of Urban Resilience. *Applied spatial modeling and planning*, Routledge, Abington, forthcoming.

Haas, J.E., Kates, R. and Bowden, M. J., 1977. Reconstruction Following Disaster, *In Reconstruction following disaster (MIT Press)*, Cambridge, MA.

Han, S.-R., Guikema, S. D., Quiring, S. M., Lee, K.-H., Rosowsky, D., and Davidson, R. A. , 2009. Estimating the spatial distribution of power outages during hurricanes in the Gulf coast region. *Reliability Engineering & System Safety*, *94*(2), 199–210.

Huling, D., and Miles, S. B., 2015. Simulating disaster recovery as discrete event processes using python. In *Global Humanitarian Technology Conference (GHTC)*, pp. 248–253.

Ibarra, L. F., Medina, R. A., and Krawinkler, H., 2005. Hysteretic models that incorporate strength and stiffness deterioration. Earthquake engineering & structural dynamics, 34(12), 1489-1511.

Iervolino, I., and Giorgio, M., 2015. Stochastic Modeling of Recovery from Seismic Shocks, *Proceedings of the 12th International Conference on Applications of Statistics and Probability in Civil Engineering*, Vancouver, Canada

Isumi, M., Nomura, N., and Shibuya, T., 1985. Simulation of post-earthquake restoration for lifeline systems, *International Journal of Mass Emergencies and Disasters*, 3(1), 87-105.

Jennings, E., Van De Lindt, J. W., Ziaei, E., Bahmani, P., Park, S., Shao, X., and Gershfeld, M., 2015. Full-scale experimental verification of soft-story-only retrofits of wood-frame buildings using hybrid testing. *Journal of Earthquake Engineering*, 19(3), 410-430.

Jerry, B., 1984. *Discrete-event system simulation*. book, Pearson Education India.

Jones, L. M., Bernknopf, R., Cox, D., Goltz, J., Hudnut, K., Mileti, D., and Seligson, H. , 2008. The shakeout scenario. US Geological Survey Open-File Report, 1150, 308.

Kang, D., and Lansey, K., 2013. Post-earthquake restoration of water supply infrastructure. In *World Environmental and Water Resources Congress*, Vol. 2013, 913–922

Kang, H. and Burton, H. V., 2018. "Replicating the recovery following the 2014 South Napa earthquake using stochastic process models," *Earthquake Spectra* (accepted for publication).

Karamlou, A., and Bocchini, P., 2016. From Component Damage to System-Level Probabilistic Restoration Functions for a Damaged Bridge, *Journal of Infrastructure Systems*, 04016042.

Kesete, Y., Peng, J., Gao, Y., Shan, X., Davidson, R. A., Nozick, L. K., and Kruse, J., 2014. Modeling Insurer-Homeowner Interactions in Managing Natural Disaster Risk, *Risk analysis*, 34(6), 1040-1055.

Kim, D. J., Ferrin, D. L., and Rao, H. R., 2008. A trust-based consumer decision-making model in electronic commerce: The role of trust, perceived risk, and their antecedents, *Decision support systems*, 44(2), 544-564.

Koppelman, F. S., and Bhat, C., 2006. A self instructing course in mode choice modeling: multinomial and nested logit models.

Kozin, F., and Zhou, H., 1990. System study of urban response and reconstruction due to earthquake, *Journal of Engineering Mechanics*, 116(9), 1959–1972.

Krawinkler, H., Parisi, F., Ibarra, L., Ayoub, A., and Medina, R., 2001. Development of a testing protocol for woodframe structures (Vol. 102). Richmond, CA.

Krejcie, R. V., and Morgan, D. W., 1970. Determining sample size for research activities, *Educational and psychological measurement*, 30(3), 607-610.

Kumar, S., Diaz, R., Behr, J. G. and Toba, A. L., 2015. Modeling the effects of labor on housing reconstruction: A system perspective. International Journal of Disaster Risk Reduction, 12, 154–162.

LADBS, 2015. Mandatory wood frame soft-story retrofit program: Structural Design Guidelines. Los Angeles Department of Building and Safety, Los Angeles.

Lignos, D. G., and Krawinkler, H., 2012. Development and utilization of structural component databases for performance-based earthquake engineering. *Journal of Structural Engineering*, 139(8), 1382-1394.

Lin, P., and Wang, N., 2017. Stochastic post-disaster functionality recovery of community building portfolios I: Modeling. *Structural Safety*, 69, 96-105.

Lindell, M. K., and Prater, C. S., 2003. Assessing community impacts of natural disasters. *Natural hazards review*, 4(4), 176-185.

Liu, H., Davidson, R. A., and Apanasovich, T. V., 2007. Statistical forecasting of electric power restoration times in hurricanes and ice storms. *IEEE Transactions on Power Systems*, *22*(4), 2270–2279. http://doi.org/10.1109/TPWRS.2007.907587

Lowes, L. N., Mitra, N., and Altoontash, A., 2003. A beam-column joint model for simulating the earthquake response of reinforced concrete frames.

Luna, R., Asce, F., Balakrishnan, N., and Dagli, C. H., 2011. Postearthquake Recovery of a Water Distribution System : discrete event simulation using colored petri nets, *Journal of Infrastructure Systems*, 17(1), 25–34.

Massey Jr, F. J., 1951. The Kolmogorov-Smirnov test for goodness of fit, *Journal of the American statistical Association*, 46(253), 68-78.

Mckenna, F. T., 1997. Object-oriented finite element programming: Frameworks for analysis, algorithms and parallel computing, PhD Dissertation, University of California, Berkeley.

Miles, S. B., 2014. Modeling and visualizing infrastructure-centric community disaster resilience. *Proceedings of the 10th US National Conference on Earthquake Engineering*, Anchorage, Alaska.

Miles, S.B., Burton, H. V., and Kang, H., 2018. "Towards a community of practice for disaster recovery modeling," *Natural Hazards Review* (accepted for publication).

Miles, S. B., and Chang, S. E., 2003. *Urban disaster recovery: A framework and simulation model*, MCEER.

Miles, S. B., and Chang, S. E., 2006. Modeling community recovery from earthquakes, *Earthquake Spectra*, 22(2), 439–458.

Miles, S. B., and Chang, S. E., 2011. ResilUS: a community based disaster resilience model, *Cartography and Geographic Information Science*, 38(1), 36–51.

Mishalani, R. G., and Madanat, S. M., 2002. Computation of Infrastructure Transition Probabilities Using Stochastic Duration Models, *Journal of Infrastructure Systems*, 8(4), 139–148.

Morss, R. E., Lazo, J. K., and Demuth, J. L., 2010. Examining the use of weather forecasts in decision scenarios: results from a US survey with implications for uncertainty communication, *Meteorological Applications*, 17(2), 149-162.

Nateghi, R., Guikema, S. D., & Quiring, S. M., 2011. Comparison and Validation of Statistical Methods for Predicting Power Outage Durations in the Event of Hurricanes, *Risk analysis*, 31(12), 1897-1906.

National Institute of Standards and Technology (NIST), 2010. *Disaster resilience: A guide to the literature, NIST Special Publication, 1117,* Gaithersburg, Maryland.

National Institute of Standards and Technology (NIST), 2015. Community resilience planning guide for buildings and infrastructure systems – Volume 1 (NIST Special Publication 1190). NIST, Washington, DC.

National Institute of Standards and Technology (NIST), 2016. Community Resilience Planning Guide for Buildings and Infrastructure Systems – Volume 2 (NIST Special Publication 1190-1). NIST, Washington, DC.

Nejat, A., 2011. Modeling dynamics of post disaster recovery, Ph.D. Dissertation, Texas A&M University, College Station, TX.

Nejat, A., and Damnjanovic, I., 2012. Modeling dynamics of disaster recovery. In *Construction Research Congress 2012: Construction Challenges in a Flat World*, pp. 2200-2210.

Nejat, A., and Ghosh, S., 2016. LASSO Model of Post-disaster Housing Recovery: Case Study of Hurricane Sandy, *Natural Hazards Review*, 4016007.

Nicholson, W., and Snyder, C. M., 2011. Microeconomic theory: Basic principles and extensions. Nelson Education.

Nojima, N., and Kameda, H., 1992. Optimal strategy by use of tree structure for post-earthquake restoration of lifeline network systems, *Proceedings of the 10th World Conference on Earthquake Engineering*, Madrid, Spain.

O'Rourke, T. D., and Shi, P., 2006. Seismic Response Modeling of Water Supply Systems. article.

Pacific Earthquake Engineering Research Center (PEER), 2016. *The Mw 6.0 South Napa Earthquake of August 24, 2014. PEER Report No. 2016/04*, Sacramento, CA.

Raileanu, L. E., and Stoffel, K., 2004. Theoretical comparison between the gini index and information gain criteria, *Annals of Mathematics and Artificial Intelligence*, 41(1), 77-93.

Rathfon, D., Davidson, R., Bevington, J., Vicini, A., and Hill, A., 2013. Quantitative assessment of post-disaster housing recovery: a case study of Punta Gorda, Florida, after Hurricane Charley. *Disasters*, 37(2), 333-355.

Shinozuka, M., Murata, M., and Iwata, T., 1992. Strategies for repair and restoration of seismically damaged gas pipeline systems, *Proceedings of the 4th US-Japan Workshop on Earthquake Disaster Prevention for Lifeline Systems*, Los Angeles, CA.

SEAOSC, 2017. SEAOSC design guide: City of Los Angeles soft, weak and open-front wall line building ordinance. Structural Engineers Association of Southern California, Los Angeles, CA.

Stewart, J. P., 1996. An empirical assessment of soil-structure interaction effects on the seismic response of structures, Ph.D. dissertation, University of California, Berkeley.

Tabucchi, T. H. P., 2007. Modeling Post-earthquake Restoration of the Los Angeles Water Supply System, Ph.D. Thesis, Cornell University.

Tabucchi, T., Davidson, R., and Brink, S., 2008. Restoring the Los Angeles water supply system following an earthquake. *Proceedings of the 14th World Conference on Earthquake Engineering*, Beijing, China.

Tabucchi, T., Davidson, R., and Brink, S., 2010. Simulation of post-earthquake water supply system restoration, *Civil Engineering and Environmental Systems*, 27(4), 263–279.

Tibshirani, R., 1996. Regression shrinkage and selection via the lasso. *Journal of the Royal Statistical Society. Series B (Methodological)*, 267–288. article.

Trifunac, M. D., and Todorovska, M. I., 1997. Northridge, California, earthquake of 1994: density of red-tagged buildings versus peak horizontal velocity and intensity of shaking. *Soil Dynamics and Earthquake Engineering*, 16(3), 209-222.

US The Aspen Global Change Institute (AGCI), 1996. *Creating sustainable and disaster resistant communities: Elements of change natural hazards and global change.*

Varian, H. R. and Repcheck, J., 2010. *Intermediate microeconomics: a modern approach* (Vol. 6). New York: WW Norton & Company.

Von Neumann, J. and Morgenstern, O., 2007. *Theory of games and economic behavior*, Princeton university press.

Wang, Y., 2006. Seismic performance evaluation of water supply systems (Ph. D. dissertation). *Cornell University, Ithaca, New York, NY, USA*.

Whitman, R. V, Anagnos, T., Kircher, C. A., Lagorio, H. J., Lawson, R. S., & Schneider, P., 1997. Development of a national earthquake loss estimation methodology, *Earthquake Spectra*, 13(4), 643–661.

Wilson, R., 1991. Rebuilding after the Loma Prieta Earthquake in Santa Cruz. *International City Management Association, Washington, DC. Philip R. Berke, Iack Kartez and Dennis Wenger Hazard Reduction and Recovery Center College of Architecture Texas A&M University College Station Texas*, 77843.

Wu, J. Y., and Lindell, M. K., 2004. Housing reconstruction after two major earthquakes: the 1994 Northridge earthquake in the United States and the 1999 Chi-Chi earthquake in Taiwan. *Disasters*, *28*(1), 63–81.

Xia, R., and Schleuss, J., 2016. L.A. releases addresses of 13,500 apartments and condos likely to need earthquake retrofitting. http://www.latimes.com/local/california/la-me-quake-risk-20160415-story.html

Xu, N., Guikema, S. D., Davidson, R. A., Nozick, L. K., Çağnan, Z., and Vaziri, K., 2007. Optimizing scheduling of post-earthquake electric power restoration tasks, *Earthquake Engineering & Structural Dynamics*, 36(2), 265–284.

Zhang, Y., and Peacock, W. G., 2009. Planning for Housing Recovery? Lessons Learned From Hurricane Andrew. *Journal of the American Planning Association*, *76*(1), 5–24. http://doi.org/10.1080/01944360903294556